



UNIVERSIDADE ESTADUAL PAULISTA
“JÚLIO DE MESQUITA FILHO”
Campus de São José do Rio Preto

ESTRUTURAS VESICULARES EM MISTURAS DE SURFACTANTES
CATIÔNICOS

Fernanda Rosa Alves

Orientador: Prof. Dr. Eloi da Silva Feitosa

Tese apresentada ao programa de pós-graduação em Biofísica Molecular do Instituto de Biociências, Letras e Ciências Exatas da Universidade Estadual Paulista, como parte das exigências para a obtenção do título de Doutor em Biofísica Molecular.

São José do Rio Preto - SP

2008

Alves, Fernanda Rosa.

Estruturas vesiculares em misturas de surfactantes catiônicos /
Fernanda Rosa Alves. - São José do Rio Preto, SP: [s.n.], 2008.

121 f. : il. ; 30 cm.

Orientador: Eloi da Silva Feitosa.
Tese (doutorado) – Universidade Estadual Paulista, Instituto de
Biociências, Letras e Ciências Exatas.

1. Físico-química. 2. Vesículas catiônicas. 3. DODAB. 4.
Calorimetria diferencial de varredura. I. Feitosa, Eloi da Silva. II.
Universidade Estadual Paulista, Instituto de Biociências, Letras e
Ciências Exatas. III. Título.

CDU - 544

*“É melhor tentar e falhar, que preocupar-se e ver a vida passar.
É melhor tentar, ainda que em vão que sentar-se, fazendo nada até o final.
Eu prefiro na chuva caminhar, que em dias frios em casa me esconder.
Prefiro ser feliz embora louco, que em conformidade viver.”*

Martin Luther King

Aos meus pais
Mauro e Lázara
(*in memoriam*)

Agradecimentos

Ao Prof. Dr. Eloi Feitosa pela orientação, paciência e confiança depositadas em mim.

Ao Prof. Dr. Watson Loh pela colaboração e disponibilidade do equipamento DSC sempre que necessário.

À Profa. Dra. Maria Elisabete Darbello Zaniquelli pela colaboração e disponibilidade do equipamento para as medidas de DLS.

Às Profas. Elisabete M. S. Castanheira e Maria Elisabete C. D. Real Oliveira, pela grande colaboração e interpretação dos resultados e discussões de fluorescência.

Ao Prof. Dr. Marcio José Tiera pela disponibilização do espectrofotômetro.

A todos os meus colegas do grupo Física de Colóides, que durante este período foram muito prestativos e companheiros.

Principalmente aos meus irmãos Christiane e Mauro César pelo incentivo, carinho e união.

Ao CNPq como auxílio financeiro para o desenvolvimento desse trabalho.

Resumo

Estudos de calorimetria diferencial de varredura (DSC) e fluorescência de estado estacionário da sonda Vermelho do Nilo indicam a formação de vesículas de DODAX ($X = \text{Cl}^-$ ou Br^-) em concentrações de surfactantes tão baixas quanto $10 \mu\text{M}$. Estas vesículas foram denominadas microvesículas (μV), cuja T_m diminui monotonicamente com a concentração de DODAX até valores de T_m das vesículas tradicionais preparadas em 1.0 mM do surfactante. O efeito do contra-íon (Br^- e Cl^-) no comportamento termotrópico de fase das vesículas mistas de DODAB-DODAC foi investigado por DSC, condutimetria e espalhamento dinâmico de luz (DLS). Observou-se que a T_m aumenta sigmoidalmente de 45.8 a $48.9 \text{ }^\circ\text{C}$ com a fração molar de DODAC (x_{DODAC}), com um ponto de inflexão no ponto equimolar. A condutividade e o diâmetro hidrodinâmico das vesículas variam muito pouco com x_{DODAB} , indicando que a densidade superficial de carga das vesículas de DODAX é semelhante entre si, e o efeito do contra íon na T_m de DODAX se deve a interações específicas desses contra-íons na interface das vesículas. Medidas de DSC, fluorescência e turbidez de misturas de DODAB-DDAB indicam que as vesículas de DODAB têm maior afinidade por DDAB do que o oposto, resultando na formação de duas populações de vesículas mistas de DDAB-DODAB, com propriedades distintas. Além disso, medidas de fluorescência mostraram que a presença de pequena quantidade de DODAB incorporado nas vesículas de DDAB causa um efeito significativo na emissão da sonda devido ao aumento do tamanho das vesículas, sugerido por medidas de turbidez. O estudo dos sistemas DODAB/ C_n TAB/água na concentração total de surfactante igual a $1,0$ e $5,0 \text{ mM}$, variando a concentração de C_n TAB, e também mantendo a concentração de DODAB fixa em $1,0 \text{ mM}$, revelou uma forte dependência do comprimento da cadeia de hidrocarbonetos n e da concentração relativa dos surfactantes, nas propriedades das vesículas mistas de DODAB- C_n TAB. Através deste estudo, foi possível analisar o comportamento termotrópico de fase das vesículas contendo diferentes quantidades de DODAB, e o mecanismo de transição vesícula-micela com o aumento da concentração de C_n TAB, abaixo e acima da CMC. Em geral, a interação C_n TAB-DODAB aumenta com n , e a T_m pode ser menor, igual ou maior do que a T_m de DODAB em água.

Palavras-chaves: DODAB, C_n TAB, DSC, DLS, Turbidez, Tensiometria, Condutimetria, Fluorescência, Vermelho do Nilo, vesículas catiônicas, transição gel-líquido cristalina.

Abstract

Differential scanning calorimetry (DSC) and fluorescence of the probe Nile Red studies reveal the formation of DODAX vesicles ($X = \text{Br}^-$ and Cl^-) at surfactant concentrations as low as $10 \mu\text{M}$. These vesicles were referred to as microvesicles (μV), whose T_m decreases monotonically with increasing DODAX concentration to the value for the ordinary vesicles at 1 mM . The effect of counterion (Br^- and Cl^-) on the thermotropic phase behavior of mixed DODAB-DODAC vesicles were investigated by differential scanning calorimetry (DSC), conductimetry and dynamic light scattering (DLS). T_m increases sigmoidally from 45.8 to $48.9 \text{ }^\circ\text{C}$ with DODAC molar fraction (x_{DODAC}), with an inflection point at the equimolarity. The conductivity and the apparent hydrodynamic diameter vary little with x_{DODAB} , indicating that the surface charge density is similar for DODAX, evidencing that the effect of counterion on T_m is due to the counterion specific interactions. DSC, fluorescence and turbidity measurements indicate a higher affinity of DDAB for DODAB vesicles than the reverse, resulting in two populations of mixed DDAB-DODAB vesicles with different properties. Besides, fluorescence measurements show that the presence of a small amount of DODAB in DDAB vesicles causes a pronounced effect on the Nile Red emission, due to the increase in vesicle size, as suggested from turbidity results. The study of DODAB/ C_n TAB/água systems at 1.0 and 5.0 total surfactant concentration, and varying C_n TAB concentrations with constant 1.0 mM DODAB revealed a strong dependence of the chain length n and relative concentration of the surfactante in the properties of mixed DODAB- C_n TAB vesicles. This study allowed analyzing the thermotropic phase behavior containing different amount of DODAB, and the mechanism of vesicle-micelle transition with increasing C_n TAB concentration, below and above CMC. Overall, the C_n TAB-DODAB interaction increases with n , and T_m can be lower, equal or higher than T_m of neat DODAB in water.

Keywords: DODAB, C_n TAB, DSC, DLS, Turbidity, Tensiometry, Conductimetry, Fluorescence, Nile Red, Cationic vesicles, Melting temperature.

Lista de trabalhos

Artigo 1: FEITOSA, E.; ALVES, F. R.; LOH, W.; CASTANHEIRA E. M. S.; REAL OLIVEIRA, M. E. C. **Cationic vesicles in the micromolar concentration domain of dioctadecyldimethylammonium bromide and chloride in water.** Manuscrito.

Artigo 2: FEITOSA, E.; ALVES, F. R. **The role of counterion on the thermotropic phase behavior of mixed dioctadecyldimethylammonium bromide and chloride vesicles.** Submetido.

Artigo 3: FEITOSA, E.; ALVES, F. R.; NIEMIEC, A.; REAL OLIVEIRA, M. E. C. D.; CASTANHEIRA, E. M. S.; BAPTISTA, A. L. F. **Cationic liposomes in mixed didodecyldimethylammonium bromide and dioctadecyldimethylammonium bromide aqueous dispersions studied by differential scanning calorimetry, Nile red fluorescence, and turbidity.** Langmuir, 22, 3579-3585, 2006.

Artigo 4: ALVES, F. R.; ZANIQUELLI, M. E. D.; LOH, W.; CASTANHEIRA, E. M. S.; REAL OLIVEIRA, M. E. C. D.; FEITOSA, E. **Vesicle-micelle transition in aqueous mixtures of the cationic dioctadecyldimethylammonium and octadecyltrimethylammonium bromide surfactants.** J. Colloid Interface Sci., 316, 132-139, 2007.

Artigo 5: ALVES, F. R.; FEITOSA, E. **Thermotropic phase behavior in aqueous mixtures of dioctadecyldimethylammonium bromide and alkyltrimethylammonium bromide surfactant series studied by differential scanning calorimetry.** Thermochemica Acta, 472, 41-45, 2008.

Artigo 6: FEITOSA, E.; ALVES, F. R.; LOH, W. **Vesicle-micelle transitions in aqueous mixtures of C_n TAB and DODAB studied by differential scanning calorimetry and turbidity.** Submetido.

Índice

1. Introdução e objetivos	<i>1</i>
1.1. Colóides de associação	<i>1</i>
1.2. Vesículas de surfactantes sintéticos	<i>4</i>
1.3. Histerese no comportamento termotrópico de vesículas de DODAX	<i>7</i>
1.4. Temperaturas de transição	<i>8</i>
1.5. Objetivos	<i>11</i>
2. Microvesículas de DODAX	<i>12</i>
3. Efeito do contra-íon	<i>16</i>
4. Efeito de co-surfactante	<i>19</i>
4.1. Sistema DDAB/DODAB/água	<i>19</i>
4.2. Sistema C ₁₈ TAB/DODAB/água	<i>22</i>
4.3. Sistemas C _n TAB/DODAB/água (<i>n</i> = 12, 14, 16 e 18)	<i>29</i>
5. Considerações finais	<i>35</i>
6. Referências bibliográficas	<i>37</i>

Artigo 1: **Cationic vesicles in the micromolar concentration domain of dioctadecyldimethylammonium bromide and chloride in water.** *42*

Artigo 2: **The role of counterion on the thermotropic phase behavior of mixed dioctadecyldimethylammonium bromide and chloride vesicles.** *69*

Artigo 3: **Cationic liposomes in mixed didodecyldimethylammonium bromide and dioctadecyldimethylammonium bromide aqueous dispersions studied by differential scanning calorimetry, Nile red fluorescence, and turbidity.** *85*

Artigo 4: **Vesicle-micelle transition in aqueous mixtures of the cationic dioctadecyldimethylammonium and octadecyltrimethylammonium bromide surfactants.** *93*

Artigo 5: Thermotropic phase behavior in aqueous mixtures of dioctadecyldimethylammonium bromide and alkyltrimethylammonium bromide surfactant series studied by differential scanning calorimetry. 102

Artigo 6: Vesicle-micelle transitions in aqueous mixtures of C_nTAB and DODAB studied by differential scanning calorimetry and turbidity. 108

Lista de abreviações e símbolos

DODAB	brometo de dioctadecildimetilamônio
DODAC	cloreto de dioctadecildimetilamônio
DDAB	brometo de didodecildimetilamônio
C ₁₂ TAB	brometo de dodeciltrimetilamônio
C ₁₄ TAB	brometo de tetradeciltrimetilamônio
C ₁₆ TAB	brometo de hexadeciltrimetilamônio
C ₁₈ TAB	brometo de octadeciltrimetilamônio
DNA	ácido desoxirribonucléico
LUV	vesículas unilamelares grandes
SUV	vesículas unilamelares pequenas
MLV	vesículas multilamelares
MEV	vesículas multiestruturais
μV	microvesículas
CMC	concentração micelar crítica
CVC	concentração vesicular crítica
<i>P</i>	parâmetro de empacotamento
<i>v</i>	volume das cadeias de hidrocarboneto
<i>a</i>	área efetiva do grupo de cabeça polar
<i>l</i>	comprimento das cadeias de hidrocarboneto
DSC	calorimetria diferencial de varredura
DLS	espalhamento de luz dinâmico
cryo-TEM	microscopia eletrônica de transmissão criogênica
T _k	temperatura de Krafft
T _m	temperatura de transição de estado gel-líquido cristalino
T _s	pré-transição
T _p	pós-transição
ΔT _{1/2}	largura do pico de transição medida na metade da altura do pico
ΔH	variação de entalpia
ΔC _p	variação da capacidade calorífica
R _H	raio hidrodinâmico
<i>r</i>	anisotropia

I_{VV} e I_{VH}	intensidade de radiação polarizada vertical e horizontal quando a radiação de excitação é polarizada verticalmente
I_{HV} e I_{HH}	intensidade de radiação polarizada vertical e horizontal quando a radiação de excitação é polarizada horizontalmente
G	fator de correção instrumental
I_{total}	intensidade de fluorescência total
λ	comprimento de onda
κ	condutividade
α	grau de dissociação

1. Introdução e objetivos

Esta tese trata do estudo de propriedades físico-químicas de vesículas catiônicas de DODAB e DODAC em diferentes concentrações, e na presença de co-surfactantes homólogos C_n TAB e DDAB. A Tese compreende seis artigos ou manuscritos sobre o tema, que serão discutidos a seguir.

1.1. Colóides de associação






Surfactantes, ou moléculas tensoativas são anfifílicas que consistem de uma porção hidrofílica e outra hidrofóbica ligadas covalentemente entre si. A parte polar ou hidrofílica pode ser iônica (catiônica ou aniônica), não iônica ou zwitteriônica, enquanto a parte apolar ou hidrofóbica é normalmente uma ou duas cadeias flexíveis de hidrocarbonetos contendo de 10 a 18 átomos de carbono.

Em solução aquosa, surfactantes tendem a formar uma variedade de agregados denominados colóides de associação, com dimensão média entre 1 nm e 1 μ m. O tipo de estrutura formada depende de fatores como a composição química dos componentes, do solvente, da temperatura e da presença de co-solutos, e pode ser aproximadamente estimada a partir do parâmetro de empacotamento do surfactante $P = v/al$, onde v e l são, respectivamente, o volume e o comprimento da parte apolar, e a é a área ocupada pela região polar. Quando $P < 1/3$ micelas esféricas tendem se formar, enquanto vesículas se formam quando $1/2 < P < 1$ (ISRAELACHVILLI, 1991) (ver Tabela 1). Estruturas reversas são formadas quando $P > 1$.

Uma das características fundamentais dos surfactantes é o potencial de diminuir a tensão superficial da água (isto é, a quantidade de trabalho necessária para expandir a interface água-ar). Quanto maior for a adsorção de surfactante na interface, maior é a redução

da tensão superficial. Outra propriedade fundamental de anfifílicos é a formação de estruturas supramoleculares, que também consiste em um fenômeno de interface.

Tabela 1 – Estruturas e formas de surfactantes e agregados, e os respectivos parâmetros de empacotamento.

Estrutura geométrica	 Cone	 Cone truncado	 Cone truncado	 Cilindro	 Cone truncado invertido
$P = v/al$	$P < 1/3$	$1/3 < P < 1/2$	$1/2 < P < 1$	$P \approx 1$	$P > 1$
Estruturas dos agregados	Micelas esféricas	Micelas globulares ou cilíndricas	Vesículas	Bicamadas	Estruturas reversas

Em ambiente aquoso, os surfactantes se associam não-covalentemente em estruturas supramoleculares, tais como micelas, bicamadas ou vesículas (Figura 1), e as interações hidrofóbicas, que minimizam o contato entre as cadeias de hidrocarbonetos com moléculas de água, são as principais responsáveis pela formação desses agregados (TANFORD, 1991). Os surfactantes podem ser solúveis ou insolúveis em um dado solvente. Os surfactantes solúveis em água formam micelas de tamanhos variados acima de uma concentração e temperatura críticas, a concentração micelar crítica (CMC) e a temperatura de Krafft (T_K). Alguns surfactantes são pouco solúveis em água em temperatura ambiente e alcançam a CMC a uma certa temperatura, a temperatura de Krafft; a partir desta temperatura, micelas são formadas (JÖNSSON et al., 1998). Surfactantes insolúveis formam vesículas. Em geral, os surfactantes monoalquilados são solúveis e os surfactantes dialquilados são insolúveis em água. Em concentrações maiores, todos os surfactantes tendem a formar estruturas e fases mais complexas.

Os surfactantes em solução se encontram na fase líquido-cristalina ou isotrópica. As micelas normais e reversas e vesículas são estruturas dominantes na fase isotrópica, enquanto

que a fase líquido-cristalina pode ser hexagonal ou lamelar. As fases cúbicas são também isotrópicas. Neste trabalho limitamo-nos a pequenas concentrações de surfactante, nas quais se têm micelas ou vesículas em água.

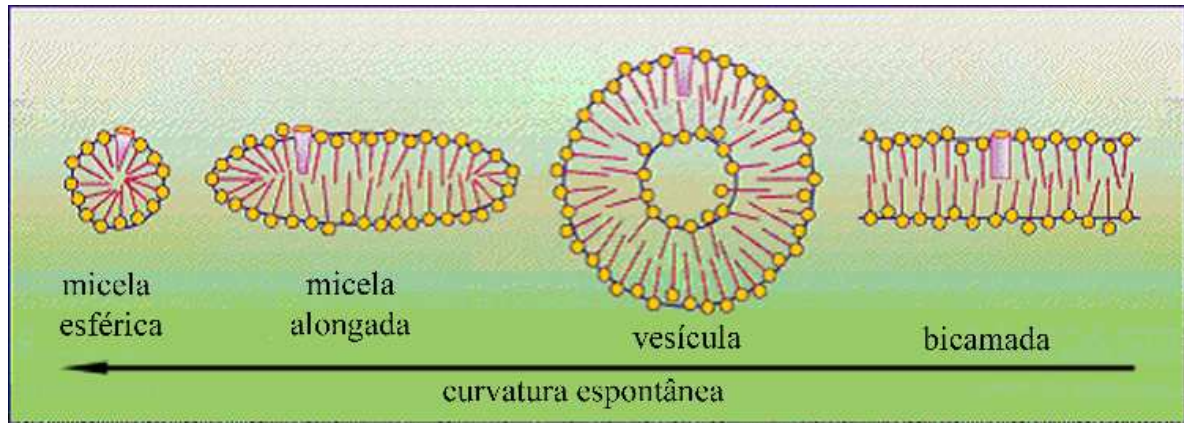


Figura 1: Algumas estruturas formadas pela associação de surfactantes em meio aquoso.

As micelas são colóides de associação mais simples formados por surfactantes em água (LINDMAN e WENNERSTRÖN, 1980). São, em geral, esféricas, podendo também ser encontradas na forma cilíndrica ou discoidal. As micelas são formadas espontaneamente acima da CMC e acima da T_K . A CMC diminui e a T_K aumenta com o aumento do comprimento da cauda do surfactante. A Tabela 2 mostra valores da CMC (MATA et al., 2005; SWANSON-VETHAMUTHU et al, 1998) e T_K (DAVEY et al., 1998; SWANSON-VETHAMUTHU et al, 1998) dos surfactantes da série brometo alquiltrimetilamônio (C_n TAB, $n = 12-18$) utilizados nesta pesquisa. Deste modo, nos experimentos realizados, exceto para C_{12} TAB, a concentração de C_n TAB ($n = 14, 16$ e 18) está tanto acima quanto abaixo da CMC, e a temperatura está tanto abaixo quanto acima da T_K . À temperatura de $25\text{ }^\circ\text{C}$, e concentrações de até 5 mM , aqui investigados, C_n TAB interage com as vesículas de DODAB como monômeros, micelas ou cristais hidratados.

Tabela 2: Valores da CMC e T_K dos surfactantes da série C_n TAB ($n = 12-18$).

n	12	14	16	18
CMC / mM	15,2 ^a	3,98 ^a	1,0 ^a	0,34 ^c
T_K / °C	< 0 ^b	≈ 0 ^b	25 ^b	38 ^c

^aMATA et al., 2005. ^bDavey et al., 1998. ^cSWANSON-VETHAMUTHU et al., 1998.

1.2. Vesículas de surfactantes sintéticos

As vesículas consistem de uma ou mais bicamadas de anfífilos separando a fase aquosa interna da externa às vesículas, formando agregados aproximadamente esféricos com um centro aquoso interno. Os surfactantes formadores de vesículas podem ser naturais, como os fosfolípidios, ou sintéticos, tais como os haletos dialquilados de amônia quaternária. Os surfactantes formadores de vesículas e micelas usados neste estudo são mostrados na Figura 2.

Brometo e cloreto de dioctadecildimetilamônio (DODAX, $X = Br^-$ e Cl^-) e brometo de didodecildimetilamônio (DDAB) são surfactantes catiônicos com duas cadeias de hidrocarbonetos, contendo 18 e 12 átomos de carbono, respectivamente. Em solução aquosa diluída esses surfactantes formam espontaneamente vesículas unilamelares acima da temperatura de transição do estado gel para líquido-cristalino do surfactante $T_m \approx 45, 49$ e $16^\circ C$, respectivamente, e concentrações relativamente baixas, tipicamente 1 mM (MARQUES et al., 2002; FEITOSA et al., 2006b).

Vesículas multilamelares e multiestruturais de DODAX e DDAB também podem ser formadas em concentrações maiores de surfactantes, assim como na presença de sais inorgânicos (MARQUES et al., 2002; FEITOSA e BARRELEIRO, 2004). Deste modo, a concentração de surfactante, a força iônica e a temperatura contribuem para determinar a estrutura vesicular em dispersões aquosas de DODAX. A Figura 3 mostra um esquema de

possíveis estruturas vesiculares formadas em solução aquosa variando a concentração do surfactante.

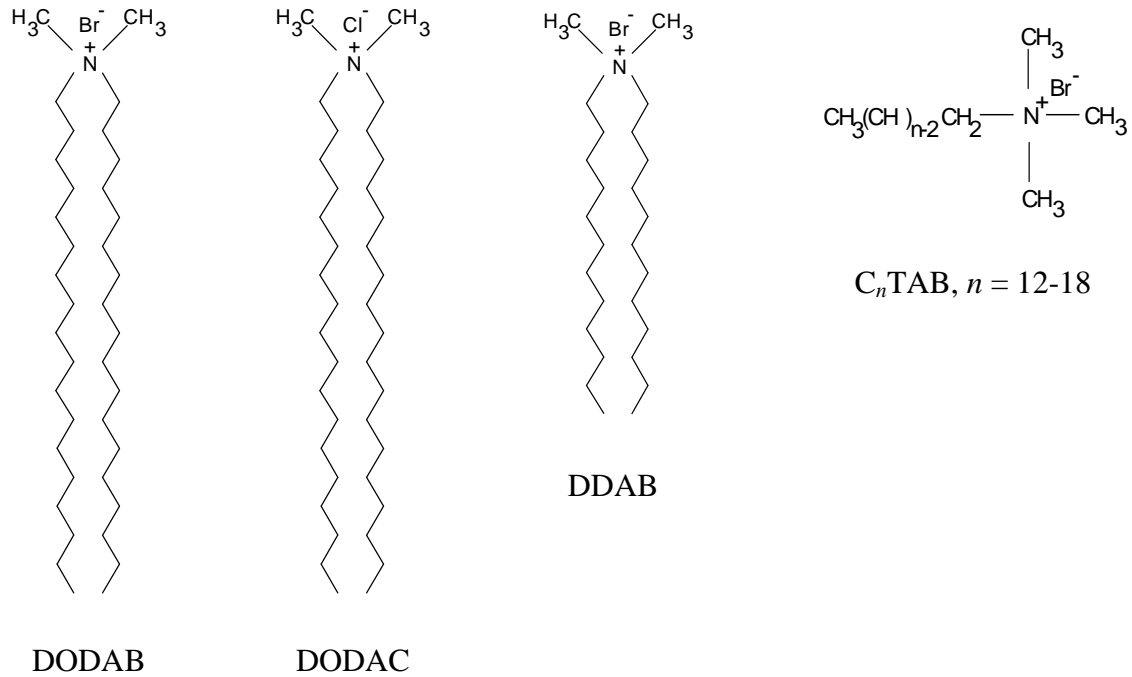


Figura 2: Estruturas moleculares de surfactantes formadores de vesículas e micelas usados neste estudo: DODAB, brometo de dioctadecildimetilamônio; DODAC, cloreto de dioctadecildimetilamônio; DDAB, brometo de dodecildimetilamônio e C_nTAB, brometo de alquiltrimetilamônio.

O estudo e a aplicação de vesículas vem crescendo muito desde a primeira formação dessas estruturas em laboratório, na década de 60, pela mistura de lipídio em solução aquosa (BANGHAM E HORNE, 1964), e na década de 70, pela mistura de anfífilos sintéticos derivados de amônia quaternária em água (KUNITAKE e OKAHATA, 1977). A partir de então, diferentes métodos foram desenvolvidos com o objetivo de formar vesículas com tamanho, estrutura, polidispersidade e estabilidade controladas (LASIC, 1993).

O controle das propriedades das vesículas espontâneas catiônicas derivadas da amônia quaternária, como DODAX e DDAB, é de grande importância na aplicação destas vesículas

no campo da ciência e tecnologia, como por exemplo, na mimetização de membranas naturais, no encapsulamento e transporte de drogas para tratamento médico ou na compactação de moléculas de DNA para terapia gênica (LASIC, 1993; FENDLER, 1982). A grande vantagem dessas vesículas, em relação às vesículas preparadas por métodos convencionais de sonicação (FEITOSA e BROWN, 1997; CUCCOVIA et al., 1990), extrusão (FEITOSA et al., 2000), injeção (CUCCOVIA et al., 1990; CARMONA-RIBEIRO, 1992) ou remoção de surfactante (FEITOSA e KARLSSON, 2006), está na maior reprodutibilidade de suas propriedades físico-químicas e no maior controle das condições de preparo das vesículas, como a temperatura e concentração de surfactante.

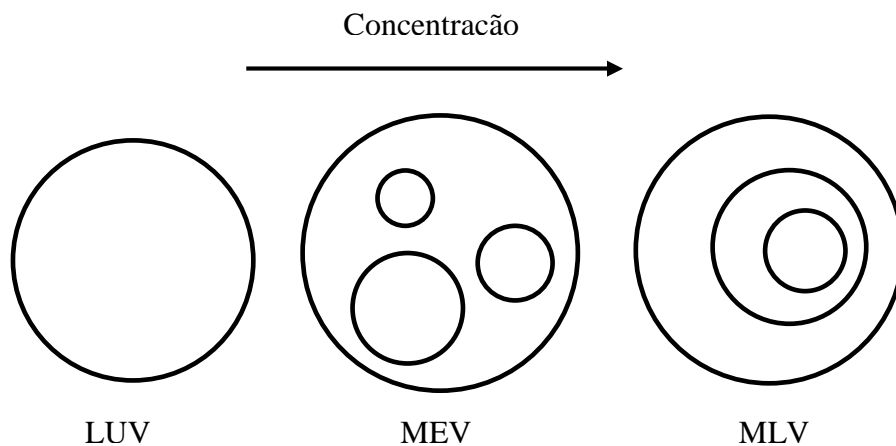


Figura 3: Representação esquemática de vesículas formadas em solução aquosa variando a concentração de surfactantes. As linhas de contorno das vesículas representam bicamadas anfifílicas. LUV: vesículas unilamelares grandes, MEV: vesículas multiestruturais e MLV: vesículas multilamelares.

Feitosa e colaboradores investigaram através de calorimetria diferencial de varredura (DSC) e espalhamento dinâmico de luz (DLS) a T_m e R_H (raio hidrodinâmico) das vesículas catiônicas de brometo de dialquildimetilamônio (D_n DAB), com $n = 12, 14, 16$ e 18 carbonos

(FEITOSA et al., 2006c). Os resultados mostraram que além da T_m aumentar (não linearmente) com o número de carbonos nas cadeias dialquiladas, R_H também aumenta.

Feitosa e colaboradores verificaram também que a T_m não é uma característica de DODAX, pois depende do método de preparação, e tende a aumentar com o tamanho das vesículas (FEITOSA et al., 2000). A T_m de DODAX diminui com o aumento da curvatura das vesículas extrudadas, porém, a T_m das vesículas sonicadas desses surfactantes é maior do que a das vesículas não sonicadas (espontâneas), provavelmente devido à predominância de estruturas do tipo lente (estruturas planares), resultantes de fragmentação das vesículas durante o processo de sonicação.

As vesículas de DODAX possuem algumas propriedades que as caracterizam. Uma dessas propriedades é o fenômeno de histerese do comportamento termotrópico, conforme descrito abaixo.

1.3. Histerese no comportamento termotrópico das vesículas de DODAX

Os valores de T_m das vesículas de DODAX, obtidos por medidas de ESR, turbidez e DSC são maiores quando obtidos por aquecimento do que por resfriamento da amostra, fenômeno este conhecido como histerese do comportamento termotrópico (NASCIMENTO et al., 1998; FEITOSA et al., 2000; BENATTI et al., 2001). Ou seja, os valores espectrais de ESR, turbidez e DSC em função da temperatura não coincidem para dispersões aquosas de vesículas de DODAX, quando obtidas por aquecimento e resfriamento da amostra, dentro de uma faixa de temperatura em torno da T_m . Resultados apresentados por Nascimento e colaboradores (1998), mostraram que a histerese diminui com o tamanho e a hidratação do contra-íon. Além disso, foi observada uma histerese maior para vesículas menores de DODAC, enquanto que as vesículas maiores de DODAB apresentaram uma histerese menor

(NASCIMENTO et al., 1998). No entanto, ainda não foi reportado na literatura qualquer relação entre histerese e o tamanho dessas vesículas.

A Figura 4 mostra algumas curvas de DSC de vesículas de DODAB e DODAC obtidos por aquecimento e resfriamento das amostras, para diferentes valores de tempo de espera entre um aquecimento e o resfriamento seguinte e diferentes taxas de aquecimento. A T_m obtida dessas curvas é de 42,5 e 39,5 °C para DODAB, e 48,8 e 43,5 °C para DODAC, resultando em uma histerese de aproximadamente 3 e 5 °C, respectivamente. Após o segundo resfriamento, aparece uma pré-transição bem próxima ao pico da T_m de DODAC de aproximadamente 42 °C, a qual é mantida nas curvas de aquecimento e resfriamento seguintes. A causa dessa pré-transição ainda está sendo investigada.

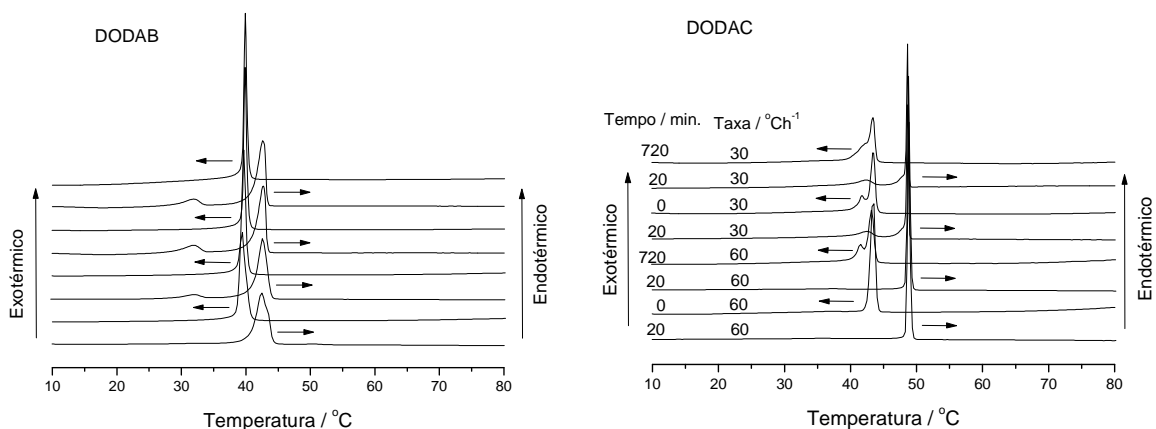


Figura 4 - Curvas de DSC de dispersões aquosas de DODAB 1,0 mM e DODAC 2,0 mM, obtidos por aquecimento (endotérmico) e resfriamento (exotérmico) das amostras, para diferentes valores de tempo de espera e diferentes taxas de aquecimento, indicados nas curvas. No resfriamento a T_m é sempre menor. (Resultados não publicados).

1.4. Temperaturas de transição

As vesículas sintéticas e naturais em geral apresentam uma temperatura de transição de estado gel para líquido-cristalino, T_m . Abaixo da T_m (estado gel) as cadeias de

hidrocarbonetos na bicamada estão mais ordenadas e rígidas, enquanto que acima da T_m (estado líquido-cristalino) as caudas são flexíveis e desordenadas (CEVEC e MARSH, 1987; EVANS e WENNERSTRÖM, 1999). A transição de um para o outro estado, em geral, ocorre numa estreita faixa de temperatura.

Além da transição de estado gel para líquido-cristalino, algumas vesículas, como as de DODAB, também apresentam uma temperatura de pré e uma pós-transição de fase, com temperaturas bem definidas, $T_s \approx 33.3 \text{ }^\circ\text{C}$ e $T_p \approx 51 \text{ }^\circ\text{C}$, respectivamente (FEITOSA e BARRELEIRO, 2004). T_s está relacionada à transição de um estado gel para um estado gel ondulado, enquanto que T_p está associada à transição de fases lamelares locais para uma fase totalmente isotrópica de vesículas uni ou multilamelares (Figura 5). A técnica de calorimetria diferencial de varredura (DSC) é uma ferramenta importante para investigar essas transições de estados. Essas três transições são endotérmicas quando a amostra é aquecida e exotérmica no resfriamento.

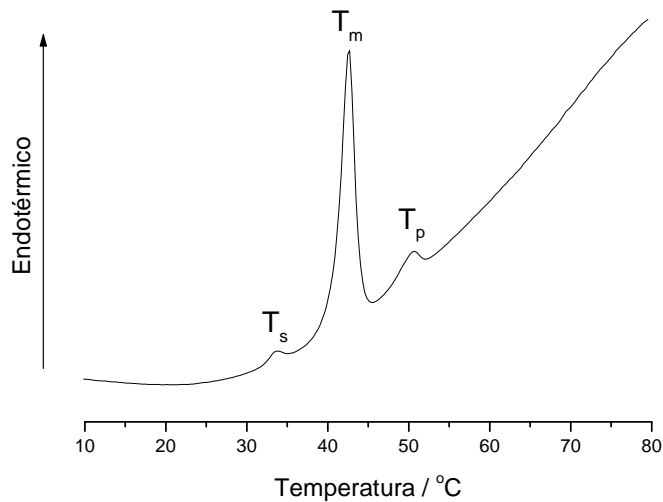


Figura 5 – Curva de DSC típica das vesículas de DODAB 1,0 mM em água, indicando os picos endotérmicos de pré-transição, transição principal e pós-transição.

A Figura 6 mostra o esquema de estruturas de bicamadas para diferentes transições de estados com a variação da temperatura. As estruturas das transições de estado associadas à pré-transição, T_s , e a transição de estado gel-líquido cristalino, T_m , são indicadas. A transição do estado gel para líquido-cristalino é uma característica do sistema, pois depende do tipo de agregado formado e está relacionada à configuração das cadeias de hidrocarbonetos da bicamada.

As vesículas de fosfolípidios naturais possuem valores menores de T_m , devido à alta proporção de cadeias insaturadas, evitando, portanto, uma maior rigidez das cadeias em temperaturas mais baixas (estado gel) (ROBINSON e ROGERSON, 2001). Com o aumento da temperatura, as moléculas são menos empacotadas, passando a ocupar uma área maior, e a espessura da bicamada diminui (ROBINSON e ROGERSON, 2001). A presença de ramificações gera um aumento do volume livre, devido ao aumento de número de terminais de cadeia. Isto facilita o movimento das cadeias, reduzindo a T_m .

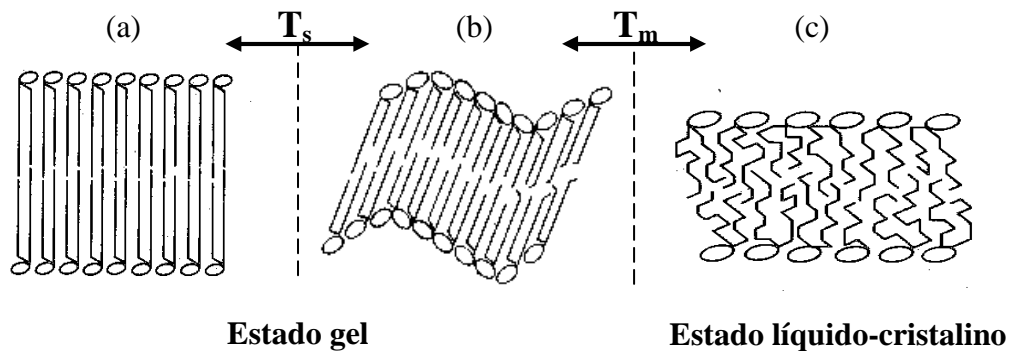


Figura 6 – Representação esquemática de estruturas de bicamadas nos estados gel e líquido-cristalino. Extraída de Cevc e Marsh (1987). (a) estado gel, (b) estado gel ondulado e (c) estado líquido-cristalino.

1.5. Objetivos

Misturas de surfactantes com características diferentes é um campo de pesquisa bastante promissor e visa estabilizar o sistema ou promover a formação de novas estruturas. Além disso, as misturas de surfactantes podem ser usadas para controlar as propriedades dos agregados formados, que podem ser essenciais em aplicações específicas na ciência e tecnologia. Neste trabalho investigamos a mistura de surfactantes catiônicos homólogos com uma ou duas cadeias de hidrocarbonetos, formadores de micelas e vesículas, através das técnicas de calorimetria diferencial de varredura (DSC), fluorescência de estado estacionário, espalhamento de luz, tensiometria e condutimetria. Os sistemas investigados foram: DODAB, DODAC, DODAB-DDAB, DODAB-DODAC, DODAB-C₁₈TAB e DODAB-C_nTAB, em água, para $n = 12, 14, 16$ e 18 .

A realização desta pesquisa visa:

- Verificar a formação de vesículas de DODAB e DODAC no regime de concentração micromolar.
- Investigar a influência dos contra-íons Br⁻ e Cl⁻ nas propriedades termotrópicas das vesículas de DODAB e DODAC.
- Estudar o comportamento termotrópico de dispersões de vesículas mistas de DODAB com surfactantes catiônicos mono e dialquilados.
- Estudar o efeito do comprimento da cadeia de hidrocarbonetos de C_nTAB no comportamento termotrópico das vesículas de DODAB.
- Caracterizar as estruturas formadas nas misturas de surfactantes catiônicos.

2. Microvesículas de DODAX

Vesículas unilamelares estáveis podem ser preparadas numa faixa de concentração de surfactantes bastante limitada. Em concentrações maiores de surfactante, vesículas multilamelares e multiestruturais são formadas, favorecendo a fusão, precipitação e formação de fases lamelares (FEITOSA et al., 2000; FEITOSA e BARRELEIRO, 2004). Comportamento inverso pode ser esperado em dispersões de DODAX muito diluídas em relação às vesículas tradicionais preparadas em 1,0 mM. Espera-se, portanto, que as soluções de vesículas diluídas (na faixa de concentração micromolar), sejam mais estáveis e menos polidispersas do que as vesículas tradicionais, principalmente porque a interação intervesicular é desprezível em concentrações tão pequenas. O artigo 1 trata do estudo por DSC e fluorescência¹ da formação de vesículas de DODAX na região micromolar desses surfactantes. Estas vesículas diluídas foram denominadas em nosso artigo de microvesículas (μV) a fim distinguí-las das vesículas tradicionais preparadas, por exemplo, a 1,0 mM. Sob diluição da amostra, foi possível observar através da Figura 7 que os picos relacionados à T_m de DODAB e DODAC permanecem até 10 μM de surfactante, enquanto os picos da pré e pós-transição de DODAB desaparecem ao redor de 40 e 80 μM , respectivamente. Nota-se que as vesículas de DODAC não apresentam pré- e pós-transição, mas apenas a transição principal.

A Figura 8 mostra os valores de T_m em função da concentração de DODAB e DODAC na região micromolar e milimolar. Para ambas as vesículas de DODAB e DODAC um aumento contínuo da T_m com a diluição das dispersões de 1,0 mM para 10 μM foi observado, com DODAB apresentando um aumento mais pronunciado da T_m .

¹ Os resultados de fluorescência desta Tese foram obtidos e discutidos por Elisabete M. S. Castanheira e M. Elisabete C. D. Real Oliveira, colaboradoras da Universidade de Minho, Campus de Gualtar, Portugal.

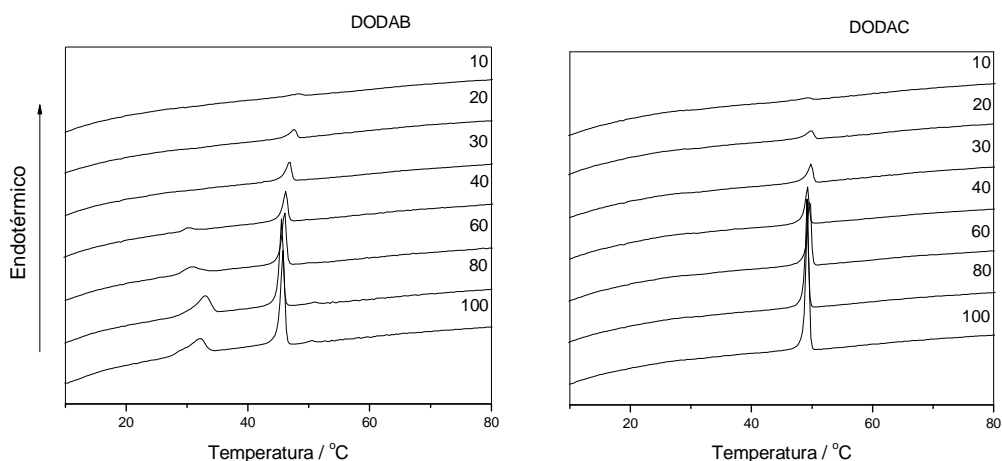


Figura 7 – Curvas de DSC de 10 a 100 μM de DODAB e DODAC em solução aquosa.

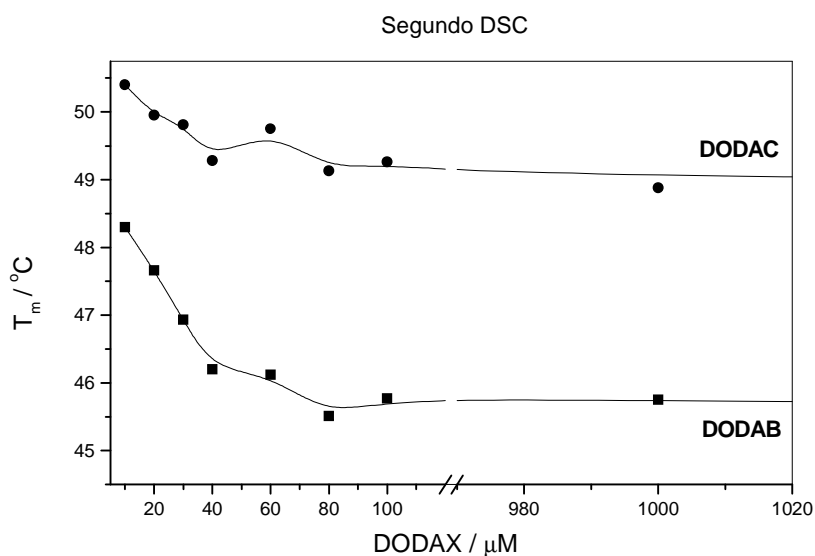


Figura 8 – Efeito da concentração de surfactante na T_m de DODAB e DODAC em água.

A T_m de DODAX em água aumenta com o aumento de tamanho das vesículas induzido por extrusão, e a T_m de DODAC é sempre maior (FEITOSA et al., 2000; FEITOSA e BARRELEIRO, 2004). O aumento da T_m com a diluição das dispersões de DODAX sonicadas e não sonicadas também foi observado por FEITOSA et al. (2000). Deste modo, a

Figura 8 sugere que as microvesículas de DODAX são maiores em relação às vesículas tradicionais, e as microvesículas de DODAB apresentam uma variação maior no tamanho com a diluição das amostras. Comportamento oposto foi observado para a T_m de dispersões de dipalmitoilfosfatidilcolina (DPPC) (CEVC e MARSH, 1987) e dihexadecilfosfato, DHP (FEITOSA, 2008), que observaram uma diminuição da T_m com a diluição das amostras.

A Figura 9 mostra os espectros de fluorescência da sonda Vermelho do Nilo (NR) incorporada nos sistemas DODAB/água, a 25 e 60 °C, ou seja, abaixo e acima da T_m desse surfactante.

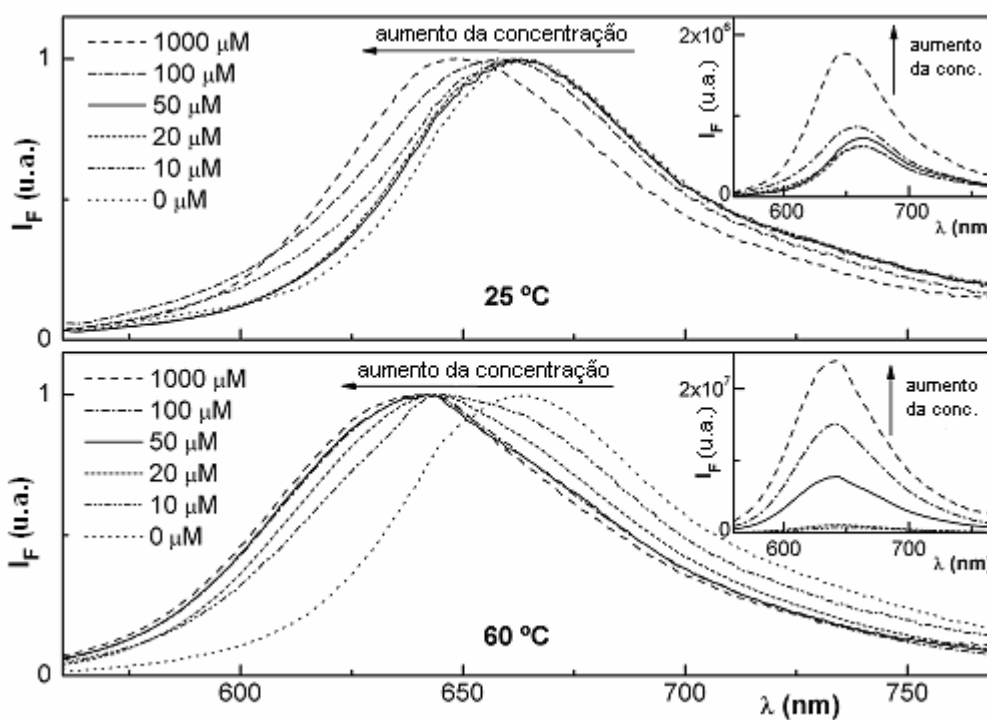


Figura 9 – Espectros de fluorescência normalizados ($\lambda_{exc} = 550$ nm) de 5×10^{-7} M NR nos sistemas DODAB/água para várias concentrações de DODAB, a 25 e 60 °C. O espectro normalizado de NR em água é mostrado para comparação. Figura inserida: Espectros de fluorescência correspondentes não-normalizados de NR dos sistemas DODAB/água.

De acordo com a figura, um deslocamento para o azul na emissão máxima foi observado com o aumento da concentração de DODAB (artigo 1) em relação aos espectros da água, indicando que a sonda sente um meio menos hidratado (mais hidrofóbico), indicando a presença de agregados. Verificou-se também um aumento na intensidade de fluorescência com o aumento da concentração de surfactante (Figuras 9 inserida), sugerindo que em baixas concentrações, a sonda está mais exposta à água, devido ao fato de nem todas as sondas serem acomodadas no interior (bicamada) das vesículas. Comportamento semelhante foi observado para DODAC (ver Figura 5 do artigo 1).

3. Efeito do contra-íon

O contra-íon do surfactante é de grande importância no comportamento termotrópico de vesículas iônicas em geral, e das vesículas catiônicas em particular. Na ausência de sais inorgânicos, como NaBr ou NaCl, a T_m é maior para as vesículas de DODAC do que para DODAB (FEITOSA et al., 2000, FEITOSA e BARRELEIRO, 2004), provavelmente devido à afinidade específica dos contra-íons na interface das vesículas, e o raio hidrodinâmico (R_H) aparente das vesículas de DODAB é maior do que as de DODAC (FEITOSA et al., 2006d). Além do mais, NaCl aumenta, enquanto NaBr diminui a T_m de DODAB em dispersões aquosas de vesículas preparadas espontaneamente, ou seja, na presença de NaCl, as vesículas de DODAB se assemelham às de DODAC (FEITOSA e BARRELEIRO, 2004).

Nascimento e colaboradores (1998) estudaram o efeito de contra-íons na T_m e no tamanho das vesículas de haleto de dioctadecildimetilamônio e observaram que contra-íons menos hidratados produzem bicamadas menos rígidas com valores de T_m menores. Assim, o contra-íon Cl^- , mais hidratado, gera uma interação eletrostática repulsiva mais forte entre os grupos polares adjacentes nas dispersões de DODAC, tornando assim, as bicamadas das vesículas mais rígidas em relação a DODAB. Esses autores verificaram também que repulsões eletrostáticas mais fracas entre os monômeros adjacentes na bicamada, contendo Br^- como contra-íon, formam vesículas maiores.

Cavalli et al. (2001) investigaram monocamadas de DODAB em água através de medidas de pressão de superfície com os contra-íons monovalentes F^- , Cl^- , Br^- , I^- e OH^- , mostrando que as monocamadas de DODAB são mais expandidas quando a eletronegatividade do contra-íon aumenta, ou seja, mais expandida para F^- e menos expandida para I^- na subfase.

Apesar das informações existentes sobre a influência do contra-íon nas propriedades de mono e bicamadas de DODAX, o efeito de Br^- e Cl^- nas propriedades dessas vesículas

ainda não foi satisfatoriamente esclarecido. Resultados obtidos através de DSC da mistura de vesículas de DODAB e DODAC em solução aquosa (artigo 2) mostraram que a adição de Cl^- às vesículas de DODAB inibe completamente a pós-transição ($T_p \approx 51,5 \text{ }^\circ\text{C}$), enquanto a pré-transição desaparece quando $x_{\text{DODAC}} > 0.25$ e diminui de $T_s = 33.5$ para $31.6 \text{ }^\circ\text{C}$ (Figura 10). O aumento da quantidade relativa de Cl^- aumenta a T_m de DODAB de $45,8$ para $48,9 \text{ }^\circ\text{C}$, ou seja, os valores da T_m estão entre as temperaturas de transição das vesículas puras de DODAB e DODAC (Figura 11).

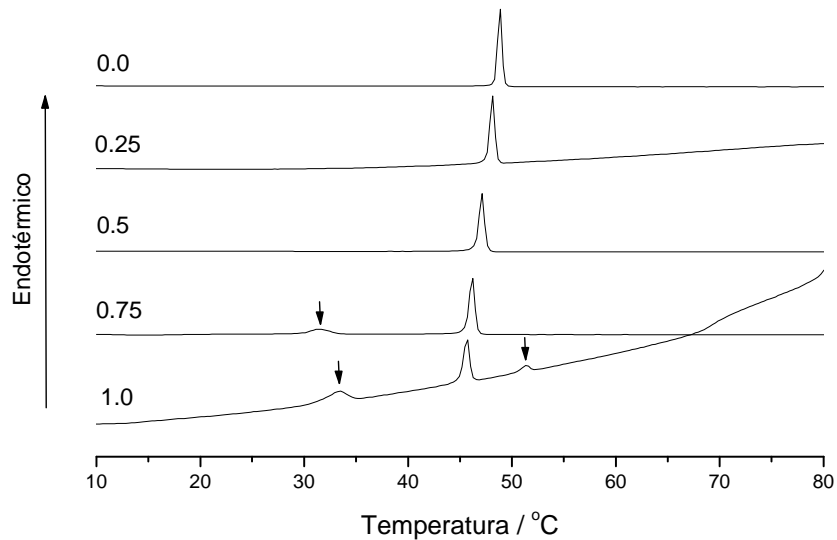


Figura 10 - Curvas de DSC das vesículas de DODAB e DODAC em solução aquosa, para 1,0 mM de concentração total de surfactantes. Os números referem-se à concentração de DODAB em mM, e as setas indicam os picos da pré- e pós-transição.

A T_m maior das vesículas de DODAC em relação a DODAB não pode ser justificado somente pelo tamanho das vesículas, já que, as vesículas de DODAB são maiores do que as de DODAC (Nascimento et al., 1998; FEITOSA et al., 2006d). Além disso, a T_m e o tamanho das vesículas tendem a aumentar com o comprimento das cadeias de hidrocarbonetos (FEITOSA et al., 2006c). Como os dois surfactantes diferem somente pela natureza dos

contra-íons, Br^- e Cl^- , a especificidade na ligação dos contra-íons na interface das vesículas de DODAX deve ser o fator principal para a T_m de DODAC ser maior. Portanto, o efeito de Br^- e Cl^- na T_m de misturas DODAB-DODAC deve estar relacionado não somente ao tamanho e a compactação da bicamada das vesículas, mas também ao efeito dos contra-íons na estrutura formada, já que DODAB tende a formar vesículas multiestruturais em concentrações menores de surfactante do que DODAC (FEITOSA et al., 2006d).

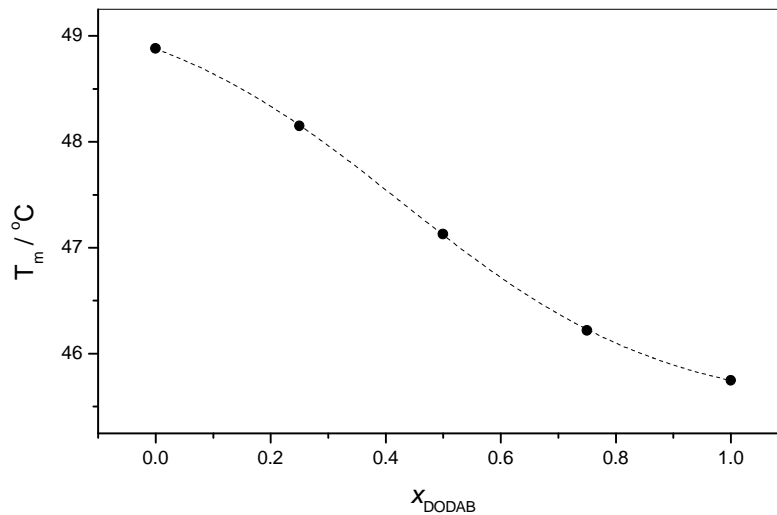


Figura 11 – Efeito da concentração de DODAB e DODAC na T_m da mistura DODAB-DODAC em água, para 1,0 mM de concentração total de surfactante.

4. Efeito de co-surfactante

4.1. Sistema DDAB/DODAB/água

Co-surfactantes podem ter grande efeito nas propriedades das vesículas devido à sua solubilização na bicamada das vesículas, afetando, portanto, o comportamento termotrópico, que pode ser monitorado por DSC, espalhamento de luz, turbidez e fluorescência. Recentemente, reportamos a formação de vesículas em misturas de DODAB-DDAB em solução aquosa (artigo 3). Apesar da semelhança estrutural desses dois surfactantes, que diferem somente no comprimento das caudas, têm pouca afinidade entre si e se misturam muito pouco em solução, formando duas populações de vesículas com diferentes valores de T_m , sendo uma rica em DDAB e a outra rica em DODAB (FEITOSA et al., 2006a).

A fim de entender esse sistema misto, investigamos as vesículas de DODAB e DDAB 1,0 mM separadamente; nas primeiras, $T_m \approx 43$ °C, $T_s \approx 33,2$ °C e $T_p \approx 53$ °C. Na presença de pequena quantidade de DDAB, a T_p , mas não T_s , de DODAB desaparece. Aumentando a concentração de DDAB, T_m diminui, e os picos correspondentes à T_m e T_s se sobrepõem, resultando, portanto, num pico largo (Figura 12). A posição dos picos centrados em $T_{m(1)} \approx 16$ °C e $T_{m(2)} \approx 43$ °C indicam as transições de estado gel para líquido-cristalino para as dispersões de DDAB e DODAB, respectivamente.

De acordo com a Figura 13, pôde-se observar que a adição de DODAB mantém a $T_{m(1)}$ aproximadamente constante e igual à T_m de DDAB puro ($\approx 15,6$ °C), mostrando que DODAB não afeta a T_m de DDAB até $x_{DODAB} \approx 0,8$. Quando $x_{DODAB} > 0,2$, um segundo pico aparece ao redor de 30 °C, correspondente à temperatura de transição maior, $T_{m(2)}$. Aumentando x_{DODAB} , $T_{m(2)}$ aumenta linearmente até atingir a T_m de DODAB puro ($\approx 42,8$ °C). Estes resultados indicam que a incorporação de DDAB nas vesículas de DODAB resulta numa maior fluidez da bicamada de DODAB com o aumento de x_{DDAB} , levando a um

decréscimo na $T_{m(2)}$ de DODAB. Por outro lado, monômeros de DODAB interagem muito pouco com as vesículas de DDAB, mantendo, portanto, a $T_{m(1)}$ de DDAB constante.

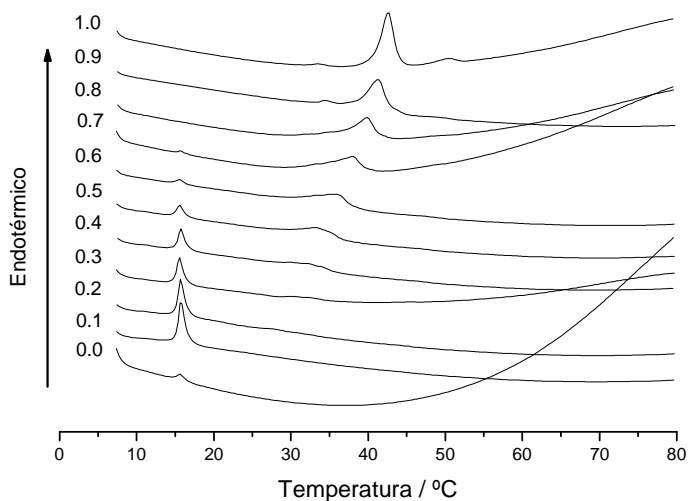


Figura 12 – Curvas de DSC de aquecimento de DODAB e DDAB em água e da mistura DODAB/DDAB para 1mM de concentração total de surfactante.

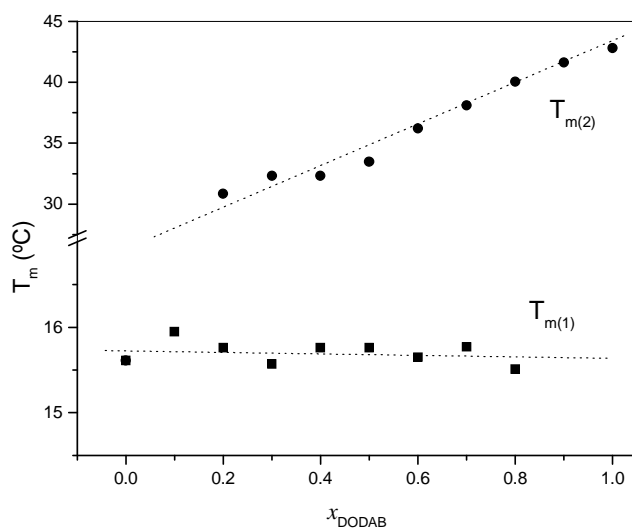


Figura 13 – Efeito da fração molar de DODAB ou DDAB na T_m da mistura DODAB/DDAB/água, para 1,0 mM de concentração total de surfactantes. Dados obtidos do primeiro DSC de aquecimento.

O efeito de x_{DODAB} na turbidez da mistura DODAB/DDAB em água, e 1,0 mM de concentração total de surfactantes, é mostrado na Figura 14. Com o aumento da fração molar de DODAB a turbidez aumenta suavemente até $x_{\text{DODAB}} \approx 0,9$ e, em seguida, aumenta rapidamente até atingir o valor para DODAB 1,0 mM, indicando uma variação de tamanho ou estrutura das vesículas. Estudos anteriores mostraram que o raio hidrodinâmico (R_H) das vesículas espontâneas de DDAB e DODAB têm $R_H \approx 350 \text{ \AA}$ (MARQUES et al., 1999) e 3370 \AA (FEITOSA et al., 2006d), respectivamente. Depois de sonicadas a banho, as vesículas de DODAB apresentaram R_H de 220 \AA (FEITOSA e BROWN, 1997) ou 325 \AA , depois de sonicadas com ponta de titânio (CUCCOVIA et al., 1990).

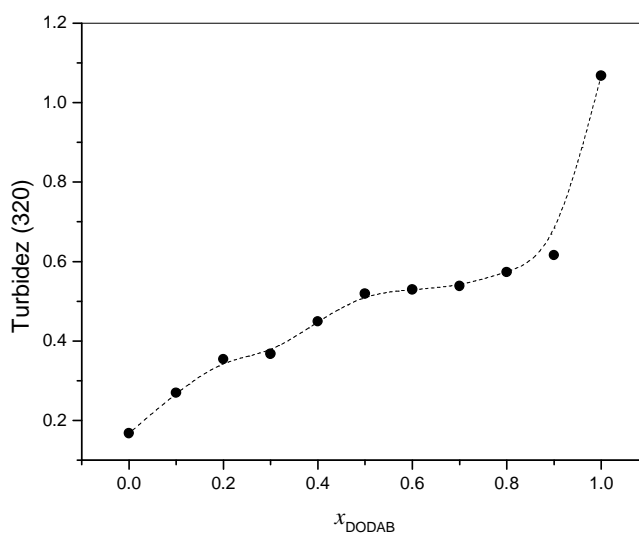


Figura 14 – Efeito da fração molar de DODAB na Turbidez (320 nm) para a mistura DODAB/DDAB/água a 1,0 mM de concentração total de surfactantes e $22 \text{ }^\circ\text{C}$.

A Figura 15 mostra o efeito da temperatura na intensidade de fluorescência total de NR nas vesículas de DODAB e DDAB e mistas de DODAB/DDAB para várias frações molares de DODAB. Para $x_{\text{DODAB}} = 1$, observou-se um máximo ao redor de $45 \text{ }^\circ\text{C}$ (região da

T_m de DODAB). Comportamento semelhante, mas não tão nítido, foi observado para quantidades maiores de DODAB ($x_{\text{DODAB}} > 0,5$), com um máximo ao redor de 40 °C. Para quantidades maiores de DDAB ($x_{\text{DODAB}} \leq 0,6$) verificou-se uma emissão máxima entre 10 e 15 °C, indicando a presença de vesículas de DDAB praticamente sem DODAB, como sugerido por DSC (Figura 12). Verificou-se também que acima de 15 °C e $x_{\text{DODAB}} \leq 0,4$, a intensidade diminui com a temperatura, mostrando que os sistemas ricos em DDAB estão principalmente no estado líquido-cristalino. Porém os sistemas ricos em DODAB ($x_{\text{DODAB}} \geq 0,6$) estão predominantemente no estado gel até aproximadamente 35 °C, ou seja, um máximo foi observado em 40 °C para $x_{\text{DODAB}} = 0,75$, e entre 35 e 40 °C para $x_{\text{DODAB}} = 0,6$.

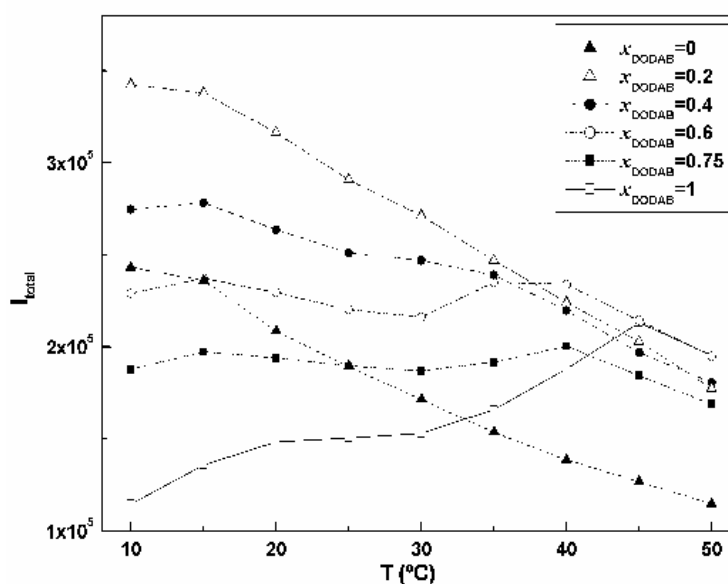


Figura 15 – Variação da intensidade de fluorescência total de NR nas vesículas de DODAB e DDAB e mistas de DODAB/DDAB com o aumento da temperatura para várias frações molares de DODAB.

4.2. Sistema $C_{18}TAB/DODAB/água$

A interação entre os surfactantes catiônicos DODAB e $C_{18}TAB$ (artigo 4) foi estudada a fim de obter informações sobre o comportamento termotrópico dos agregados mistos e o mecanismo de transição vesícula-micela nesse sistema (ALVES et al., 2007).

Como mencionado anteriormente, em regime diluído, DODAB e $C_{18}TAB$ formam vesículas e micelas, respectivamente. Com a mistura desses surfactantes, vesículas e/ou micelas mistas podem ser formadas, dependendo da concentração relativa desses surfactantes. Acima da CMC de $C_{18}TAB$ ($\approx 0,34$ mM, 40 °C) e 25 °C (abaixo da temperatura de Krafft, $T_K \approx 38$ °C) (SWANSON-VETHAMUTHU et al., 1998), $C_{18}TAB$ em solução aquosa precipita como cristais hidratados (*HC*), depois de aproximadamente 24 horas pós-preparo da amostra. O diagrama de fase do sistema $C_{18}TAB/DODAB/$ água para $1,0$ mM de concentração total de surfactante e 25 °C é mostrado na Figura 16. Esse diagrama foi construído preparando-se amostras em concentrações relativas desses surfactantes entre 0 e 1,0 e mantendo as mesmas à temperatura ambiente (25 °C) por meses, antes do diagrama de fases ser definido. Inicialmente todas as amostras eram homogêneas e a formação de cristais foi verificada periodicamente através de observação visual das amostras. Através do diagrama observa-se que até $x_{DODAB} = 0,25$ ($x_{C_{18}TAB} > 0,75$) a dispersão é rica em micelas de $C_{18}TAB$ e existem cristais precipitados em equilíbrio com vesículas mistas ($L_1 + HC$). Para $x_{DODAB} > 0,25$, a dispersão é azulada e rica em vesículas de DODAB (L_1), com algumas moléculas de $C_{18}TAB$ incorporadas na bicamada das vesículas ou livres em solução como monômeros. Provavelmente, os surfactantes de $C_{18}TAB$ que não estão ligados aos agregados precipitam como *HC*.

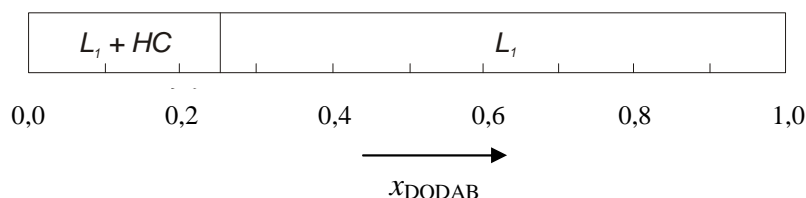


Figura 16 – Diagrama de fase para a mistura DODAB/ $C_{18}TAB/$ água, para $1,0$ mM de concentração total de surfactante e 25 °C.

O mesmo comportamento foi observado para 5,0 mM de concentração total de surfactante desta mistura. A T_K de $C_{18}TAB$ em água foi obtida por aquecimento da amostra e verificação da temperatura na qual os cristais desaparecem, e também por DSC. Em ambos os casos obtivemos $T_K = 37$ °C. Interessante é que na presença de DODAB o valor da T_K não foi alterado, indicando que a presença das vesículas não afeta a formação de cristais de $C_{18}TAB$.

A Figura 17 mostra curvas de DSC da mistura DODAB/ $C_{18}TAB$ em solução aquosa 1,0 mM de concentração total de surfactante. A pré-transição, $T_s \approx 33,3$ °C, presente na curva de DODAB ($x_{DODAB} = 1,0$) desaparece em pequena quantidade de $C_{18}TAB$ ($x_{C_{18}TAB} = 0,1$). O pico relacionado à $T_m \approx 42,5$ °C de DODAB em água desloca-se para temperaturas ligeiramente maiores com o aumento de $x_{C_{18}TAB}$ até aproximadamente 0,3, quando um novo pico sobreposto aparece com temperatura um pouco mais elevada. Com um aumento de $C_{18}TAB$, a intensidade do pico da T_m diminui enquanto a intensidade do pico adicional aumenta. Quando $x_{DODAB} \approx 0,5$, o pico da T_m de DODAB desaparece, indicando a presença de vesículas mistas dominadas por moléculas de $C_{18}TAB$ com valores de T_m maiores.

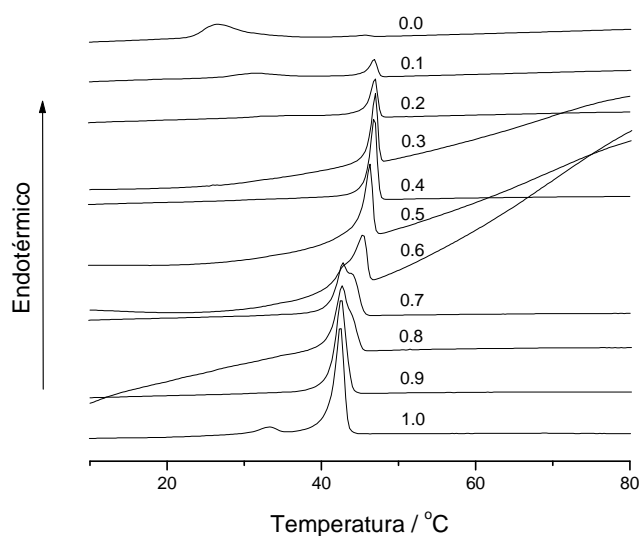


Figura 17 – Curvas de DSC da mistura DODAB/ $C_{18}TAB$ em solução aquosa para 1,0 mM de concentração total de surfactante. Os números indicam a fração molar de DODAB, x_{DODAB} .

O efeito da concentração de C₁₈TAB na T_m de DODAB é do tipo “sino”, ou seja, inicialmente aumenta e depois diminui para valores maiores que as vesículas de DODAB 1,0 mM em água (Figura 18). Até $x_{C_{18}TAB} \approx 0,3$, a T_m aumenta ligeiramente, indicando que monômeros de C₁₈TAB são incorporados na bicamada das vesículas de DODAB até formar vesículas mistas de DODAB-C₁₈TAB. Com o aumento da concentração de C₁₈TAB ($x_{C_{18}TAB} \geq 0,3$), observou-se um pronunciado aumento na T_m até $x_{DODAB} \approx 0,3$ ($x_{C_{18}TAB} \approx 0,7$), quando T_m ≈ 47 °C, relacionada ao pico adicional da curva de DSC sobreposto ao pico original. Aumentando ainda mais a concentração de C₁₈TAB, a T_m é mantida aproximadamente constante, indicando que monômeros de C₁₈TAB não são mais solubilizados na bicamada das vesículas e micelas mistas de DODAB-C₁₈TAB são formadas. O valor obtido da T_m para C₁₈TAB 1,0 mM pode estar relacionado à formação de bicamadas (SWANSON-VETHAMUTHU et al., 1998) que, na presença de DODAB, origina vesículas cuja T_m varia de acordo com a curva superior mostrada na Figura 18.

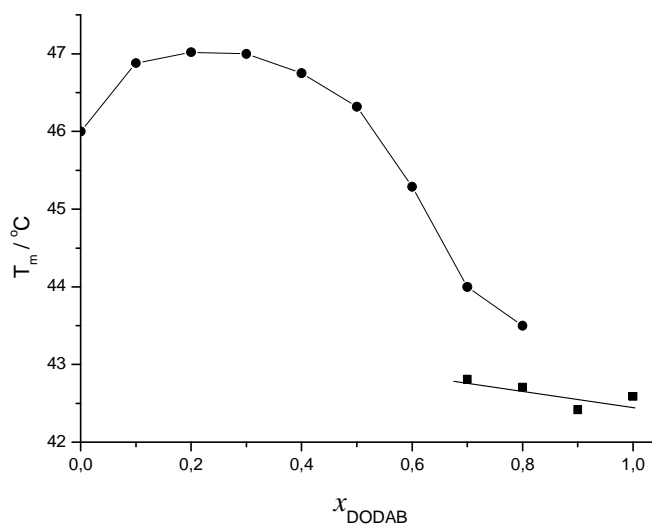


Figura 18 – Efeito da fração molar de DODAB (ou C₁₈TAB) na T_m para a mistura DODAB/C₁₈TAB/água, 1,0 mM de concentração total de surfactante.

A Figura 19 mostra a variação do raio hidrodinâmico aparente (R_H) dos agregados no sistema DODAB/ C_{18} TAB/água para 0,5 mM de concentração total de surfactante em função da fração molar de DODAB. Com a adição de C_{18} TAB R_H aumenta até atingir um valor máximo de $R_H \approx 820$ nm quando $x_{\text{DODAB}} \approx 0,3$, e em seguida, diminui para o valor de R_H correspondente às micelas de C_{18} TAB ($R_H \approx 180$ nm). O crescimento das vesículas deve ser atribuído à incorporação de C_{18} TAB na bicamada de DODAB favorecendo assim, a formação de vesículas maiores. O valor máximo de R_H observado em $x_{\text{DODAB}} \approx 0,3$ indica o início de formação de micelas devido à desestabilização da bicamada das vesículas. Acima deste ponto ($x_{\text{DODAB}} < 0,3$), observou-se o predomínio de micelas mistas no sistema, com tamanho médio menor.

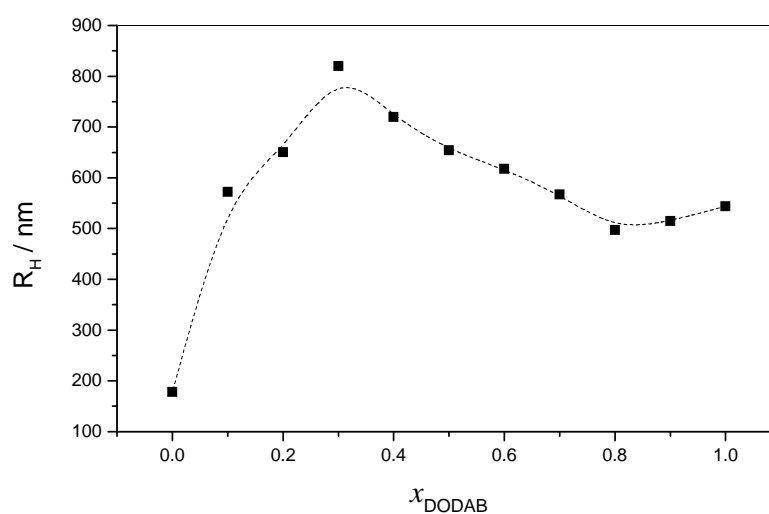


Figura 19 – Efeito da fração molar de DODAB (ou C_{18} TAB) no raio hidrodinâmico aparente, R_H , para a mistura DODAB/ C_{18} TAB/água a 0,5 mM de concentração total de surfactantes. Os dados foram coletados a 25 °C.

Feitosa e colaboradores (2006b) mostraram que a adição de surfactantes não iônicos derivados do polióxido de etileno, PEO, ($C_{12}E_n$, $n = 5, 7$ e 8) e zwitteriônico 3-(N-hexadecil-

N,N-dimetilamônio)propano sulfonato (HPS) às vesículas de DODAB e DODAC diminui a T_m , e induz transição vesícula-micela. Além disso, observaram que a solubilidade das vesículas de DODAX é mais forte na presença de $C_{12}E_n$ do que HPS, ou seja, a região polar do surfactante desempenha importante papel na interação com vesículas catiônicas.

Surfactantes aniônicos e catiônicos também modificam a T_m das vesículas de DODAX. Sulfato dodecil de sódio, SDS, aumenta, mas colato de sódio, NaC, diminui a T_m de DODAB e DODAC, respectivamente (COCQUYT et al., 2004; ALVES e FEITOSA, 2006). A adição de SDS às vesículas de DODAB induz a fusão de vesículas, com posterior formação de micelas, enquanto a adição de NaC as vesículas de DODAB induz à transição vesícula-micela-agregado, sendo a transição vesícula-micela lenta e a micela-agregado muito rápida. Esses agregados são, provavelmente, micelas planas grandes, devido ao aspecto turvo da solução. C_n TAB ($n = 12-18$) pode aumentar, diminuir ou manter constante a T_m de DODAB, dependendo do comprimento da cadeia destes surfactantes, conforme observado por Kacperska e colaboradores (1995) e confirmado pelo nosso trabalho.

A Figura 20 mostra os espectros de emissão de fluorescência da sonda NR incorporada a misturas DODAB/ C_{18} TAB/água, 25 °C. Observou-se que o espectro de fluorescência aumenta com a redução da quantidade de DODAB, e o espectro de emissão mais baixo observado para DODAB em água ($x_{DODAB} = 1$) indica que a sonda está em meio mais rico em água na bicamada de DODAB, provavelmente devido ao fato que em temperatura ambiente (abaixo da $T_m \approx 42,5$ °C) as bicamadas das vesículas estão na fase gel, dificultando, portanto, a sonda penetrar mais profundamente na bicamada das vesículas. Observou-se também que quando x_{DODAB} diminui, a intensidade de fluorescência aumenta monotonicamente, indicando que a sonda fica menos exposta a água nos agregados mistos, que pode ser explicado pela formação de estruturas maiores devido à incorporação de C_{18} TAB na bicamada de DODAB, como mostrado por dados de DLS na Figura 19. A maior intensidade de fluorescência para

quantidades maiores de $C_{18}TAB$ ($x_{DODAB} < 0,3$) pode ser justificada pelo aumento da quantidade de micelas mistas formadas, onde a sonda sente um meio mais fluído (menos viscoso), devendo alcançar uma penetração mais profunda.

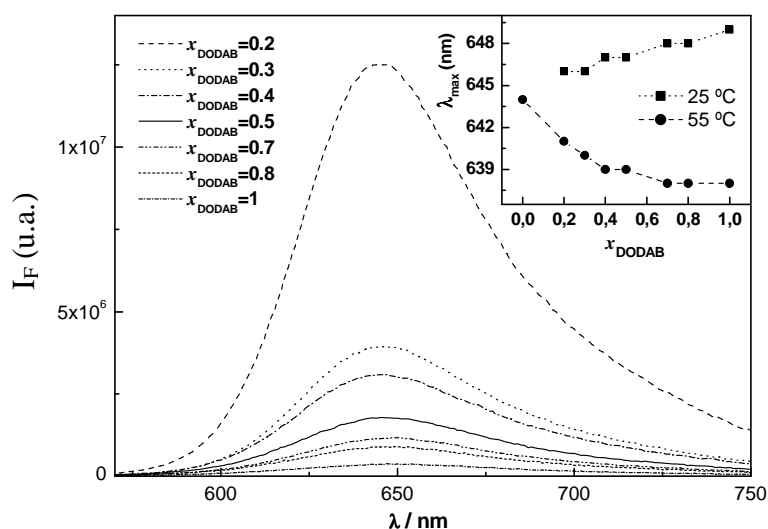


Figura 20 – Espectros de fluorescência de NR nos sistemas mistos DODAB/ $C_{18}TAB$ /água para várias frações molares de DODAB a 25 °C. Figura inserida: Comprimento de onda de máxima emissão de NR nos sistemas mistos DODAB/ $C_{18}TAB$ /água abaixo (25 °C) e acima (55 °C) da T_m , em função de x_{DODAB} .

A variação do comprimento de onda de máxima emissão (λ_{max}) de NR com o aumento da quantidade de DODAB (Figura 20 inserida) mostra a mesma tendência. A 25 °C, no estado gel, λ_{max} diminui com o aumento de $x_{C_{18}TAB}$, indicando um aumento da hidrofobicidade do meio local onde a sonda se encontra. Um comportamento oposto de λ_{max} é observado a 55 °C (acima da T_m), no estado líquido-cristalino, mostrando que a sonda sente um meio mais hidrofóbico em quantidades maiores de DODAB.

4.3. Sistemas C_n TAB/DODAB/água ($n = 12, 14, 16$ e 18)

Depois de estudar o comportamento termotrópico das vesículas de DODAB e caracterizar as diferentes fases da mistura C_{18} TAB-DODAB em água e 1 mM de concentração total de surfactantes (artigo 4), estudos também foram feitos da interação DODAB- C_n TAB ($n = 12, 14, 16$ e 18), para 1,0 e 5,0 mM (artigo 5) de concentração total de surfactante, a fim de investigar o efeito do comprimento da cadeia de hidrocarbonetos de C_n TAB no comportamento termotrópico das vesículas de DODAB, e o mecanismo de interação entre os surfactantes em diferentes concentrações. Investigou-se também misturas de C_n TAB-DODAB ($n = 12-18$) variando a concentração de C_n TAB, com a concentração de DODAB mantida constante a 1,0 mM (artigo 6), de modo que os surfactantes estejam acima e abaixo da CMC. Este estudo possibilitou a análise do comportamento termotrópico das vesículas contendo diferentes quantidades de DODAB e a possível transição vesícula-micela com o aumento da quantidade de C_n TAB. Em geral, C_{12} TAB e C_{14} TAB não interagem muito com as vesículas de DODAB nas misturas contendo 1,0 mM de surfactante, e do mesmo modo, C_{12} TAB em 5,0 mM de concentração total, que pode estar associado à baixa concentração deste surfactante, abaixo da CMC, contendo apenas monômeros, além da maior diferença do comprimento das caudas em relação a DODAB. Assim, o comprimento das cadeias e a fração relativa dos surfactantes na bicamada das vesículas podem influenciar as propriedades, estrutura e tamanho dos agregados formados.

Os valores obtidos da T_m das misturas DODAB- C_n TAB-água, para 1,0 e 5,0 mM de concentração total de surfactante, em função da fração molar de C_n TAB são mostrados na Figura 21. Verificou-se que ao adicionar C_n TAB às vesículas de DODAB, Figura 21(a), até $x_{C_nTAB} \approx 0,2$, a T_m é mantida aproximadamente constante. Com o aumento da quantidade de C_{16} TAB ($x_{C_{16}TAB} > 0,2$), a T_m desloca-se para temperaturas menores, aumentando, portanto, a fluidez da bicamada das vesículas no estado gel. Por outro lado, C_{12} TAB e C_{14} TAB não

afetam a T_m de DODAB, indicando fraca interação entre esses monômeros e as vesículas de DODAB.

Ao aumentar a concentração total de surfactante para 5,0 mM, Figura 21(b), observou-se que até $x_{C_nTAB} \approx 0,1$, a T_m não é afetada por C_nTAB . Com o aumento da quantidade de C_nTAB , até $x_{C_nTAB} \approx 0,6$, $C_{18}TAB$ aumenta a T_m de DODAB até atingir um valor máximo de 47, 2 °C, enquanto que $C_{14}TAB$ e $C_{16}TAB$ diminuem a T_m , com efeito ligeiramente maior para $C_{16}TAB$. Para $x_{DODAB} < 0,4$ ($x_{C_nTAB} > 0,6$), $C_{18}TAB$ diminui a T_m para valores maiores que DODAB 5,0 mM em água. $C_{14}TAB$ e $C_{16}TAB$ diminuem a T_m , com um efeito maior de $C_{14}TAB$. Porém, $C_{12}TAB$ não afeta a T_m de DODAB, conforme já observado anteriormente para a concentração total de surfactante igual a 1,0 mM. O motivo desta fraca interação pode estar associado à baixa concentração de $C_{12}TAB$ em solução a 1,0 e 5,0 mM, estando abaixo da CMC, além da maior diferença do comprimento da cadeia de hidrocarbonetos em relação a DODAB, indicando pequena afinidade.

Ao comparar as misturas de $C_{16}TAB$ -DODAB para 1,0 e 5,0 mM de concentração total de surfactante, Figuras 21(a) e (b), verifica-se que a adição de $C_{16}TAB$ às vesículas de DODAB diminui a T_m , mas o efeito é mais pronunciado para o sistema mais concentrado. Para as misturas contendo $C_{18}TAB$, a T_m variou aproximadamente na mesma ordem de grandeza. Como a T_m é influenciada por perturbações causadas por moléculas de C_nTAB solubilizadas na bicamada das vesículas, o efeito da concentração de $C_{18}TAB$ na T_m de DODAB do tipo “sino” indica que a bicamada da mistura DODAB- $C_{18}TAB$ é mais densamente empacotada do que DODAB em água. Por outro lado, na presença de $C_{14}TAB$ e $C_{16}TAB$, as bicamadas são mais maleáveis e menos organizadas, diminuindo, portanto, a T_m . $C_{12}TAB$ não afeta muito a T_m , pois a concentração está abaixo da CMC e os monômeros de $C_{12}TAB$ solubilizados na bicamada não são suficientes para afetar as propriedades das vesículas. Portanto, de acordo com os resultados, além do comprimento da cadeia de

hidrocarbonetos, a fração relativa dos surfactantes e o fato do surfactante estar na forma de monômeros ou agregados, podem influenciar a T_m .

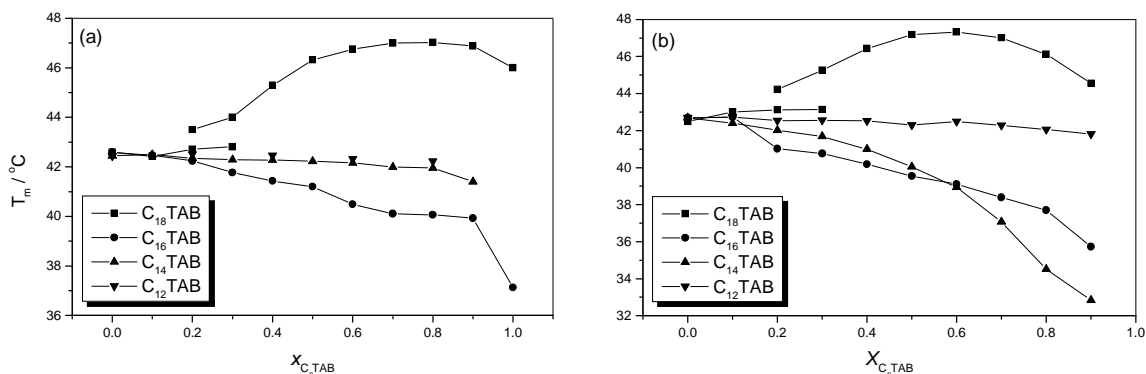


Figura 21 – Efeito da fração molar de DODAB (ou C_n TAB) na T_m para a mistura DODAB/ C_n TAB/água (a) 1,0 mM e (b) 5,0 mM de concentração total de surfactante.

A Figura 22 mostra a variação da T_m em função da concentração de C_n TAB para a mistura DODAB/ C_n TAB/água mantida constante a concentração de DODAB em 1,0 mM. A T_m aumenta até atingir um valor máximo de 47 °C para 2,0 mM de C_{18} TAB e diminui para valores menores que DODAB (1,0 mM) em água, tendendo ao valor da T_m de C_{18} TAB em água. Por outro lado, a adição C_{12} TAB, C_{14} TAB e C_{16} TAB diminuem a T_m de DODAB. Em todos os casos, as vesículas de DODAB são totalmente solubilizadas por C_n TAB formando micelas mistas, devido ao desaparecimento da T_m em concentrações relativamente altas de C_n TAB. Estes dados sugerem, portanto, que a T_m do sistema C_n TAB-DODAB em água (como consequência da alteração do empacotamento das cadeias da bicamada) e o mecanismo de transição estrutural, apresenta uma significativa dependência em relação ao comprimento da cadeia de hidrocarbonetos e da concentração relativa de cada surfactante.

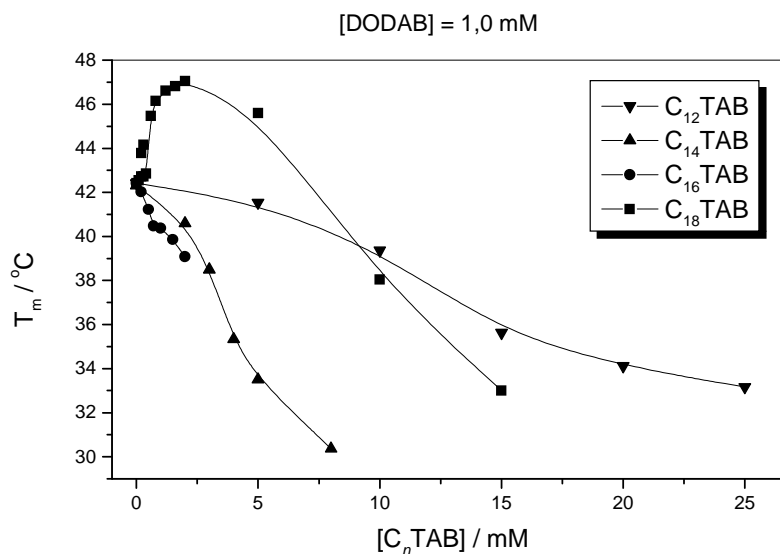


Figura 22 – Efeito da concentração de C_n TAB na T_m da mistura DODAB/ C_n TAB/água, para 1,0 mM de DODAB. O ponto correspondente a 15 mM corresponde à T_m de C_{18} TAB em água.

A variação da turbidez da mistura DODAB- C_n TAB em água em função da concentração de C_n TAB, para 1,0 mM de DODAB, é mostrada na Figura 23. Quando C_n TAB é adicionado às vesículas de DODAB, a turbidez aumenta inicialmente até atingir um valor máximo, devido à incorporação de C_n TAB na bicamada das vesículas de DODAB, formando vesículas mistas maiores. Quando a bicamada é saturada pelo surfactante, as vesículas são rompidas iniciando o processo de solubilização de DODAB pelas micelas então formadas, diminuindo a turbidez da amostra, até as vesículas serem completamente solubilizadas pelas micelas, como sugerido por medidas de DSC (Figura 22). A turbidez alcança o patamar mais elevado nas concentrações de surfactantes $[C_n$ TAB] = 5,0, 1,0, 1,5 e 0,8 mM para $n = 12, 14, 16$ e 18 , respectivamente. Com o aumento da concentração de C_n TAB, a turbidez diminui progressivamente, indicando que agregados menores são formados nas misturas, provavelmente micelas e vesículas mistas coexistindo em solução, nessa região intermediária. Aumentando mais a concentração de surfactante, a turbidez não é mais afetada pela adição de

C_n TAB, mantendo-se em seu valor mínimo, indicando que apenas micelas mistas de C_n TAB-DODAB estão presentes em solução. De acordo com os resultados, as variações na T_m e o mecanismo de transição vesícula-micela ocorridos nas misturas não estão relacionados somente com o grau de afinidade de C_n TAB pelas vesículas de DODAB, mas também com o tamanho da cauda do surfactante. De acordo com esses resultados, o efeito do comprimento da cauda de C_n TAB na completa transição vesícula-micela obedece a seguinte ordem $n = 18 > 16 > 14 > 12$, indicando que a afinidade de C_n TAB pelas vesículas de DODAB aumenta, como se espera, com o tamanho da cauda e ocorre em três etapas: formação de vesículas mistas (etapa I), formação de micelas e vesículas (etapa II) e formação de micelas (etapa III).

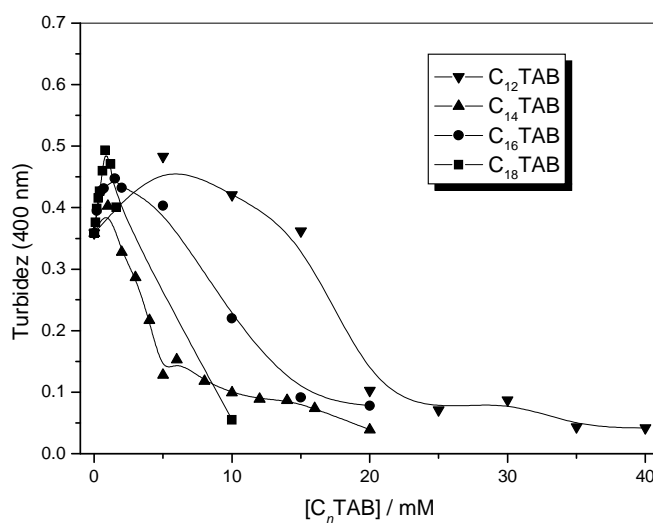


Figura 23 – Efeito da concentração de C_n TAB na turbidez para a mistura DODAB/ C_n TAB/água a 1,0 mM de DODAB.

Apesar dos estudos feitos das vesículas de DODAX, alguns aspectos físico-químicos dessas vesículas ainda não estão completamente esclarecidos. Por exemplo, no que diz

respeito ao efeito de co-solutos e co-surfactantes na estrutura e estabilidade dessas vesículas ainda tem muito para ser explorado, além das propriedades das microvesículas.

Embora DSC seja um dos métodos essenciais para medir a T_m , outras técnicas dão informações complementares do comportamento termotrópico das vesículas de DODAX. Além de DSC, utilizamos fluorescência de estado estacionário, espalhamento de luz, condutividade e tensão superficial para investigar o comportamento termotrópico das misturas DODAB-DODAC e DODAB-DDAB em água, e também o efeito do comprimento da cauda de C_n TAB ($n = 12, 14, 16$ e 18) nas propriedades termotrópicas das vesículas de DODAB e o mecanismo de interação entre os surfactantes. Estes surfactantes têm grupo de cabeça polar semelhante a DODAB (amônia quaternária), porém com um grupo metila a mais no lugar de uma das caudas (o que confere uma região ligeiramente maior do grupo polar de C_{18} TAB), mas diferem um do outro no comprimento e no número de caudas. Este estudo visa, portanto, um melhor entendimento das propriedades de vesículas catiônicas para aplicação em diferentes áreas de pesquisa.

5. Considerações finais

Dentre os resultados obtidos, destacamos os seguintes:

➤ Microvesículas de DODAB e DODAC podem ser formadas em concentrações tão baixas quanto 10 μM , cuja T_m diminui monotonicamente com o aumento da concentração de surfactantes. Essas microvesículas são, muito provavelmente, unilamelares grandes e estáveis em relação às vesículas tradicionais preparadas em 1 mM de DODAX. Outra diferença consiste no aspecto azulado das dispersões de vesículas e transparente das microvesículas.

➤ A T_m das vesículas mistas de DODAB-DODAC em solução aquosa aumenta sigmoidalmente com x_{DODAC} , com um ponto de inflexão ao redor do ponto equimolar, e os valores obtidos da T_m estão entre os valores dos surfactantes puros. A condutividade, assim como o diâmetro das vesículas não variou com a fração molar do surfactante. Considerando que os surfactantes se diferem somente pelos contra-íons, a especificidade dos contra-íons na interface das vesículas desempenha um papel importante no comportamento termotrópico dessas vesículas mistas.

➤ Estudos do comportamento termotrópico do sistema DODAB/DDAB/água revelaram a existência de duas populações de vesículas de DODAB e DDAB que coexistem, com propriedades distintas, dependendo da composição do surfactante. Os resultados apresentados mostraram maior afinidade das vesículas de DODAB por DDAB do que o oposto.

➤ Resultados de DSC do sistema DODAB/ $C_{18}\text{TAB}$ /água a uma concentração total de 1,0 e 5,0 mM de surfactante mostraram que o efeito da concentração de $C_{18}\text{TAB}$ na T_m de DODAB é do tipo “sino”, ou seja, inicialmente aumenta e depois diminui para valores ainda maiores do que DODAB em água, indicando que o estado conformacional das cadeias de hidrocarbonetos vem a ser mais rígido e ordenado.

➤ O estudo dos sistemas DODAB/ $C_n\text{TAB}$ /água, para 1,0 e 5,0 mM de concentração total de surfactantes, e variando a concentração de $C_n\text{TAB}$ mas mantendo a concentração de

DODAB fixa em 1,0 mM mostrou uma forte dependência do comprimento da cadeia de hidrocarbonetos n e da concentração individual de cada surfactante nas propriedades das vesículas mistas de DODAB- C_n TAB. Ao realizar este estudo foi possível analisar o comportamento termotrópico das vesículas de DODAB e o mecanismo de transição vesícula-micela com o aumento da concentração de C_n TAB, acima ou abaixo da CMC. Quanto maior n mais forte é a interação de C_n TAB com as vesículas de DODAB e a T_m pode ser menor, igual ou maior que a T_m de DODAB em água. Para os sistemas DODAB/ C_n TAB/água, para 1,0 e 5,0 mM de concentração total de surfactante, mesmo em concentrações mais elevadas de C_n TAB, vesículas mistas estão presentes em solução.

Com base nessas conclusões, observamos que a mistura de surfactantes catiônicos com uma ou duas cadeias de hidrocarbonetos ainda é um campo de pesquisa em aberto que requer maior atenção no sentido de entender o efeito de diferentes surfactantes na estrutura e propriedade das vesículas, assim como o mecanismo de transição estrutural nas misturas. Este trabalho sugere a continuidade da pesquisa para outros surfactantes catiônicos monoalquilados derivados da amônia quaternária no comportamento termotrópico de vesículas de surfactantes dialquilados, variando o comprimento da cauda, para D_n DAB e C_n TAB, pois há uma variedade de combinação de mistura desses surfactantes que pode ser explorada. Este estudo sugere, portanto, que misturas de surfactantes catiônicos homólogos, variando o comprimento da cadeia e o número de cadeias, pode levar a um controle das propriedades das estruturas formadas, que podem ser essenciais em aplicações práticas de surfactantes.

6. Referências bibliográficas

- ALVES, F. R.; FEITOSA, E. Interaction of sodium cholate with dioctadecyldimethylammonium chloride vesicles in aqueous dispersion. *Thermochimica Acta*, 450, 76-80, 2006.
- ALVES, F. R.; ZANIQUELLI, M. E. D.; LOH, W.; CASTANHEIRA, E. M. S.; REAL OLIVEIRA, M. E. C. D.; FEITOSA, E. Vesicle-micelle transition in aqueous mixtures of the cationic dioctadecyldimethylammonium and octadecyltrimethylammonium bromide surfactants. *J. Colloid Interface Sci.*, 316, 132-139, 2007.
- BANGHAM, A. D.; HORNE, R. W. Negative staining of phospholipids and their structural modification by surface-active agents as observed in the electron microscope. *Journal of Molecular Biology*, 8, 660-668, 1964.
- BARRELEIRO, P. C. A.; OLOFSSON, G.; BROWN, W.; EDWARDS, K.; BONASSI, N. M.; FEITOSA, E. Interaction of octaethylene glycol n-dodecyl monoether with dioctadecyldimethylammonium bromide and chloride vesicles. *Langmuir*, 18, 1024-1029, 2002.
- BENATTI, C. R.; FEITOSA, E.; FERNANDEZ, R. M.; LAMY-FREUND, M. T. Structural and thermal characterization of dioctadecyldimethylammonium bromide dispersions by spin labels. *Chem. Phys. Lipids*, 111, 93-104, 2001.
- CARMONA-RIBEIRO, A. M. Synthetic amphiphile vesicles. *Chem. Soc. Reviews*, 21, 209-214, 1992.
- CAVALLI, A.; DYNAROWICZ-ŁĄTKA, P.; OLIVEIRA JR., O. N.; FEITOSA, E. Using an effective surface charge to explain surface potentials of Langmuir monolayers from dialkyldimethylammonium halides with the Gouy-Chapman theory. *Chem. Phys. Letters*, 338, 88-94, 2001.

- CEVEC, G.; MARSH, D. Phospholipid Bilayers-Physical Principles and Models, v. 5, New York, 1987.
- COCQUYT, J.; OLSSON, U.; OLOFSSON, G.; VAN DER MEEREN, P. Temperature quenched DODAB dispersions: fluid and solid state coexistence and complex formation with oppositely charged surfactant. *Langmuir*, 20, 3906-3912, 2004.
- CUCCOVIA, I. M.; FEITOSA, E.; CHAIMOVICH, H.; SEPULVEDA, L.; REED, W. Size, electrophoretic mobility, and ion dissociation of vesicles prepared with synthetic amphiphiles. *J. Phys Chem.* 94, 3722-3725, 1990.
- DAVEY, T. W.; DUCKER, W. A.; HAYMAN, A. R.; SIMPSON, J. Krafft temperature depression in quaternary ammonium bromide surfactants. *Langmuir*, 14, 3210-3213, 1998.
- EVANS, D. F.; WENNERSTRÖM, H. *The Colloidal Domain: Where Physics, Chemistry, Biology and Technology Meet*, 2nd Ed., Wiley/VCH, New York/Weinheim, 1999.
- FEITOSA, E. Spontaneous vesicles of sodium dihexadecylphosphate in HEPES buffer. *J. Colloid Interface Sci.*, 320, 608-610, 2008.
- FEITOSA, E.; ALVES, F. R.; NIEMIEC, A.; REAL OLIVEIRA, M. E. C. D.; CASTANHEIRA, E. M. S.; BAPTISTA, A. L. F. Cationic liposomes in mixed didodecyldimethylammonium bromide and dioctadecyldimethylammonium bromide aqueous dispersions studied by differential scanning calorimetry, Nile red fluorescence, and turbidity. *Langmuir*, 22, 3579-3585, 2006a.
- FEITOSA, E.; BARRELEIRO, P. C. A.; OLOFSSON, G. Phase transition in dioctadecyldimethylammonium bromide and chloride vesicle prepared by different methods. *Chem. Phys. Lipids*, 105, 201-213, 2000.

- FEITOSA, E.; BARRELEIRO, P. C. A. The effect of ionic strength on the structural organization of dioctadecyldimethylammonium bromide in aqueous solution. *Progr. Colloid Polym. Sci.*, 128, 163-168, 2004.
- FEITOSA, E.; BONASSI, N. M.; LOH, W. Vesicle-micelle transition in mixtures of dioctadecyldimethylammonium chloride and bromide with nonionic and zwitterionic surfactants. *Langmuir*, 22, 4512-4517, 2006b.
- FEITOSA, E.; BROWN, W. Fragment and vesicle structures in sonicated dispersions of dioctadecyldimethylammonium bromide. *Langmuir* 13, 4810-4816, 1997.
- FEITOSA, E.; JANSSON, J.; LINDMAN, B. The effect of chain length on the melting temperature and size of dialkyldimethylammonium bromide vesicles. *Chem. Phys. Lipids*, 142, 128-132, 2006c.
- FEITOSA, E.; KARLSSON, G. Dioctadecyldimethylammonium bromide vesicles prepared by the surfactant removal method. *J. Colloid Interface Sci.*, 298, 1000-1001, 2006.
- FEITOSA, E.; KARLSSON, G.; EDWARDS, K. Unilamellar vesicles prepared by simple mixing dioctadecyldimethylammonium chloride and bromide with water. *Chem. Phys. Lipids*, 140, 66-74, 2006d.
- FENDLER, J. H.; *Membrane Mimetic Chemistry*. 1st ed. Nova Iorque, Ed. Wiley-Interscience, 1982.
- ISRAELACHVILLI, N. J. *Intermolecular and Surface Forces*. 2nd ed. Londres, Ed. Academic Press, 1991.
- JÖNSSON, B.; LINDIMAN, B.; HOLMBERG, K.; KRONBERG, B. *Surfactants and polymers in aqueous solution*, John Wiley, 1998.
- KACPERSKA, A. The effect of alkyltrimethylammonium bromides on the thermal stability of dioctadecyldimethylammonium bromide (DOAB) vesicles in aqueous solutions *J. Thermal Analysis*, 45, 703-714, 1995.

- KUNITAKE, T.; OKAHATA, Y. A totally synthetic bilayer membrane. *Journal of the American Chemical Society*, 99, 3860-3861, 1977.
- LASIC, D. D. *Liposomes. From Physics to Applications*; 1st ed. Amsterdam-Holanda, Ed. Elsevier: Amsterdam, 1993.
- LINDMAN, B.; WENNERSTRÖN, H. Micelles. Amphiphile aggregation in aqueous solution. *Topics in current chemistry*, 1980.
- MARQUES, E. F.; KHAN, A.; LINDMAN, B. A calorimetric study of the gel-to-liquid crystal transition in cationic surfactant vesicles. *Thermochimica Acta*, 394, 31-37, 2002.
- MARQUES, E. F.; REGEV, O.; KHAN, A.; MIGUEL, M. G.; LINDMAN, B. Vesicle formation and general phase behavior in the cationic mixture SDS-DDAB-water. The cationic-rich side. *Journal Phys. Chem. B*, 103, 8353-8363, 1999.
- MATA, J.; VARADE, D.; BAHADUR, P. Aggregation behavior of quaternary salt based cationic surfactants. *Thermochimica Acta*, 428, 147-155, 2005.
- NASCIMENTO, D. B.; RAPUANO, R.; LESSA, M. M.; CARMONA-RIBEIRO, A. M. Counterion effects on properties of cationic vesicles. *Langmuir*, 14, 7387-7391, 1998.
- ROBINSON, B. H.; ROGERSON, M. *Handbook of Applied Surface and Colloid Chemistry*, Ed. John Wiley, 2001.
- SWANSON-VETHAMUTHU, M.; FEITOSA, E.; BROWN, W. Salt-induced sphere-to-disk transition of octadecyltrimethylammonium bromide micelles. *Langmuir*, 14, 1590-1596, 1998.
- TANFORD, C. *The Hydrophobic Effect: Formation of micelles and biological membranes*. 2nd ed. Nova Iorque, Ed. John Wiley, 1991.

Artigo 1

Cationic vesicles in the micromolar concentration domain of DODAB and DODAC

Eloi Feitosa,¹ Fernanda Rosa Alves,¹ Elisabete M.S. Castanheira² and M. Elisabete C.D. Real
Oliveira²

¹Physics Department, São Paulo State University, São José do Rio Preto – SP, Brazil

²Physics Department, University of Minho, Campus de Gualtar, 4710-057 Braga, Portugal

Correspondence address:

Eloi Feitosa

Physics Dept., IBILCE/UNESP

Rua Cristovao Colombo, 2265

Sao Jose do Rio Preto, SP - Brazil

CEP: 15054-000

Voice: +55 17 3221 22 40

Telefax: +55 17 3221 22 47

e-mail: eloi@ibilce.unesp.br

Abstract

Diocetadecyldimethylammonium bromide and chloride (DODAX, X representing Br⁻ or Cl⁻ counterions) molecules assemble in water as large unilamellar vesicles in the millimolar domain of the surfactant concentration – typically 1 mM. Differential scanning calorimetry (DSC) is a suitable technique to obtain the melting temperature (T_m) characteristic of surfactant bilayers, while fluorescence spectroscopy detects formation of surfactant bilayers. At 1 mM surfactant, $T_m \approx 45$ and 49 °C for DODAB and DODAC, respectively. DSC and fluorescence of the probe Nile Red were used to show the formation of DODAX vesicles at surfactant concentrations as low as 10 μ M, referred to as “microvesicles” (μ V), whose T_m decreases monotonically with increasing DODAX concentration to the value for the ordinary vesicles. DSC and fluorescence data indicate that the microvesicles should exhibit larger stabilized non-interacting unilamellar structure relative to the ordinary vesicles.

Keywords: DODAB, DODAC, DSC, Nile Red, surfactant, cationic vesicle, microvesicle, melting temperature, steady-state fluorescence, fluorescence anisotropy.

Introduction

There is a class of surfactants suitable to form vesicles in aqueous solutions, that is, closed bilayers entrapping a limited portion of the aqueous solvent, the water core, where hydrophilic solutes can be solubilized [1]. These vesicles have potential applications in drug delivery as well as to mimic biomembranes [1,2]. Other solubilization sites for small particles are the vesicle bilayer, where hydrophobic molecules can be solubilized, and the inner and outer vesicle interfaces where polar and amphiphilic molecules can be anchored.

It is well established that dioctadecyldimethylammonium bromide and chloride (DODAB and DODAC) molecules assemble as cationic vesicles with properties and structure that depend on the surfactant concentration, solvent condition (ionic strength and temperature) and method of vesicle preparation [3-11]. Large unilamellar vesicles (LUV) can be formed by simply warming an aqueous mixture of DODAX (typically 1 mM) to 55-60 °C (i.e., safely above the T_m of these surfactants). Multilamellar and multistructural vesicles (Fig. SM1) can also be formed at higher surfactant concentrations, as well as in presence of single inorganic salts [9]. Thus, surfactant concentration, ionic strength and temperature contribute to determine the vesicle structure in DODAX aqueous dispersions. Overall, the structure of the surfactant aggregates becomes more complex when the surfactant concentration is raised or temperature is lowered below T_m (Fig. SM1). The vesicle instability and polydispersity tend to increase with the surfactant concentration, because at higher concentrations the vesicles are closer together and the intervesicle interactions are destabilizing.

Stable (or meta-stable) unilamellar vesicles can thus be prepared within a quite limited range of surfactant concentrations. Higher surfactant concentrations favor the formation of more complex structures as well as vesicle fusion and precipitation [7,9]. The opposite behavior is thus expected for very dilute DODAX dispersions relative to the 1 mM surfactant

commonly used in vesicle preparation. That is, very dilute vesicles might be more stable and less polydisperse than the ordinary vesicles at 1 mM.

Long-chain vesicle-forming surfactants like DODAX exhibit a small critical vesicle concentration (CVC) above which vesicles are formed. The CVC of DODAB or DODAC is too low to be measured by ordinary techniques (for instance surface tension, conductimetry, light scattering, etc.) [5], thus allowing the formation of cationic vesicles in the domain of micromolar concentrations – these vesicles will be referred to as “microvesicles” (μV) to be distinguished from the ordinary vesicles in the typical bluish dispersions at 1 mM surfactant concentration. Unlike the ordinary dispersions, the μV dispersions of DODAX are optically clear (transparent) and low viscous resembling pure water. The term “microvesicles” is to remind that the surfactant concentration lies within the micromolar concentration domain and has no relation to the vesicle size.

In this communication, it was used high sensitive differential scanning calorimetry (DSC) and steady-state fluorescence of the probe Nile Red (NR) to detect μV structures of DODAB and DODAC at surfactant concentrations as low as 10 μM . The data are compared to those for ordinary millimolar vesicles. The DSC thermograms for the μV dispersions exhibit a single endothermic peak characteristic of T_m for unilamellar vesicles. The effect of DODAX concentration on T_m allows the comprehension of some properties of the microvesicles that may be highly suitable as host for microamount of solute molecules.

Materials and Methods

DODAB (from Sigma) was recrystallized and DODAC obtained from DODAB by ion exchange and recrystallized as reported [4]. Ordinary 1.0 mM DODAB and DODAC vesicles were prepared by mixing the surfactant and water at room temperature (ca 22 °C) and warming the mixture to 60 °C until complete dissolution of the surfactant. The homogeneous

dispersions were then cooled to room temperature for storage. These vesicles can alternatively be stored at the fridge temperature (5 °C), where they are as well stable for months [9,11]. The microvesicles (μV) were obtained by diluting at room temperature (below T_m) the stock vesicle dispersions of DODAX 1.0 mM to the desired micromolar concentration of the surfactant for DSC and fluorescence measurements. For comparison, ordinary 1.0 mM DODAX dispersions were also investigated by DSC and fluorescence. Ultrapure Milli-Q-Plus quality water was used in sample preparations.

Differential scanning calorimetry (DSC)

DSC experiments were performed in a high-sensitive differential scanning calorimeter (DSC) model VP-DSC MicroCal MC-2 (MicroCal Inc., Northampton, MA, USA), equipped with 0.542 ml twin cells for the reference and sample solutions. Heat was supplied to or removed from the sample and reference and the equipment recorded the power removed from or supplied to the sample, to keep its temperature equal to the reference temperature, as the cell temperature was varied at a constant rate. The power was then converted to heat and the equipment supplied the heat capacity at constant pressure (ΔC_p) for the sample, as a function of temperature (thermogram). Associated to the melting transition (and other transitions), there is a peak in the DSC traces which maximum is positioned at T_m . The melting enthalpy is proportional to the peak area, that is, $\Delta H = \int C_p dT$; the width of the peak is inversely proportional to the transition cooperativity. The measurements were performed with the scan rate of 1 °C/min and temperature range of 5-85°C. Details on the experimental procedures can be found elsewhere [7,9].

Steady-state fluorescence

The fluorescence probe 9-(diethyl-amino)-5H-benzo[*a*]phenoxazin-5-one (Nile Red) was used as supplied by Aldrich. Nile Red was introduced in the DODAX/water systems by evaporating the appropriate volume of a 1 mM stock solution of the probe in ethanol, under an argon stream. Then, the required amount of 1.0 mM DODAX dispersion in water was added and the system was heated to 60 °C under vigorous stirring. The solutions were then cooled to room temperature and left standing for several hours (ca 24 h) to stabilize. The final concentration of Nile Red in the solutions is 0.5 μ M.

Fluorescence measurements were performed using a Fluorolog 3 spectrofluorimeter, equipped with a temperature controlled cuvette holder. Polarized emission spectra were recorded using Glan-Thompson polarizers. All spectra were corrected for the instrumental response of the system.

Fluorescence measurements were performed below and above the melting temperature of both surfactants, respectively, at 25 °C and 60 °C. The spectra at both temperatures were repeated in different days to check reproducibility. All measurements were reproducible. Emission of Nile Red in pure water was obtained for comparison immediately after solution preparation.

Results

DODAB and DODAC molecules assemble in water as vesicles, whose structure is determined by the surfactant concentration, counterion nature and temperature. In general, the vesicle structure tends to be more complex at higher surfactant concentration and lower temperature, as outlined in Fig. SM1. The counterion Br⁻ also gives more complex vesicles than Cl⁻. At 1.0 mM, DODAB and DODAC vesicles exhibit typical DSC thermograms, as shown in Fig. SM2. These surfactants exhibit, respectively, three and one peaks, indicating that the structure of DODAB vesicles is more complex at this concentration. At 10 μ M,

however, the DSC thermograms are single-peak, thus indicating the structures of DODAB and DODAC microvesicles are rather similar, differing mainly in size, because for these surfactants T_m increases with vesicle size [7].

The effect of diluting the 1.0 mM DODAB and DODAC vesicle dispersions on the DSC thermogram is shown in Fig. 1. The main- (melting), pre- and post-transition temperatures, the melting enthalpy and the peak width obtained from the thermograms are summarized in Table 1. The fluorescence spectra of the probe Nile Red (NR) incorporated in DODAB vesicles and in pure water are depicted in Figs. 4 and 5 at 25 and 60 °C, that is, below and above T_m . The NR spectral modifications due to change in surfactant concentration and temperature can give important information on the surfactant packing and bilayer structure. The results indicate that the probe feels environments with different levels of hydration, because the maximum emission wavelength lowers on increasing surfactant concentration. The effect of surfactant concentration on the variation of NR maximum emission wavelength, λ_{max} , and on the steady-state fluorescence anisotropy, is depicted in Figs. 6 and 7, respectively, at 25 and 60 °C. The fitting of the NR emission spectra to a sum of lognormal functions is shown in Fig. 8 for 10 μ M DODAC at 25 °C, as an example.

Discussion

DSC results

DSC and fluorescence measurements for 1.0 mM DODAX dispersions were performed for comparison with the data in the micromolar concentration domain. At 1.0 mM, DODAC vesicles in water exhibit a single peak DSC thermogram due to the melting temperature at $T_m \approx 49.0$ °C, whereas DODAB vesicles exhibit two additional peaks to the main transition ($T_m \approx 45.8$ °C): the pre-transition ($T_s \approx 33.3$ °C) and the post-transition ($T_p \approx$

51.5 °C) peaks, in good agreement with previously reported data [7,9]. At 10 μM , however, both DODAB and DODAC exhibit single peak thermogram.

Figure SM2 compares the typical single- and three-peak DSC traces, respectively for DODAC and DODAB. Upon dilution, however, only the main transition peak remains up to 10 μM , while the pre- and post-transition peaks vanish around 40 and 80 μM , respectively (Fig. 1). Thus, the single peak in the DSC thermograms for 10 μM DODAX aqueous dispersions is undoubtedly related to the main transition (chain melting) temperature, T_m , indicating that at this quite low concentration microvesicles (μV) are formed.

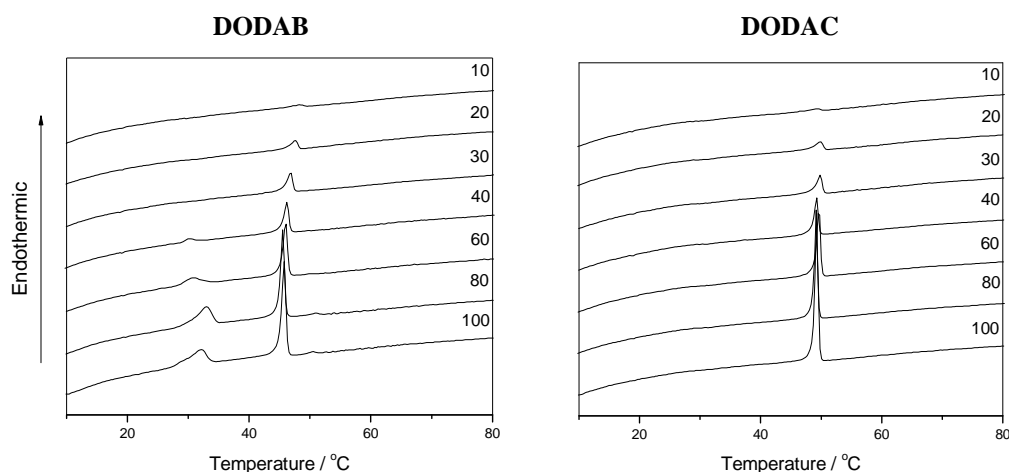


Figure 1 – Second DSC upscan thermograms for 10-100 μM DODAB and DODAC in aqueous dispersions. The numbers besides the curves refer to DODAX concentration.

Since the pre-transition is related to undulation in the vesicle bilayers [7], the absence of the pre-transition peak does not necessarily mean there is no undulation associated with the vesicle bilayer but, instead, the undulation energy is too low to be detected by the calorimeter. The post-transition temperature may be related to the formation of local lamellar phases in the gel state (below T_m) yielding flow-birefringency, and the peak height tends to increase with surfactant concentration [7]. As the microvesicles exhibit no post-transition temperature, the

dispersion is dominated by unilamellar vesicle structures and contains no local lamellar phases and the samples exhibit no flow-birefringency.

For both DODAB and DODAC, T_m increases continuously on dilution of the vesicle dispersions from 1 mM to 10 μM , with DODAB exhibiting a more pronounced increase (Fig. 2). Previously it was reported that the T_m for DODAX in water increases when the vesicle size increases and planar bilayers (or bilayer fragments) exhibit even larger T_m [7]. In that communication, the vesicle size was controlled by extrusion while bilayer fragments were obtained by sonication. The data in Fig. 2 thus suggest that the microvesicles are slightly larger relative to the ordinary vesicles, and DODAB microvesicles exhibit higher change in size than DODAC ones. It is worth of mentioning that DODAX vesicles were prepared spontaneously, that is, without sonication or extrusion that could influence the final vesicle structure or T_m .

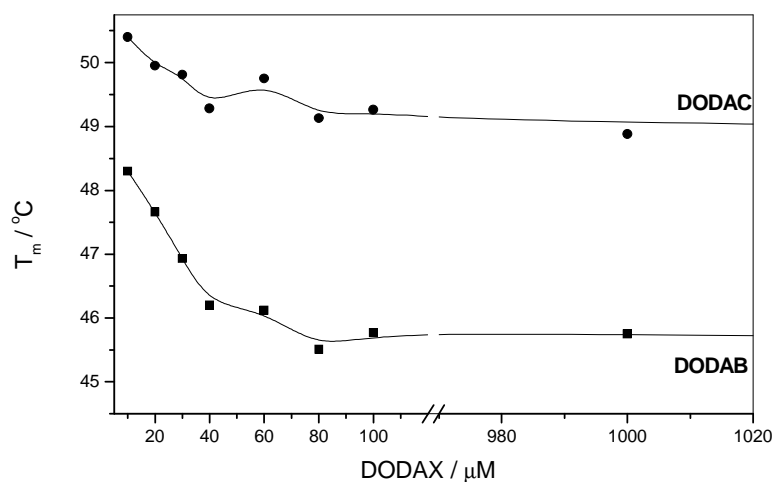


Figure 2 – The effect of surfactant concentration on the melting temperature, T_m , of DODAC and DODAB in water, obtained from the second DSC upscans. For comparison, the values of T_m for 1 mM were included.

The lower T_m of DODAB may indicate that DODAB vesicles are smaller than DODAC ones and/or that the surfactants are less densely packed in the DODAB bilayers. Below ca 40 μM , T_m increases on sample dilution at a higher rate for DODAB, suggesting that at infinite dilution T_m for DODAB is only slightly smaller than that for DODAC, indicating that DODAB microvesicles may be slightly smaller than DODAC microvesicles. A linear fit of the first four points in the T_m curves (Fig. 2) gives $T_{m,0} = 49.0$ and 50.7 $^\circ\text{C}$, respectively for DODAB and DODAC vesicles at infinite dilution.

Alternatively, the higher T_m for the microvesicles relative to the ordinary vesicles could suggest the presence of bilayer fragments (planar structures), as reported [5,12]. This may be, however, not the case because the change in T_m on sample dilution is rather smooth to indicate integral vesicle-bilayer fragment structure transition in the systems. In previous works [5,12] such a transition was forced by dispersion sonication.

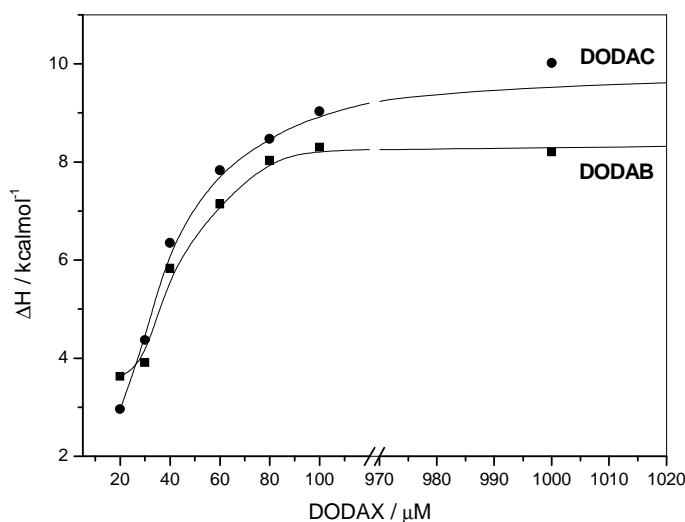


Figure 3 – The effect of surfactant concentration on the melting enthalpy, ΔH , of DODAC and DODAB in water, obtained from the second DSC upscans. For comparison, the values of ΔH for 1 mM DODAX were included.

The melting enthalpy increases as DODAX concentration is increased, with the enthalpy for DODAB being slightly smaller (Fig. 3), except at 20 μM . Overall, the melting enthalpy of DODAB is smaller than that for DODAC in agreement with the lower T_m of DODAB that requires smaller amount of heat to melt the surfactant chains. As the surfactant concentration increases, T_m decreases but ΔH increases, indicating the formation of more complex bilayer structures. One should realize that this is not a general behavior for lipid vesicles. An opposite behavior was reported for the anionic dihexadecylphosphate (DHP) vesicles in a HEPES buffer solution, for which both T_m and the melting enthalpy increase when DHP concentration is increased [13]. The width of the main transition peak, $\Delta T_{1/2}$, on the other hand, presents no clear dependence on surfactant concentration, but it lies between 0.5-1.0 (Table 1), characteristic of “sharp” cooperative transitions. The deviation in the $\Delta T_{1/2}$ data at the lowest DODAX concentrations may be due to the much smaller area of the peaks that leads to pronounced error in the calculation of this parameter.

Table 1 – Values of melting temperature (T_m), melting enthalpy (ΔH) and width of the melting transition peak ($\Delta T_{1/2}$) for different DODAB and DODAC molar concentrations. Data obtained from the second DSC upscans. Data for 10 μM not calculated because the peak is too small for data analyses.

DODAB				DODAC		
Conc. / μM	$T_m / ^\circ\text{C}$	$\Delta H / \text{kcal mol}^{-1}$	$\Delta T_{1/2} / ^\circ\text{C}$	$T_m / ^\circ\text{C}$	$\Delta H / \text{kcal mol}^{-1}$	$\Delta T_{1/2} / ^\circ\text{C}$
1000	45.8	8.20	0.54	48.9	10.02	0.53
100	45.8	8.30	0.80	49.3	9.03	0.53
80	45.5	8.03	0.80	49.1	8.47	0.80
60	46.1	7.14	0.80	49.8	7.83	0.53
40	46.2	5.83	0.80	49.3	6.35	0.53
30	46.9	3.91	0.80	49.8	4.37	0.80
20	47.7	3.63	1.06	50.0	2.96	1.06

Since the melting temperature is a characteristic of the surfactant bilayer system, rather than the surfactant itself, in the domain of micromolar concentrations DODAX should assemble as bilayer structures, most probably as unilamellar vesicles, although they may assemble as bilayer fragments due to larger T_m , as reported [5,12]. The actual structure of DODAX microvesicles requires further investigation. The light scattering signal for the 10 μM DODAX vesicles is too weak, comparable to that for water (results not shown), thus giving no information on the vesicle size.

Table 2 summarizes the DSC data related to the pre-transition at different DODAB concentrations. Accordingly, undulations (indicated by the pre-transition temperature) in the microvesicle bilayers are attenuated, giving small enthalpy and large peak width values. The weak signal for the pre-transition hinders the analysis of this transition in the micromolar concentration domain, meaning that this phenomenon is negligible for microvesicles.

Table 2 – Values of pre-transition temperature (T_s), enthalpy (ΔH) and width of the transition peak ($\Delta T_{1/2}$) for different DODAB molar concentrations. Data obtained from the second DSC upscan. Data for smaller concentrations could not be obtained owing to the quite low intensity of the transition DSC peak.

DODAB / μM	$T_s / ^\circ\text{C}$	$\Delta T_{1/2(s)} / ^\circ\text{C}$	$\Delta H_{(s)} / \text{kcalmol}^{-1}$
80	33.01	2.39	4.84
100	32.21	2.13	1.85
1000	33.22	2.23	5.95

These data indicate that, in the micromolar domain, DODAX molecules assemble as bilayer structures, most probably as microvesicles, since these bilayers cannot be either infinite or fragmented, due to the quite low concentration and energetic impeachment, respectively. In other words, it is unlikely the bilayers are fragmented because of the unfavorable contact of water molecules with the exposed surfactant chains from the bilayer

lateral boundaries; they also cannot be extended bilayers because of the quite reduced amount of surfactant in the dispersion. Furthermore, there is no clear reason for the integral vesicles to be fragmented upon sample dilution.

DSC data thus clearly indicate the existence of bilayer structures in the surfactant micromolar domain, whereas the existing microvesicles (closed bilayers) is inferred from the behavior of T_m with decreasing DODAX concentration, that is, T_m increases continuously with sample dilution, indicating that, on dilution, slightly larger vesicles are formed. Furthermore, the microvesicles might be rather monodisperse in size and structure, because the polydispersity of DODAX dispersions tends to decrease as the surfactant concentration decreases and $\Delta T_{1/2}$ (peak width) for the microvesicles is comparable to that for ordinary vesicles that lies between 0.5-1.0 °C (Table 1). It was not found a clear dependence of $\Delta T_{1/2}$ on the μV concentration, however.

Fluorescence results

The fluorescence probe Nile Red (NR) has been extensively used as a probe for microheterogeneous systems, such as vesicles, micelles and microemulsions, due to its hydrophobic nature [14-19]. In polar media NR exhibits a solvatochromic behavior and displays a red shift of the emission maximum and fluorescence quenching, due to its capability to establish hydrogen bonds with protic solvents [20].

The hydrophobic nature of NR allows the probe to incorporate into the vesicle bilayer. The emission spectra of NR incorporated in the DODAX/water systems (Figs. 4 and 5) at 25 and 60 °C, respectively below and above the melting temperature of these surfactants, indicate a blue shift in the emission maximum with increasing surfactant concentration, relative to the spectrum in pure water. This indicates that, as the surfactant concentration increases, the environment surrounding the probe is in average less hydrated, pointing to the presence of

lipid aggregates. An increase in fluorescence intensity with DODAB concentration is also observed (inserts of Figs. 4 and 5), showing that at low surfactant concentrations the probe is more exposed to water.

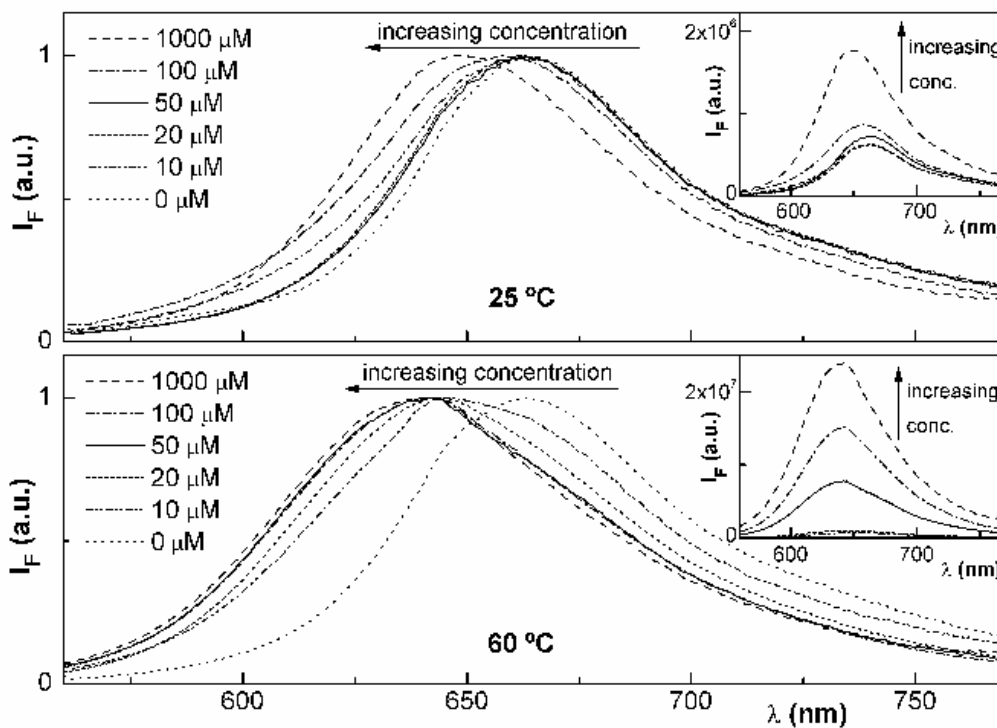


Figure 4 – Normalized fluorescence spectra ($\lambda_{\text{exc}} = 550 \text{ nm}$) of $5 \times 10^{-7} \text{ M}$ NR in DODAB aqueous dispersions for several DODAB concentrations, at 25 and 60 °C, respectively below and above T_m . Normalized emission of NR in pure water is shown for comparison. Insert: Corresponding non-normalized emission spectra of NR in DODAB/water system.

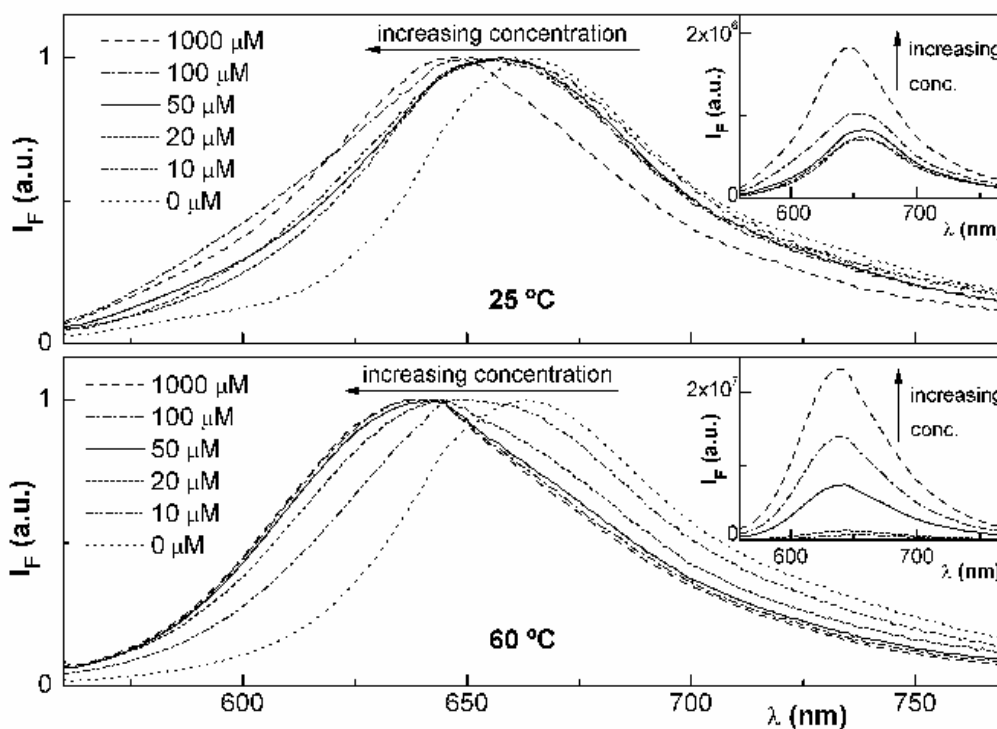


Figure 5 – Normalized fluorescence spectra ($\lambda_{\text{exc}} = 550 \text{ nm}$) of $5 \times 10^{-7} \text{ M}$ NR in DODAC aqueous dispersions for several DODAC concentrations, at 25 and 60 °C, respectively below and above T_m . Normalized emission of NR in pure water is shown for comparison. Insert: Corresponding non-normalized emission spectra of NR in DODAC/water system.

For both DODAB and DODAC, the NR fluorescence exhibits a significant blue shift (lower λ_{max}) in the liquid-crystalline state (60 °C), relative to the gel phase (25 °C) (Fig. 6). Such a blue-shift is not due only to the small thermochromic shift of the NR emission in pure water ($[\text{DODAX}] = 0$). It indicates that NR feels a more hydrophobic environment in the liquid-crystalline phase (above T_m), as previously observed for the DODAB/ C_{18}TAB /water system [21]. At room temperature the vesicle bilayers in the gel phase hinder the probe to penetrate deeper into the lipid bilayer. At 60 °C the vesicle bilayers are in the liquid-crystalline state and DODAX concentration affects little λ_{max} , but the blue-shift relative to pure water is much higher at 60 than at 25 °C (Fig. 6).

For DODAC, the NR emission is always blue-shifted relative to DODAB (Fig. 6) and slightly more intense (insert of Figs. 4 and 5). This indicates that in DODAC aggregates the NR environment is less hydrated, suggesting that DODAC vesicles are larger than those of DODAB, in accordance with the DSC data, at least in the micromolar concentration domain.

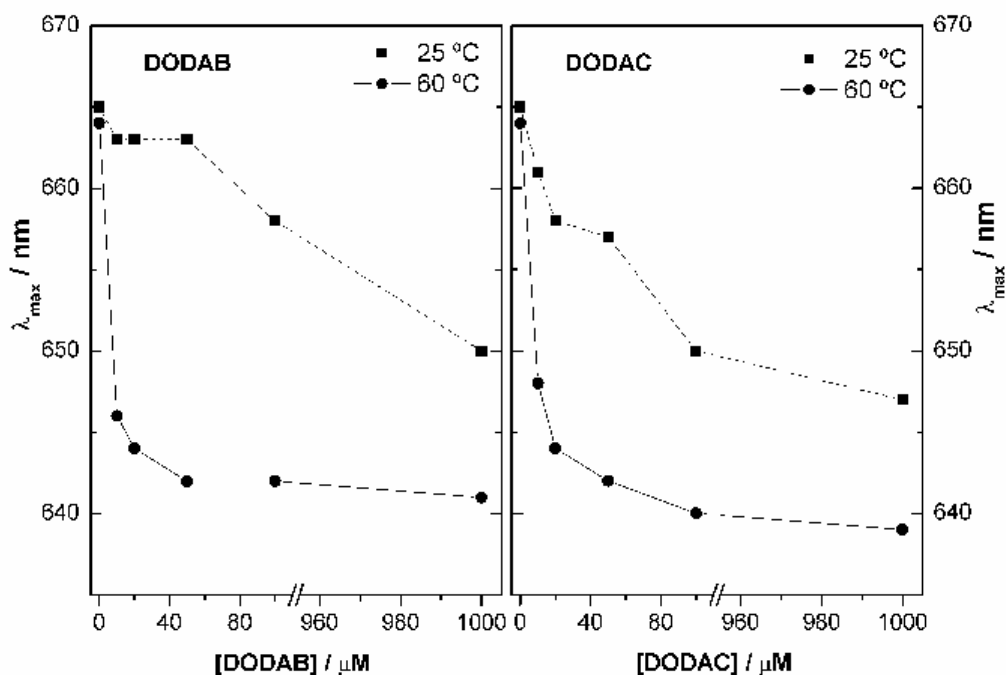


Figure 6 – Maximum emission wavelength of NR in DODAX/water systems, at 25 and 60 °C, for DODAB (left) and DODAC (right).

Complementary information can be obtained from steady-state fluorescence anisotropy measurements of NR in the DODAX/water systems. The anisotropy is given by

$$r = \frac{I_{VV} - GI_{VH}}{I_{VV} + 2GI_{VH}} \quad (1)$$

where I_{VV} and I_{VH} are the intensity of the emission spectra obtained with vertical and horizontal light polarization, respectively, for vertically polarized excitation light, and $G = I_{HV}/I_{HH}$ is the instrument correction factor, where I_{HV} and I_{HH} are the emission

intensities obtained with vertical and horizontal light polarization, for horizontally polarized excitation light.

Since a high value of steady-state fluorescence anisotropy is related to a low degree of rotation of the fluorescence probe, high anisotropy is expected when NR is located in a lipid bilayer, especially in the gel state (below T_m). On increasing temperature above T_m , a decrease in anisotropy is expected, resulting from the decrease in the bilayer microviscosity in the liquid-crystalline state.

At 1.0 mM DODAX and 25 °C, the anisotropy is high, as previously observed for DODAB [19], because the vesicle bilayers of both surfactants are in the gel state (below T_m) (Fig. 7). The data suggest a lower fluidity of DODAB bilayer in the gel state of the ordinary vesicles relative to DODAC. In the liquid-crystalline state the fluidity of both DODAB and DODAC bilayers is rather similar to each other.

At 25 °C the anisotropy is generally high at all surfactant concentrations (Fig. 7), indicating that the rotation of the NR molecule is hindered in the DODAX/water systems, even at concentrations as low as 10 μ M. Besides, the anisotropy exhibits a strong decrease by increasing temperature above T_m , reflecting the gel to liquid-crystalline state transition of DODAX (micro)vesicles.

The decrease in anisotropy (especially for 10 and 20 μ M DODAX) can be related to some fraction of NR molecules located in a water-rich environment. At such low concentrations, it is possible that the number of microvesicles is not enough to contain all the probes (at the concentration of 0.5 μ M) inside the bilayer. These molecules can be located near the inner and outer the vesicle interfaces. In fact, at low DODAX concentrations, the emission spectrum of NR seems to be composed by more than one single emission band. As the fluorescence band is asymmetric, the emission spectra can be decomposed into a sum of

lognormal functions [22], an approach previously used for this probe in microheterogeneous systems [17,23,24].

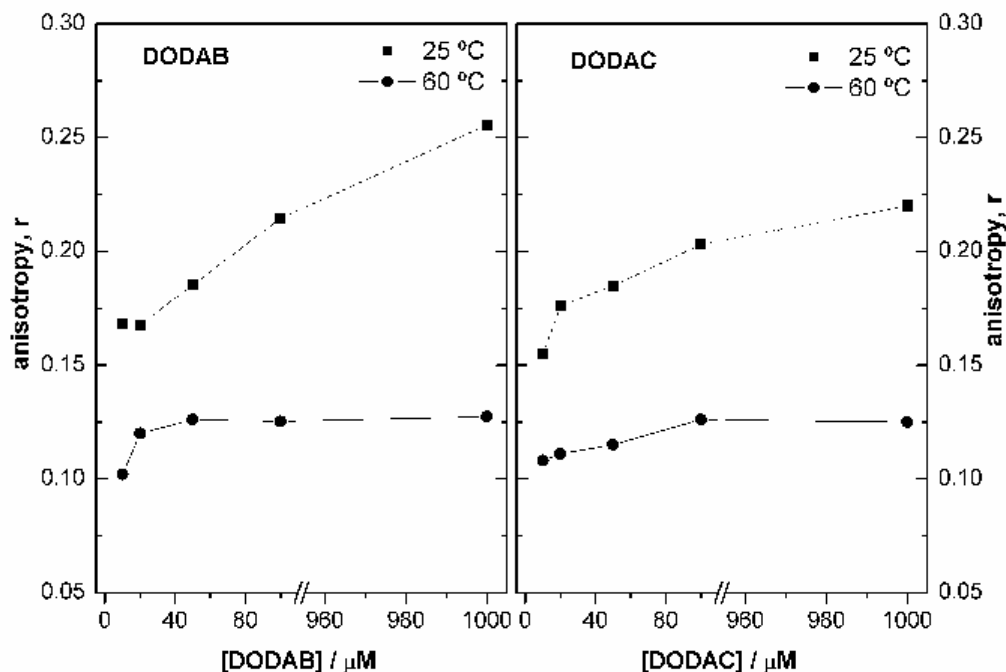


Figure 7 – Steady-state anisotropy of NR in DODAX/water systems, at 25 and 60 °C, for DODAB (left) and DODAC (right).

Here, the NR spectra in the micromolar range of surfactant concentrations (10-100 μM) were first fitted as the sum of two components (eq. 2), one corresponding to the NR experimental emission in 1.0 mM DODAX and the other to the NR emission in pure water, with variable fractions of each component, that is,

$$I_F = f_{1\text{mM}} I_{1\text{mM}} + f_{\text{water}} I_{\text{water}} \quad (2)$$

where I_F is the experimental emission spectrum, $f_{1\text{mM}}$ is the fitted fraction of NR emission in 1 mM DODAX ($I_{1\text{mM}}$) and f_{water} is the fitted fraction of NR emission in water (I_{water}). In almost all cases, the quality of these fittings is poor (an example is given in Fig. 8A).

Therefore, another approach was adopted, where one of the components is the NR emission in 1 mM DODAX (as before) and the other component, I_{fit} , is a lognormal function (or the sum of two lognormal functions, if necessary) obtained from the best fit to the experimental results (eq. 3).

$$I_F = f_{1\text{mM}} I_{1\text{mM}} + I_{\text{fit}} \quad (3)$$

with

$$I_{\text{fit}} = \frac{A}{(\lambda - \lambda_{\text{max}} + a)} \exp(-c^2) \exp\left\{-\frac{1}{2c^2} \left[\ln\left(\frac{\lambda - \lambda_{\text{max}} + a}{b}\right)\right]^2\right\}, \quad (4)$$

where A is the maximum emission intensity at wavelength λ_{max} and the parameters a , b and c are given by [23]

$$c = \ln(\rho)/\sqrt{2\ln(2)} \quad b = H \frac{\rho}{\rho^2 - 1} \exp(c^2) \quad a = H \frac{\rho}{\rho^2 - 1} \quad (5)$$

where H is the half-width of the band and ρ is the skewness.

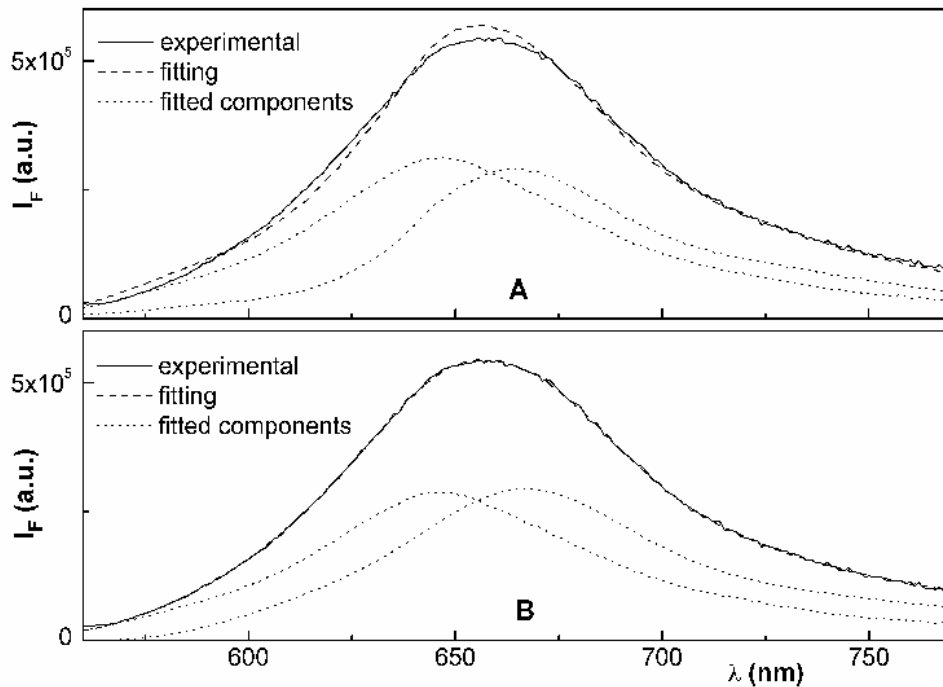


Figure 8 – Fitting of the NR emission spectrum in 10 μM DODAC at 25 $^{\circ}\text{C}$. The dotted lines correspond to the fitting components. A: Fitting to equation 2; B: Fitting to equation 3.

For both surfactants at 25 °C, the experimental emission is well described by a fitted fraction of NR emission in 1 mM DODAX and one lognormal function with λ_{\max} around 660–663 nm (Fig. 8B), which is characteristic for the probe in a water-rich environment (NR maximum emission wavelength in water at 25 °C is 665 nm). The weight of the latter component increases with the decrease in surfactant concentration (Table 3). This can explain the decrease in the NR anisotropy at low DODAX concentrations, as this water-rich medium can correspond to a less viscous environment. The weight of this component is always higher for DODAB than for DODAC. The slightly lower NR anisotropy for DODAC at room temperature (Fig. 7) points to a more fluid (less compact) bilayer than DODAB, allowing a higher fraction of probe molecules to penetrate deep into the bilayer.

Table 3 – Weights of the lognormal components obtained from the best fits to experimental NR emission in the DODAX/water systems at 25 °C (below T_m) and 60 °C (above T_m). The λ values correspond to maximum emission wavelengths.

Conc / μ M	DODAB				DODAC			
	25 °C		60 °C		25 °C		60 °C	
	$\lambda_{1\text{mM}}$ = 650 nm	$\lambda_{1\text{mM}}$ = 641 nm	$\lambda_{1\text{mM}}$ = 647 nm	$\lambda_{1\text{mM}}$ = 639 nm	λ_{fit} /nm	weight	λ_{fit} /nm	weight
100	662	61%	650	41%	660	29%	648	13%
50	662	64%	652	42%	662	43%	651	32%
20	663	65%	654	44%	663	48%	654	36%
10	663	71%	656	46%	663	51%	657	42%

The results at 60 °C confirm that in the liquid-crystalline state, the NR molecules can penetrate deeper into the bilayer, and the fitted lognormal component corresponding to a less hydrated environment has lower weight (Table 3). At this high temperature, the majority of the NR molecules feel an environment close to the one in ordinary (1 mM DODAX) vesicles.

The other fraction of molecules (component with $\lambda_{\text{max}} = 648\text{--}657\text{ nm}$) is more significant in DODAB than in DODAC microvesicles.

Summary

Microvesicles (μV) are introduced in this communication as non-interacting unilamellar vesicles formed in the micromolar domain of DODAX concentration, that is, at concentrations as low as $10\ \mu\text{M}$, according to DSC and Nile Red fluorescence data.

In theory, μV are formed above CVC, but the physical characterization of their structure is quite difficult, because a limited amount of sensitive enough techniques, such as DSC and fluorescence, is available to investigate such diluted systems. They cannot be viewed, for instance, by cryogenic transmission electron microscopy (cryo-TEM) or detected by scattering techniques.

An important characteristic of DODAB and DODAC to be well appropriate to form μV is that their CVC approaches zero [5], thus allowing the formation of bilayer structures at concentrations as low as $10\ \mu\text{M}$.

The high surfactant dilution ensures the non-existing intervesicle interaction and the μV should be stable, because bilayer fragments eventually formed from the vesicle rupture would be energetically unfavourable and the amount of DODAX molecules is not enough to form infinite bilayers.

Since T_m is a characteristic of surfactant bilayers, and since in the millimolar concentration domain (e.g. $1\ \text{mM}$) DODAX vesicles exhibit mainly the melting temperature transition, the DSC peak detected for DODAX dispersions in the micromolar concentration domain is clearly due to unilamellar vesicles, here referred to as “microvesicles” (μV). Such μV should be stable, rather monodisperse, and slightly larger in size than the ordinary $1\ \text{mM}$ DODAX vesicles.

Furthermore, since DODAX exhibit a CVC, it has to be lower than 10 μM . In fact, it is the extremely low CVC that makes DODAX potential candidates to form μV . The data here and previously reported indicate that the microvesicles can be either integral or fragmented, although we find no good reason for the integral vesicles to be fragmented on sample dilution, even because the fragments would be energetically unfavourable.

Like the ordinary vesicles, DODAX microvesicles have potential applications as vehicle for drug delivery and their properties can be modified by sonication or extrusion. One of the main characteristics of DODAX is their high capability to self-assemble as vesicles without sonication or extrusion, that is, spontaneously. Besides these characteristics, DODAX microvesicles can be formed by simple dilution of the ordinary vesicle dispersions which guarantees the high reproducibility of the microvesicle properties.

Acknowledgements

FRA and EF thank CNPq for PhD and research grant (Grant 304543/2006-3), respectively. EMSC and MECDRO thank FCT-Portugal for funding through Centro de Física da Universidade do Minho. Dr. W. Loh is acknowledged for kindly supplying the DSC equipment.

References

- [1] D.D. Lasic, *Liposomes. From Physics to Applications*. Elsevier: Amsterdam, 1993.
- [2] J.H. Fendler, *Membrane Mimetic Chemistry*. Wiley-Interscience: New York, 1982.
- [3] A.M. Carmona-Ribeiro, *Synthetic amphiphile vesicles*. *Chem. Soc. Rev.* 21 (1992) 209.
- [4] I.M. Cuccovia, A. Sesso, E.B. Abuin, P.F. Okino, P.G. Tavares, J.F.S. Campos, F.H. Florenzano, H. Chaimovich, *J. Mol. Liq.* 72 (1997) 323.
- [5] E. Feitosa, W. Brown, *Langmuir* 13 (1997) 4810.

- [6] M.J. Blandamer, B. Briggs, P.M. Cullis, P. Last, J.B.F.N. Engberts, A. Kacperska, J. Therm. Anal. Calorim. 55 (1999) 29.
- [7] E. Feitosa, P.C.A. Barreleiro, G. Olofsson, Chem. Phys. Lipids 105 (2000) 201.
- [8] C.R. Benatti, E. Feitosa, R.M. Fernandez, M.T. Lamy-Freund, Chem. Phys. Lipids 111 (2001) 93.
- [9] E. Feitosa, P.C.A. Barreleiro, Prog. Coll. Polym. Sci. 128 (2004) 163.
- [10] R.O. Brito, E.F. Marques, Chem. Phys. Lipids 137 (2005) 18.
- [11] E. Feitosa, G. Karlsson, K. Edwards, Chem. Phys. Lipids 140 (2006) 66.
- [12] M. Andersson, L. Hammarström, K. Edwards, J. Phys. Chem. 99 (1995) 14531.
- [13] E. Feitosa, J. Colloid Interface Sci., 320 (2008) 608.
- [14] P. Greenspan, E.P. Mayer, S.D. Fowler, J. Cell Biol. 100 (1985) 965.
- [15] P. Greenspan, S.D. Fowler, J. Lipid Res. 26 (1985) 781.
- [16] I. and G. Krishnamoorthy, J. Phys. Chem. B 15 (2001) 1484.
- [17] G. Hungerford, E.M.S. Castanheira, M.E.C.D. Real Oliveira, M.G. Miguel, H.D. Burrows, J. Phys. Chem. B 106 (2002) 4061.
- [18] G. Hungerford, E.M.S. Castanheira, A.L.F. Baptista, P.J.G. Coutinho, M.E.C.D. Real Oliveira, J. Fluorescence 15 (2005) 835.
- [19] E. Feitosa, F.R. Alves, A. Niemiec, M.E.C.D. Real Oliveira, E.M.S. Castanheira, A.L.F. Baptista, Langmuir 22 (2006) 3579.
- [20] A. Cser, K. Nagy, L. Biczók, Chem. Phys. Lett. 360 (2002) 473.
- [21] F.R. Alves, M.E.D. Zaniquelli, W. Loh, E.M.S. Castanheira, M.E.C.D. Real Oliveira, E. Feitosa, J. Colloid Interface Sci., 316 (2007) 132.
- [22] D.B. Siano, D.E. Metzler, J. Chem. Phys. 51 (1969) 1856.
- [23] V.J.P. Srivatsavoy, J. Lumines. 82 (1999) 17.

- [24] P.J.G. Coutinho, E.M.S. Castanheira, M.C. Rei, M.E.C.D. Real Oliveira, J. Phys. Chem. B 106 (2002) 12841.

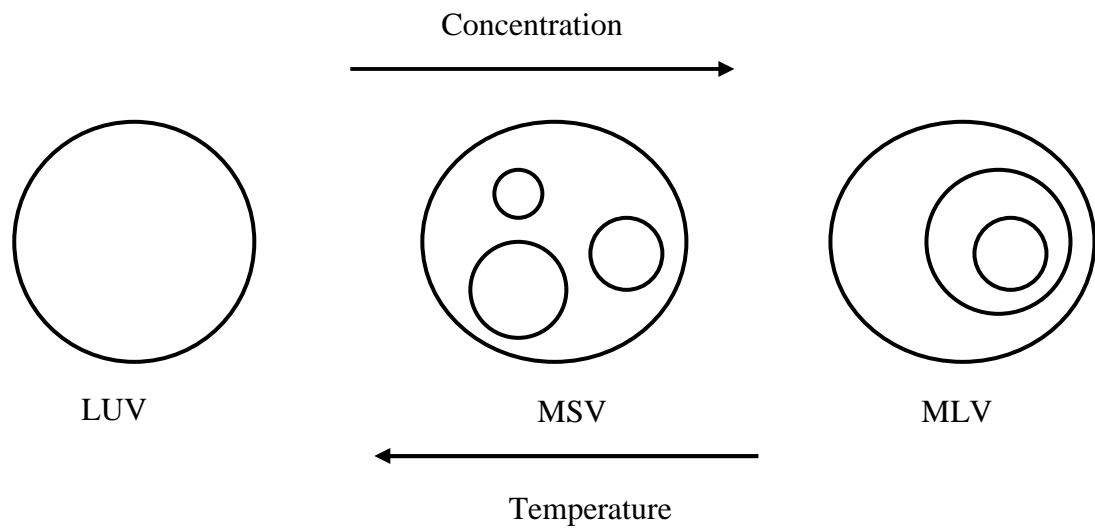
Supplementary materials

Figure SM1 – Schematic representation of possible vesicle structures formed by varying the DODAX concentration or temperature.

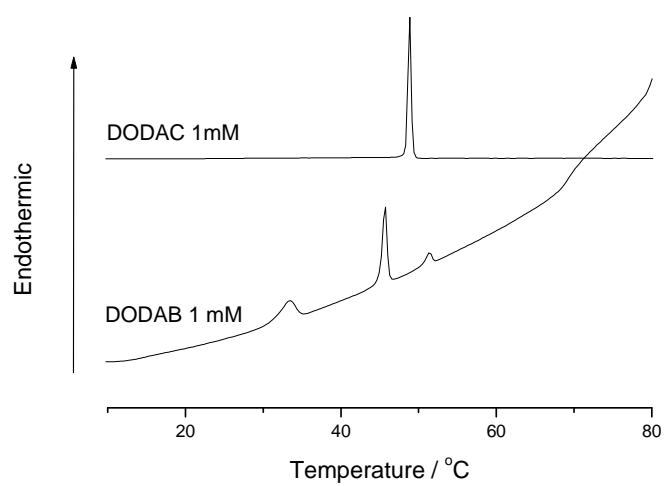


Figure SM2 – Second DSC upscan thermograms for 1 mM DODAB and DODAC in aqueous dispersions, used as reference for the DSC data from microvesicles.

Artigo 2

**The role of counterion on the thermotropic phase behavior of DODAB and DODAC
vesicles**

Eloi Feitosa,^{*} Fernanda Rosa Alves

¹Department of Physics, Sao Paulo State University, Sao Jose do Rio Preto, SP, Brazil

*Correspondence address:

Eloi Feitosa

Physics Dept., IBILCE/UNESP

Rua Cristovao Colombo, 2265

Sao Jose do Rio Preto, SP - Brazil

CEP: 15054-000

Voice: +55 17 3221 22 40

Telefax: +55 17 3221 22 47

e-mail: eloi@ibilce.unesp.br

Abstract

Diocetadecyldimethylammonium bromide and chloride surfactants (DODAX, X representing Br⁻ or Cl⁻ counterions) assemble in water, above their melting temperatures (T_m), as cationic unilamellar vesicles at the typical surfactant concentration of 1.0 mM. The larger T_m of DODAC (49 °C) relative to DODAB (45 °C) has been attributed to the differing affinity and binding specificity of the counterions to the vesicle interfaces. In this communication it is reported differential scanning calorimetry (DSC), conductimetry and dynamic light scattering (DLS) data for mixtures of DODAB and DODAC in water at 1.0 mM total surfactant concentration and varying surfactant concentration, to investigate the effect of counterion on the pre-, main- and post-transition temperatures (T_s , T_m and T_p), and the data compared to the neat surfactants in water. Accordingly, T_m increases sigmoidally from 45.8 to 48.9 °C when DODAC molar fraction (x_{DODAC}) is varied from 0 to 1. Neat DODAB exhibits in addition to T_m , T_s and T_p that are inhibited by DODAC. The main peak width $\Delta T_{1/2}$ does not depend on the surfactant molar fraction but the melting enthalpy change ΔH is smaller for DODAB-rich dispersions due to the stronger affinity of Br⁻. The conductivity and the apparent hydrodynamic diameter as well do not vary much with x_{DODAB} , indicating that the surface charge density is similar for DODAB and DODAC, evidencing that the effect of counterion on T_m is due to differing counterion binding specificity and affinity.

Keywords: DODAB, DODAC, DSC, dynamic light scattering, conductivity, cationic vesicle, melting temperature.

Introduction

There is a class of surfactants suitable to form vesicles in aqueous solutions, that is, closed bilayers entrapping a limited portion of the solvent where small hydrophilic solute molecules can be solubilized. Such vesicles have potential applications in drug delivery or to mimic biomembranes (Fendler, 1982; Lasic, 1993). In these applications, properties like vesicle stability, size, polydispersity, degree of counterion dissociation and critical temperatures (like the melting temperature T_m) should be well controlled.

Diocetadecyldimethylammonium bromide and chloride (DODAB and DODAC) assemble in water as cationic unilamellar vesicles whose properties and structures depend on the surfactant concentration, solvent condition, vesicle preparation method and nature of counterion (Romero et al., 1978; Carmona-Ribeiro, 1992; Cuccovia et al., 1990, 1990a, 1997; Feitosa and Brown, 1997; Blandamer et al., 1999; Feitosa and Barreleiro, 2004; Cocquyt et al., 2004; Brito and Marques, 2005; Feitosa et al., 2000, 2006; Alves et al., 2007). Large unilamellar vesicles (LUVs) are formed by simply warming to 55-60 °C (ie., above $T_m = 45.8$ and 48.9 °C of DODAB and DODAC) and gently shaking the aqueous surfactant solution (typically 1 mM) (Feitosa and Brown, 1997; Feitosa and Barreleiro, 2004; Feitosa et al., 2000, 2006). Once formed, these vesicles remain stable (or metastable) without precipitates for months even at room temperature, that is, in the gel state (Feitosa et al., 2006). Since these surfactants differ only by the nature of the counterion, their differing properties, such as size (Feitosa et al., 2006), melting temperature (Feitosa et al., 2000) and the degree of counterion dissociation (Cuccovia et al., 1990), might be related to the differing counterion binding specificity and affinity to the vesicle interfaces that gives vesicles with different characteristics.

To our knowledge, the effect of counterion binding on the properties of DODAX vesicles is not well understood. This work attempts to elucidate the role of Br^- and Cl^-

counterions on some properties of DODAX vesicles based on differential scanning calorimetry (DSC), conductivity and dynamic light data for aqueous dispersions of neat DODAX and mixtures of these surfactants. The findings point to the binding specificity and affinity of the counterions to the vesicle interfaces as being responsible for the differing properties in DODAX vesicles.

Materials and Methods

Scheme 1 shows the molecular structures of DODAB and DODAC. DODAB (Sigma) was recrystallized and DODAC obtained from DODAB by ion exchange and then recrystallized as reported (Cuccovia et al., 1997). Ultrapure Milli-Q quality water was used in the sample preparations. DODAX (1.0 mM) vesicles were prepared by weighing the surfactants and adding water at room temperature followed by warming and gently shaking the mixtures to 60 °C (i.e., safely above the T_m of these surfactants) until complete dissolution of the surfactants. The dispersions were then cooled to room temperature for storage. The so prepared DODAX vesicle dispersions were mixed properly to form mixed DODAB-DODAC vesicles at molar fractions of these surfactantes from 0-1 and constant up to 1.0 mM total surfactant concentration. The molar fraction for DODAB is defined as $x_{\text{DODAB}} = [\text{DODAB}]/[\text{TOTAL}]$, where $[\text{TOTAL}] = [\text{DODAB}] + [\text{DODAC}]$, and the brackets account for molar concentration.

Differential scanning calorimetry (DSC) measurements were performed in a high-sensitivity differential scanning calorimetry, model MicroCal VPDS (Microcal Inc. Northampton, MA, USA) for samples containing selected molar fractions of DODAB and DODAC and 1.0 mM total surfactant concentration. The temperature was raised from 5.0 to 85.0 °C at the scan rate of 1.0 °C/min and the thermograms recorded. The twin cells were filled with equal volume of water and solution, respectively in the reference and sample cells.

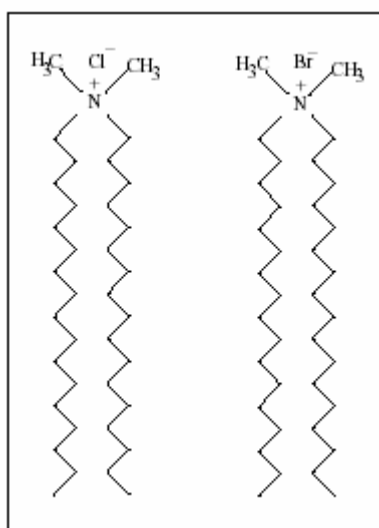
Details on the experimental setup can be found in previous communications (Alves et al., 2007).

Dynamic light scattering (DLS) measurements were made using a Zeta Sizer 3000 HS, operating with a He-Ne laser with power of 10 mW. From the normalized intensity time correlation function, the relaxation time distribution was obtained, and thus the diffusion coefficients of the vesicles (Nascimento et al., 1998). The apparent hydrodynamic diameter was then obtained using the Stokes-Einstein equation

$$D_H = \frac{kT}{3\pi\eta_0 D}$$

where D is the mean diffusion coefficient, k is the Boltzmann constant, T is the absolute temperature, and η_0 is the solvent viscosity.

The conductivity measurements were performed at 25.0 ± 0.1 °C using a conductimeter by Hanna Instrumentns, model HI9032, equipped with an electrode of 0.1 cell constant.



Scheme 1 – Molecular structures of DODAC and DODAB.

Results

DSC thermograms for DODAC-DODAB mixed vesicles in water are shown in Fig. 1 for 1.0 mM total surfactant concentration and varying the molar fraction of the individual surfactants from 0 to 1. For comparison, thermograms for neat DODAX in water were included. DODAC vesicles in water exhibit a single sharp peak characteristic of the main (melting) transition temperature. Under the same experimental condition, neat DODAB vesicles exhibit in addition to the main transition a pre- and a post-transition, in agreement with previous reported data (Feitosa et al., 2000; Feitosa and Barreleiro, 2004, Cocquyt et al., 2004; Brito and Marques, 2005; Alves et al., 2007). Table 1 summarizes the data (T_m , main transition enthalpy change, ΔH , and width of the main transition peak, $\Delta T_{1/2}$) extracted from the thermograms in Fig. 1.

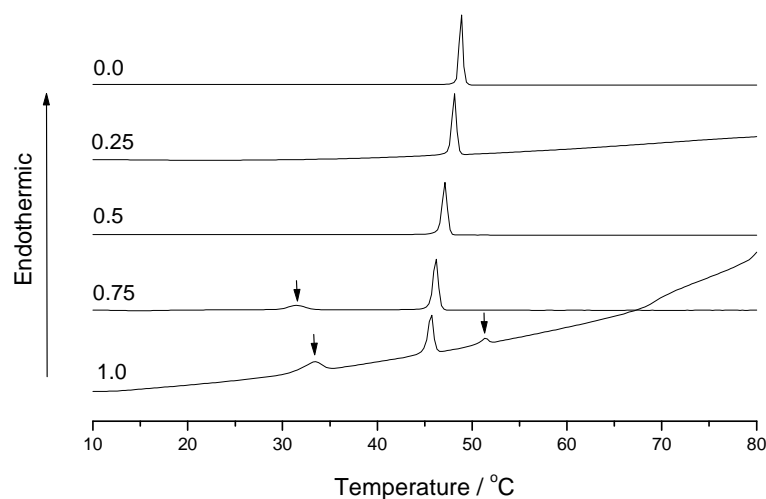


Fig. 1 – DSC upscan thermograms for mixed DODAB-DODAC aqueous dispersions at varying molar fraction of DODAB, as indicated by the numbers by the curves. All transitions are endothermic. Arrows indicate the pre- and post-transition peaks.

Table 1- Melting temperature, enthalpy change and peak width for selected x_{DODAB} . Data obtained from the analyses of the DSC traces in Figure 1.

x_{DODAB}	$T_m / ^\circ\text{C}$	$\Delta H / \text{kcalmol}^{-1}$	$\Delta T_{1/2} / ^\circ\text{C}$
0	48.9	9.96	0.53
0.25	48.2	10.24	0.53
0.50	47.1	10.33	0.53
0.75	46.2	10.35	0.53
1.00	45.8	8.37	0.54

Figs. 2 and 3 show how the T_m , enthalpy change (ΔH) and the peak width ($\Delta T_{1/2}$) of the main transition vary with surfactant molar fraction. Accordingly, T_m increases sigmoidally from 45.8 to 48.9 with the relative amount of DODAC, with the inflection point at the equimolarity. $\Delta T_{1/2}$ is constant around 0.53 ± 0.02 $^\circ\text{C}$ and the narrow peaks indicate sharp (cooperative) transitions. Up to $x_{\text{DODAB}} = 0.75$, ΔH is constant around 10.0 ± 0.1 kcalmol^{-1} , and above this value, ΔH decreases to ca. 8.4 ± 0.1 kcalmol^{-1} for neat DODAB, indicating the stronger affinity of Br^- , as suggested by Cuccovia et al. (1990a) who reported stronger exchange of the ion Γ with Cl^- and Br^- .

According to Figs. 4 and 5 the counterion causes minor effects on the conductivity and mean hydrodynamic diameter of the DODAX vesicle system. Accordingly, there is a trend of conductivity to decrease and the hydrodynamic diameter to increase with x_{DODAB} about the mean values $\sigma = 7.2$ μS and $D_H = 1350$ nm, respectively. These combined data indicate that the vesicles have about the same surface charge density, or degree of counterion dissociation (α), as reported (Cuccovia et al., 1990), and the counterion binding specificity and affinity might be the main reason for T_m being higher for DODAC.

Discussion

At 1.0 mM DODAB and DODAC assemble in water as large unilamellar vesicles (LUVs) (Feitosa and Brown, 1997; Feitosa and Barreleiro, 2004; Cocquyt et al., 2004; Feitosa et al., 2000, 2006; Alves et al., 2007). At this concentration DODAC exhibits only the main transition temperature ($T_m = 48.9$ °C) whereas DODAB exhibits, in addition to $T_m = 45.8$ °C, pre- ($T_s = 33.5$ °C) and post-transition ($T_p = 51.5$ °C) temperatures (Feitosa et al., 2000, Alves et al., 2007), that is, the phase behavior of DODAB is more complex than that of DODAC vesicles. Furthermore, T_m of neat DODAC is larger and the transition is more energetic ($\Delta H = 10$ kcalmol⁻¹) relative to DODAB ($\Delta H = 8.4$ kcalmol⁻¹) (Table 1), in good agreement with reported data (Feitosa et al., 2000) indicating that the DODAC bilayer is more densely packed, possibly due to the stronger affinity of Br⁻ relative to Cl⁻, as suggested by the fluorescence data reported by Cuccovia et al (1990a).

Since the counterion can also affect the vesicle structure, a change in the vesicle structure may as well affect the melting parameters, like T_m or ΔH . Alternatively, the change in ΔH should be corrected by the surfactant concentration used in the calculations that does not take into account the type and amount of counterion bound to the vesicle (the molar mass of Br is about twice that of Cl). In other words, the effect of counterion on ΔH may be due to a series of factors that affect both the thermotropic and structural properties. The peak width is about the same for the neat and mixed DODAX main transition (Table 1), meaning that this transition exhibits rather similar cooperativity (sharp transition). Furthermore, the degree of counterion dissociation (α) (Cuccovia et al., 1990), as well as the conductivity (Fig. 4) and hydrodynamic diameter (Fig. 5) do not depend much on the relative amount of the counterions Br⁻ and Cl⁻, indicating that the mixed and neat DODAX vesicles exhibit roughly the same surface charge density and the ion specificity and affinity should thus determine the thermotropic behavior of the DODAX single and mixed vesicle dispersions.

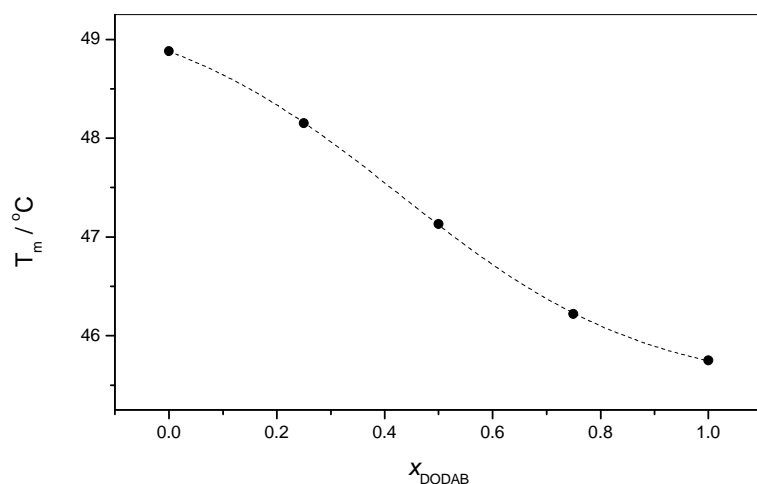


Fig. 2 – The effect of DODAB molar fraction on the melting temperature of DODAB-DODAC mixed vesicles, for total surfactant concentration equals 1.0 mM. $x_{\text{DODAB}} = 0$ and 1 account for the neat DODAC and DODAB vesicles in water, respectively. The dashed line is a sigmoidal fitting to the experimental data.

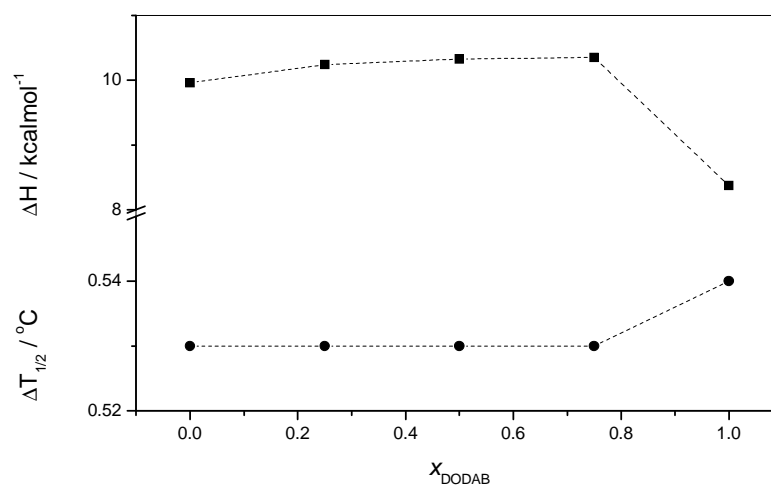


Fig. 3 – The effect of DODAB molar fraction on the enthalpy change and peak width of the main transition for the DODAB-DODAC mixed vesicles, for 1.0 mM total surfactant concentration. $x_{\text{DODAB}} = 0$ and 1 account for the neat DODAC and DODAB vesicles in water, respectively. The dashed lines just connect the experimental data.

The DSC data mainly indicate: (a) T_m of the mixed DODAX vesicles lies between those for the neat surfactants and increases sigmoidally from 45.8 to 48.9 °C with x_{DODAC} , that is, T_m increases with the relative amount of Cl^- ; and (b) DODAC inhibits completely the post-transition and partially the pre-transition of DODAB. Up to $x_{\text{DODAC}} = 0.25$, DODAC decreases T_s from 33.5 to 31.6 °C and T_s vanishes when $x_{\text{DODAC}} > 0.25$. Since the nature of the counterion (Br^- or Cl^-) is the only parameter that is varied in the experiment, most probably such a behavior has to do with the way the counterion is distributed throughout the vesicle interfaces, or the specificity and affinity of the counterion binding. The effect of the counterion on T_m might be related to the effect of the counterion on the vesicle structure and not only on the vesicle size and bilayer compactness, because at a given concentration the structure of DODAB vesicles seems to be more complex than that of DODAC vesicles, as suggested by the three and single peak thermograms for DODAB and DODAC, respectively.

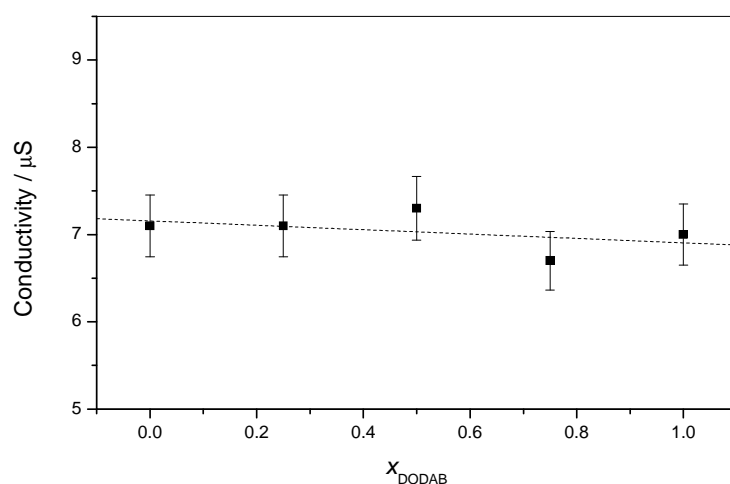


Fig. 4 – Conductivity as a function of x_{DODAB} for DODAB-DODAC mixed vesicles, for 1.0 mM total surfactant concentration and varying the surfactant concentration. Measurements performed at 25 °C. Error bars account for 5% the measured values. The dashed line is a linear fitting to the experimental data.

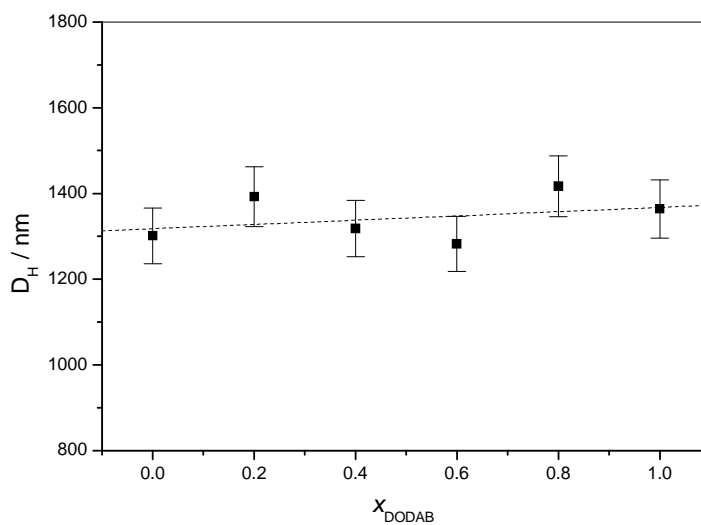


Fig. 5 – Apparent hydrodynamic diameter as a function of x_{DODAB} for DODAB-DODAC mixed vesicles, for 0.5 mM total surfactant concentration and varying the surfactant concentration. Measurements performed at 25 °C. Error bars account for 5% the measured values. The dashed line is a linear fitting to the experimental data.

The differing specificity and affinity of the counterion binding to DODAX vesicles results in the higher T_m of DODAC (Fig. 1) and the constancy of counterion dissociation (Cuccovia et al., 1990), conductivity (Fig. 4) and hydrodynamic diameter (Fig. 5). The interpretation of the data should assume that DODAB and DODAC form similar (unilamellar) vesicle structures, what is mostly likely at the surfactant concentration of 1.0 mM, although DODAB tends to assemble as multi-structural vesicles at lower concentrations than DODAC (Feitosa et al., 2006), as suggested by the more complex DSC thermograms of DODAB (Fig. 1) that indicate more polydisperse vesicle dispersion.

The larger T_m and size of DODAC vesicles relative to DODAB cannot be explained simply by the way the counterions bind to the vesicles and affects the bilayer packing and vesicle size without considering the changes in the vesicle structure, because it is expected that vesicles having larger size and T_m should exhibit more densely packed bilayers. This is

not what is observed for DODAB and DODAC, since it is well accepted that DODAB vesicles are larger than DODAC vesicles (Nascimento et al., 1998; Feitosa et al., 2000; Lopes et al., 2008). In this communication, however, the hydrodynamic diameter of DODAB vesicles is only modestly larger. One should remind that in mixtures of DODAB and DODAC, it is not easy to identify the bound counterions, thus the relative amount of counterion and their characteristics (mainly size and polarity) should be taken into account to fully explain the here reported data. The smaller and more polarizable ion (Br^-) should bind more strongly to the vesicle interfaces.

Even though the main transition is well-defined for both DODAC and DODAB, it requires more energy for DODAC (Fig. 3 and Table 1), indicating that Br^- favors more the transition than Cl^- , in other words, DODAC is more densely packed. Up to ca $x_{\text{DODAC}} = 0.25$ the transition enthalpy change (ΔH) increases from ca 8.4 to 10.4 kcalmol⁻¹, whereas above this concentration it decreases slightly and smoothly (Fig. 3). A correction factor to ion binding should be considered in the calculations of ΔH that takes into account the total concentration of vesiculated DODAX. Overall, the binding of Cl^- to the vesicles interfaces yields an increase in T_m , a decrease in T_s and the inhibition of T_p . The low dissociation degree ($\alpha \approx 0.04$) of DODAB and DODAC large unilamellar vesicles (Cuccovia et al., 1990), indicating high affinity of the counterions to the vesicle interfaces, together with the effect of the counterions on the thermotropic behavior of DODA^+ vesicles (Fig. 2), might be related to the specificity and affinity of the counterion binding to the vesicles because the hydrated Br^- is smaller and more polarizable than Cl^- (Cuccovia et al., 1990; Feitosa et al., 2000). This conclusion is supported by the conductivity, hydrodynamic diameter and degree of counterion dissociation data that are independent on the relative counterion concentration (Figs. 4 and 5), while T_m increases with the relative amount of Cl^- .

Summary and conclusions

When the relative amount of counterions Cl^-/Br^- increases, T_m varies sigmoidally with the inflection point around the equimolar concentration (Fig. 2), whereas the main transition enthalpy change (ΔH) exhibits an initial increase when x_{DODAC} increases to ca 0.25 and then a soft decrease (Fig. 3), reflecting the stronger affinity of Br^- . The peak width ($\Delta T_{1/2}$), on the other hand, is kept roughly constant (Fig. 3), as well as the conductivity and the hydrodynamic diameter, although there is a trend in conductivity and hydrodynamic diameter, respectively to decrease and increase with the relative amount of Br^- . The data thus indicate that the counterion binding specificity and affinity plays important role on the thermotropic behavior and structure of DODAX vesicles. Br^- thus exhibits stronger effect on turning the bilayer more fluid, yielding smaller T_m and only slightly larger vesicles. Most probably Br^- yields change in vesicle structure resulting in more complex vesicle structures, as indicates the DSC thermograms.

Since the counterion influences the vesicle characteristics, the understanding of the effects of the ion binding on the vesicle properties is of great importance in application, for example as catalysts, ion transport, DNA compaction and drug delivery. This work thus allows us to conclude that the properties of DODAX vesicles are sensitive to the counterion nature that have different affinity and bind specifically to the vesicle interfaces resulting in changes in physical and structural characteristics of these vesicles.

Acknowledgments

FRA and EF acknowledge CNPq for PhD and research (Grant 304543/2006-3) grants, respectively. Dr. W. Loh and Dr. M. E. D. Zaniquelli are acknowledged for kindly supplying the DSC and light scattering equipments.

References

- Alves, F.R., Zaniquelli, M.E.D., Loh, W., Castanheira, E.M.S., Real Oliveira, M.E.C.D., Feitosa, E., 2007. Vesicle-micelle transition in aqueous mixtures of the cationic dioctadecyldimethylammonium and octadecyltrimethylammonium bromide surfactants. *J. Colloid Interface Sci.* 316, 132-139.
- Blandamer, M.J., Briggs, B., Cullis, P.M., Last, P., Engberts, J.B.F.N., Kacperska, A., 1999. Effects of added urea and alkylureas on gel to liquid-crystal transitions in DOAB vesicles. *J. Therm. Anal. Cal.* 55, 29-35.
- Brito, R.O., Marques, E.F., 2005. Neat DODAB vesicles: Effect of sonication time on the phase transition thermodynamic parameters and its relation with incomplete chain freezing. *Chem. Phys. Lipids* 137, 18-28.
- Carmona-Ribeiro, A.M., 1992. Synthetic amphiphile vesicles. *Chem. Soc. Rev.* 21, 209–214.
- Cocquyt, J., Olsson, U., Olofsson, G., Van der Meeren, P., 2004. Temperature quenched DODAB dispersions: fluid and solid state coexistence and complex formation with oppositely charged surfactant. *Langmuir* 20, 3906–3912.
- Cuccovia, I.M., Feitosa, E., Chaimovich, H., Sepulveda, L., Reed, W., 1990. Size, electrophoretic mobility, and ion dissociation of vesicles prepared with synthetic amphiphiles. *J. Phys Chem.* 94, 3722-3725.
- Cuccovia, I.M., Chaimovich, H., Lissi, E., Abuin, E., 1990a. Selectivity Coefficients for Iodide/Bromide and Iodide/Chloride Counterion Exchanges at the Surfaces of Dioctadecyldimethylammonium Vesicles. *Langmuir* 6, 1601-1604.
- Cuccovia, I.M., Sesso, A., Abuin, E.B., Okino, P.F., Tavares, P.G., Campos, J.F.S., Florenzano, F.H., Chaimovich, H., 1997. Characterization of dioctadecyldimethylammonium chloride vesicles prepared by membrane extrusion and dichloromethane injection. *J. Mol. Liquids* 72, 323-336.

- Feitosa, E., Barreleiro, P.C.A., 2004. The effect of ionic strength on the structural organization of dioctadecyldimethylammonium bromide in aqueous solution. *Progr. Colloid Polym. Sci.* 128, 163-168.
- Feitosa, E., Barreleiro, P.C.A., Olofsson, G., 2000. Phase transition in dioctadecyldimethylammonium bromide and chloride vesicles prepared by different methods. *Chem. Phys. Lipids* 105, 201–213.
- Feitosa, E., Brown, W., 1997. Fragment and vesicle structures in sonicated dispersions of dioctadecyldimethylammonium bromide. *Langmuir* 13, 4810-4816.
- Feitosa, E., Karlsson, G., Edwards, K., 2006. Unilamellar vesicles prepared by simple mixing dioctadecyldimethylammonium chloride and bromide with water. *Chem. Phys. Lipids* 140, 66-74.
- Fendler, J.H., 1982. *Membrane Mimetic System*; Wiley-Interscience: New York.
- Lasic, D.D., 1993. *Liposomes. From Physics to Application*. Elsevier: Amsterdam.
- Lopes, A., Edwards, K., Feitosa, E., 2008. Extruded vesicles of dioctadecyldimethylammonium bromide and chloride investigated by light scattering and cryogenic transmission electron microscopy. *J. Colloid Interface Sci.* 322, 582-588.
- Nascimento, D.B., Rapuano, R., Lessa, M.M., Carmona-Ribeiro, A.M., 1998. Counterion effects on properties of cationic vesicles. *Langmuir* 14, 7387–7391.
- Romero, A., Tran, C.C., Klahn, P.L., Fendler, J.H., 1978. Drug entrapment in surfactant vesicles. *Life Sci.* 22, 1447-1450.

Artigo 3

Cationic Liposomes in Mixed Didodecyldimethylammonium Bromide and Dioctadecyldimethylammonium Bromide Aqueous Dispersions Studied by Differential Scanning Calorimetry, Nile Red Fluorescence, and Turbidity

Eloi Feitosa,*[†] Fernanda Rosa Alves,[†] Anna Niemiec,[‡] M. Elisabete C. D. Real Oliveira,[§] Elisabete M. S. Castanheira,[§] and Adelina L. F. Baptista[§]

Physics Department, São Paulo State University, São José do Rio Preto, SP, and Instituto de Química, Universidade Estadual de Campinas, Campinas, SP, Brazil, and Physics Department, University of Minho, Campus de Gualtar, 4710-057 Braga, Portugal

Received November 30, 2005. In Final Form: February 14, 2006

The thermotropic phase behavior of cationic liposomes in mixtures of two of the most investigated liposome-forming double-chain lipids, dioctadecyldimethylammonium bromide (DODAB) and didodecyldimethylammonium bromide (DDAB), was investigated by differential scanning calorimetry (DSC), turbidity, and Nile Red fluorescence. The dispersions were investigated at 1.0 mM total surfactant concentration and varying DODAB and DDAB concentrations. The gel to liquid-crystalline phase transition temperatures (T_m) of neat DDAB and DODAB in aqueous dispersions are around 16 and 43 °C, respectively, and we aim to investigate the T_m behavior for mixtures of these cationic lipids. Overall, DDAB reduces the T_m of DODAB, the transition temperature depending on the DDAB content, but the T_m of DDAB is roughly independent of the DODAB concentration. Both DSC and fluorescence measurements show that, within the mixture, at room temperature (ca. 22 °C), the DDAB-rich liposomes are in the liquid-crystalline state, whereas the DODAB-rich liposomes are in the gel state. DSC results point to a higher affinity of DDAB for DODAB liposomes than the reverse, resulting in two populations of mixed DDAB/DODAB liposomes with distinctive phase behavior. Fluorescence measurements also show that the presence of a small amount of DODAB in DDAB-rich liposomes causes a pronounced effect in Nile Red emission, due to the increase in liposome size, as inferred from turbidity results.

Introduction

The mixture of lipids in solution is a promising field of research, since it can be used to monitor the structure and phase behavior of lipid mixtures suitable for specific applications in science and technology; such applications may require sample preparation with well-controlled properties.^{1–5} The mixture of lipids in solution can thus be used to modify the phase behavior of the individual lipids by varying the lipid composition in the mixture and monitoring some physical properties of these mixtures.

Mixtures of lipids can also be used to control specific properties of the aggregates by investigating the interaction with other systems. For example, to overcome the precipitation problems related to the strong interaction of polyelectrolytes with oppositely charged lipids, a copolymer with neutral or opposite charge is often added to the main lipid, to reduce electrostatic effects. Homologue lipids can also be mixed to change properties such as the aggregate size and architecture and chain conformation in the lipid aggregates.

The homologue double-chain liposome-forming cationic lipids dioctadecyldimethylammonium bromide (DODAB) and didodec-

yltrimethylammonium bromide (DDAB) have been some of the most investigated cationic lipids,⁶ and liposome formation in aqueous solutions of these lipids is extensively reported,^{7–9} but the literature is scarce on the liposome formation in aqueous mixtures of these surfactants. The difference in chain length of these lipids (C_{18} and C_{12}) yields interesting characteristics and behavior for mixed solutions of these lipids, as shown in this paper.

It has been reported that micelle-forming nonionic surfactants reduce¹⁰ whereas cationic surfactants tend to increase¹¹ the T_m of DODAB. Cationic liposomes also interact with DNA to form cationic lipid–DNA complexes, resulting in DNA condensation, where the key role of cationic lipids is to provide an electrostatic attraction between the positively charged liposome and the negatively charged DNA molecule.^{12–15}

Steady-state fluorescence spectroscopy has been used to characterize the properties of cationic liposomes, such as

(6) Bunton, C. A. In *Cationic surfactants*. *Physical Chemistry*; Rubingh, D. N., Holland, P. M., Eds.; Surfactant Science Series, Vol. 37; Dekker: New York, 1991.

(7) Kunitabe, T.; Okahata, Y. *J. Am. Chem. Soc.* **1977**, *99*, 3860.

(8) Cuccovia, I. M.; Feitosa, E.; Chaimovich, H.; Sepulveda, L.; Reed, W. F. *J. Phys. Chem.* **1990**, *94*, 3722.

(9) Proverbik, Z. E.; Schulz, P. C.; Puig, J. E. *Colloid Polym. Sci.* **2002**, *280*, 1045.

(10) Barreiros, P. C. A.; Okofsson, G.; Borassi, N. M.; Feitosa, E. *Langmuir* **2002**, *18*, 1024.

(11) Kacperska, A. J. *Therm. Anal.* **1995**, *45*, 703.

(12) Campbell, R. B. *Biochim. Biophys. Acta* **2001**, *1512*, 27.

(13) Felgner, P. L.; Gadek, T. R.; Holm, M.; Roman, R.; Chan, H. W.; Wenz, M.; Northrop, J. P.; Ringold, G. M.; Danielsen, M. *Proc. Natl. Acad. Sci. U.S.A.* **1987**, *84*, 7413.

(14) Farhood, H.; Serbira, N.; Huang, L. *Biochim. Biophys. Acta* **1995**, *1235*, 289.

(15) Pires, P.; Simões, S.; Nir, S.; Gaspar, R.; Duzgunes, N.; Pedrosa de Lima, M. C. *Biochim. Biophys. Acta* **1999**, *1418*, 71.

* To whom correspondence should be addressed. Phone: +55 17 3221 22 40. Fax: +55 17 3221 22 47. E-mail: eloi@ibilce.unesp.br.

[†] São Paulo State University.

[‡] Universidade Estadual de Campinas.

[§] University of Minho.

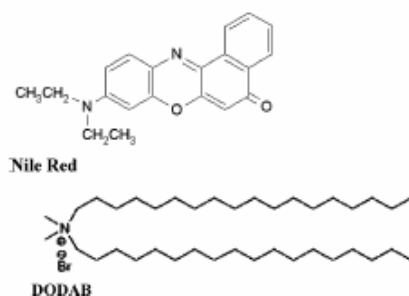
(1) Lasic, D. D. *Liposomes. From Physics to Applications*; Elsevier: Amsterdam, 1993.

(2) Fendler, J. H. *Membrane Mimetic Chemistry*; Wiley-Interscience: New York, 1982.

(3) Jönsson, B.; Lindman, B.; Holmberg, K.; Kromberg, B. *Surfactants and Polymers in Aqueous Solution*; John Wiley & Sons: New York, 1998.

(4) Evans, D. F.; Wennerström, H. *The Colloidal Domain, where Physics, Chemistry, Biology and Technology Meet*; VCH Publishers: New York, 1999.

(5) Rosoff, M., Ed. *Vesicles*; Marcel Dekker: New York, 1996.

Scheme 1. Molecular Structures of Nile Red and DODAB

hydration, polarity, and fluidity.^{16,17} The fluorescent probe chosen for this work, Nile Red, is hydrophobic with low solubility and fluorescence in water,¹⁸ and its potential application to the study of biological membranes has been demonstrated.^{19–22} It is highly solvatochromic, and both steady-state and time-resolved fluorescence emission properties are strongly medium dependent. Nile Red usually exhibits an increase in fluorescence yield with decreasing solvent polarity accompanied by a blue shift in the emission peak.^{18,23,24}

DSC has also widely been employed to investigate the phase behavior of liposomes both in the absence and in the presence of additives.^{25–31} Thus, the combination of these two methods may give important information about liposome systems, such as the DODAB/DDAB mixed system investigated here.

The work aims to characterize the thermotropic phase behavior of cationic liposome dispersions in mixtures of DDAB and DODAB by using differential scanning calorimetry (DSC) and fluorescence spectroscopy. The results undoubtedly indicate the formation of two populations of liposomes with distinctive properties. The turbidity of the mixture dispersion is dominated by the gel state, rather than by the liquid-crystalline state of the liposomes.

Experimental Section

Materials. DODAB, DDAB, and Nile Red (9-(diethylamino)-5H-benzof[α]phenoxazin-5-one) were supplied by Aldrich. All chemicals were used as received. Scheme 1 shows the molecular structures of DODAB and Nile Red. DDAB has a chemical structure similar to that of DODAB, except for the shorter C₁₂ double chain, instead of the C₁₈ DODAB.

Liposome Preparation. Stock solutions of DODAB and DDAB liposome dispersions were prepared by simple dilution of 5.0 mM lipid in water at room temperature (ca. 22 °C). The DODAB/water

mixture was then warmed to 60 °C (safely above the DODAB $T_m \approx 43$ °C) for complete DODAB solubilization.^{10,25} Since the DDAB T_m is lower than room temperature, this lipid was mixed with the aqueous solvent at room temperature and kept standing for at least 24 h. After solubilization, both lipid dispersions were kept standing at room temperature and stored. Mixed DODAB/DDAB aqueous dispersions were prepared by mixing properly 1.0 mM aqueous dispersions of DODAB and DDAB to have 1.0 mM total lipid concentration and varying the individual lipid concentrations.

For fluorescence measurements, the DODAB/DDAB aqueous mixtures were sonicated at 60 °C in a bath-type sonicator (Heat Systems W-225R), to obtain optically clear dispersions with the probes incorporated within the liposome bilayer.^{20,22} A final concentration of 3 μ M Nile Red was introduced in the liposome dispersions by injection of 10 μ L of a 10^{-3} M stock solution of this probe in ethanol. The liposome dispersions were cooled to room temperature and stored for 24 h prior to the measurements.

DODAB and DDAB liposomes, prepared by simply mixing the lipids or by sonication in aqueous solution, above their T_m , are mainly unilamellar.^{25–29} The same is expected to happen in DODAB/DDAB mixtures at different fractions of each lipid.

The DODAB molar fraction, x_{DODAB} , in the dispersions is given by eq 1 such that $x_{\text{DODAB}} + x_{\text{DDAB}}$ equals unity.

$$x_{\text{DODAB}} = \frac{[\text{DODAB}]}{[\text{DDAB}] + [\text{DODAB}]} \quad (1)$$

High-Sensitivity Differential Scanning Calorimetry Measurements. A VP-DSC (MicroCal, Northampton, MA) calorimeter equipped with 0.542 mL twin cells for the reference and sample solutions was used. The measurements for 1.0 mM total lipid concentration and varying DODAB and DDAB concentration were performed with a scan rate of 1 °C/min and in the temperature range of 5–80 °C. This method is useful for observing, for example, the gel to liquid crystal phase transition temperature that takes place in the system. Moreover, it enables one to find T_m , which is the temperature at the peak maximum. The enthalpy change associated with each transition was calculated from integration of the calorimetric curves using the equipment software (MicroCal Origin, v. 5.0). Further details on the DSC methods and setup can be found in previous papers.^{16,25,27}

Fluorescence Measurements. Fluorescence measurements were performed using a Spex Fluorolog 2 spectrofluorimeter. Polarized emission spectra were recorded using Glan-Thompson polarizers. All spectra were corrected for the instrumental response of the system.

Turbidity Measurements. Turbidity data were collected using a Cary 100 Scan spectrophotometer equipped with a quartz cuvette of 1.0 cm path length.

Results and Discussion

DSC Results. The DSC traces for neat DODAB and DDAB in water and mixtures of these surfactants, for selected concentrations such that the total lipid concentration equals 1.0 mM, are shown in Figures 1 and 2, respectively, for the first and second upscans. In dilute dispersions the T_m of these neat surfactants is constant (results not shown). All DSC traces were repeated twice, and the first and second upscans recorded. The pre-scanning time, that is, the waiting time to start the second upscan after the sample being cooled, was 20 min. At 1.0 mM the DSC traces for the neat DDAB and DODAB dispersions exhibit a single narrow peak, characteristic of the main gel to liquid crystalline phase transition (melting) temperature. The positions of these peaks, at $T_{m(1)} \approx 16$ °C and $T_{m(2)} \approx 43$ °C, give the melting temperatures of DDAB and DODAB,^{25,28} here referred to as the lower and higher main transition temperatures, $T_{m(1)}$ and $T_{m(2)}$, for the DDAB/DODAB system. The parameters T_m , $\Delta T_{1/2}$, and ΔH obtained from these traces are summarized in Tables 1 and 2, respectively, for the first and second upscans.

- (16) Zuidam, N. J.; Barenholz, Y. *Biochim. Biophys. Acta* **1997**, *1329*, 211.
- (17) Hirsch-Lerner, D.; Barenholz, Y. *Biochim. Biophys. Acta* **1998**, *1370*, 17.
- (18) Hungerford, G.; Castanheira, E. M. S.; Real Oliveira, M. E. C. D.; Miguel, M. G.; Burrows, H. D. *J. Phys. Chem. B* **2002**, *106*, 4061.
- (19) Greenspan, P.; Fowler, S. D. *J. Lipid Res.* **1985**, *26*, 781.
- (20) Krishnamoorthy, I. G. *J. Phys. Chem. B* **2001**, *105*, 1484.
- (21) Coutinho, P. J. G.; Castanheira, E. M. S.; Rei, M. C.; Real Oliveira, M. E. C. D. *J. Phys. Chem. B* **2002**, *106*, 12841.
- (22) Hungerford, G.; Castanheira, E. M. S.; Baptista, A. L. F.; Coutinho, P. J. G.; Real Oliveira, M. E. C. D. *J. Fluoresc.* **2005**, *15*, 835.
- (23) Krishna, M. M. G. *J. Phys. Chem. A* **1999**, *103*, 3589.
- (24) Ghoneim, N. *Spectrochim. Acta, A* **2002**, *50*, 1003.
- (25) Feitosa, E.; Barreiro, P. C. A.; Olofsson, G. *Chem. Phys. Lipids* **2000**, *105*, 201.
- (26) Benatti, C. R.; Feitosa, E.; Fernandez, R. M.; Lamy-Frenkel, M. T. *Chem. Phys. Lipids* **2001**, *111*, 93.
- (27) Benatti, C. R.; Tiera, M. J.; Feitosa, E.; Olofsson, G. *Thermochim. Acta* **1999**, *328*, 137.
- (28) Marques, E. F.; Khan, A.; Lindman, B. *Thermochim. Acta* **2002**, *394*, 31.
- (29) Schulz, P. C.; Puig, J. E.; Barreiro, G.; Torres, L. A. *Thermochim. Acta* **1994**, *231*, 239.
- (30) Blankamer, M. J.; Briggs, B.; Cullis, P. M.; Kirby, S. D.; Engberts, J. B. F. *N. J. Chem. Soc., Faraday Trans.* **1997**, *93*, 453.
- (31) Feitosa, E.; Barreiro, P. C. A. *Prog. Colloid Polym. Sci.* **2004**, *128*, 163.

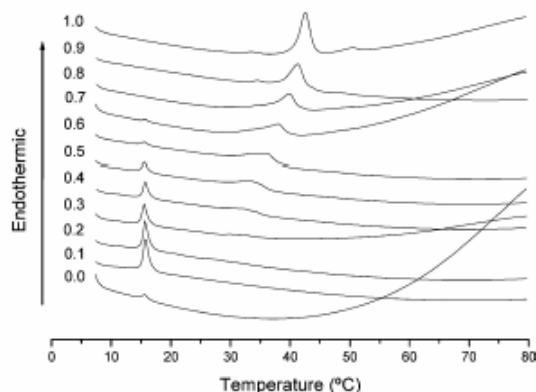


Figure 1. First DSC upscan for the mixture DODAB/DDAB/water, for 1.0 mM total lipid concentration. Numbers beside the curves correspond to the DODAB molar fraction, x_{DODAB} .

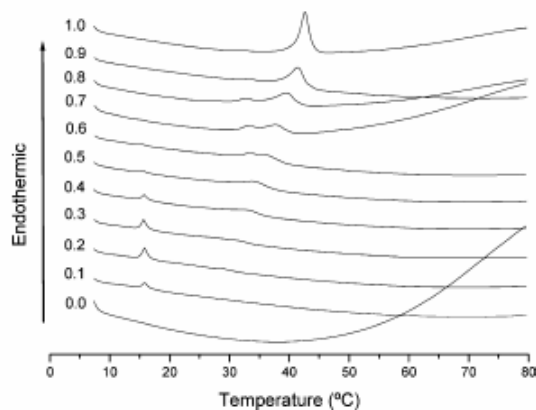


Figure 2. Second DSC upscan for the mixture DODAB/DDAB/water, for 1.0 mM total lipid concentration. Numbers beside the curves correspond to the DODAB molar fraction, x_{DODAB} .

Table 1. Parameters Obtained from the First DSC Upscan (Figure 1)

x_{DODAB}	$T_{m(1)}$ (°C)	$\Delta H_{(1)}$ (kcal/mol)	$\Delta T_{1/2(1)}$ (°C)	$T_{m(2)}$ (°C)	$\Delta H_{(2)}$ (kcal/mol)	$\Delta T_{1/2(2)}$ (°C)
0.0	15.63	0.96	1.33			
0.1	15.62	4.3	1.06			
0.2	15.65	3.8	1.06			
0.3	15.59	3.3	0.80	32.28	4.9	5.03
0.4	15.75	3.0	0.79	32.16	3.1	5.29
0.5	15.62	2.2	0.80	33.35	6.5	4.76
0.6	15.61	1.2	1.06	36.26	7.0	4.23
0.7	15.58	1.0	1.06	37.89	8.2	4.77
0.8				39.89	8.9	3.17
0.9				41.41	8.1	2.64
1.0				42.71	9.8	1.85

Note that there is no peak for the neat DDAB in the second upscan (Figure 2). This is because a longer prescanning time should be used (longer than the 20 min we used for the prescanning time in this work). After being cooled, the sample requires a time long enough for the surfactants to rearrange into the gel state of the liposome bilayer to attain a kinetic equilibrium. Of course, this time is system dependent. Accordingly, Figure 3 shows the effect of the prescanning time of 0, 0.4, 0.5, 1.0, 2.0, and 4.0 h on the DSC traces for 5.0 mM DDAB. For 1.0 mM DDAB, the peak intensity is even lower, and the prescanning time required

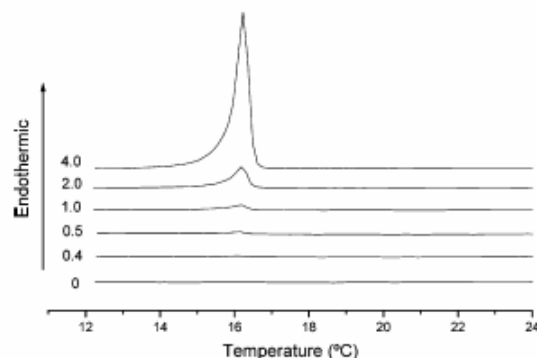


Figure 3. Effect of the prescanning time on the DSC thermograms for a 5.0 mM DDAB aqueous solution. Numbers beside the curves indicate the prescanning time in hours.

Table 2. Parameters Obtained from the Second DSC Upscan (Figure 2)

x_{DODAB}	$T_{m(1)}$ (°C)	$\Delta H_{(1)}$ (kcal/mol)	$\Delta T_{1/2(1)}$ (°C)	$T_{m(2)}$ (°C)	$\Delta H_{(2)}$ (kcal/mol)	$\Delta T_{1/2(2)}$ (°C)	
0.0							
0.1	15.87	0.8	0.79				
0.2	15.85	1.6	0.79	29.08	1.6	2.38	
0.3	15.66	1.6	0.79	31.80	2.6	5.03	
0.4	15.79	1.0	0.79	33.52	1.8	3.17	
0.5	15.62	0.3	0.79	34.67	3.1	3.70	
0.6				1.59	36.40	1.0	2.39
0.7				1.59	37.99	1.6	2.65
0.8				2.39	39.52	2.9	2.91
0.9					41.62	6.1	2.38
1.0					42.60	9.2	1.85

Table 3. Parameters Obtained from the First DSC Upscan, for Different Prescanning Times (Figure 3)

prescanning time (h)	T_m (°C)	$T_{1/2}$ (°C)	ΔH (kcalmol ⁻¹)
0	15.84	0.53	$0.84 \cdot 10^{-3}$
0.4	16.15	0.53	$6.97 \cdot 10^{-3}$
0.5	16.16	0.40	0.011
1.0	16.20	0.40	0.036
2.0	16.20	0.40	0.12
4.0	16.22	0.40	0.83

to have a measurable peak is even larger (larger than 4 h, results not shown). The T_m for 1.0 and 5.0 mM neat DDAB equals 16.2 °C. These curves clearly indicate that, for low prescanning times, the main transition peak does not come up, owing to kinetic reasons as proposed by Blandamer and co-workers;³⁰ that is, the surfactants do not have enough time to rearrange into the liposome bilayer in the gel (more rigid) state of the chains. Interestingly, the prescanning time affects only the peak intensity and the area (proportional to the melting enthalpy of the surfactant chains), but not to the peak position (related to the surfactant T_m). Table 3 summarizes the T_m , $\Delta T_{1/2}$, and ΔH for DDAB at increasing prescanning time up to 4 h. These results indicate that T_m and $\Delta T_{1/2}$ are roughly constant, but ΔH increases roughly exponentially with the prescanning time (curve not shown).

Depending on the lipid relative concentration, the DODAB/DDAB mixtures exhibit one or two main peaks in the DSC thermograms (additional peaks may appear, owing to the pretransition or posttransition observed for the neat DODAB, as discussed below). The main peaks for the mixtures approach the position of the main transition temperatures for the neat surfactants when the molar fraction of the other surfactant goes to zero, and the peak position varies systematically (or not) with surfactant

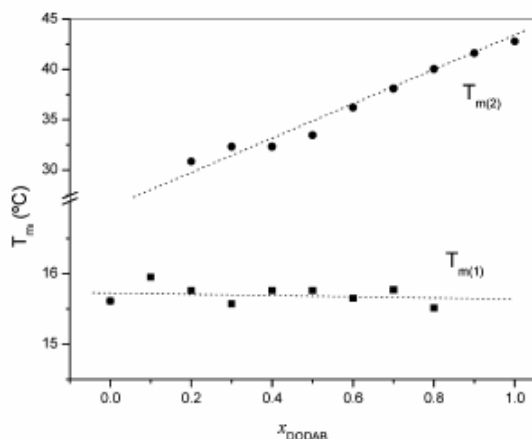


Figure 4. Effect of DODAB or DDAB concentration on T_m of the mixture DODAB/DDAB/water, for 1.0 mM total lipid concentration. DSC data were obtained from the first upscan.

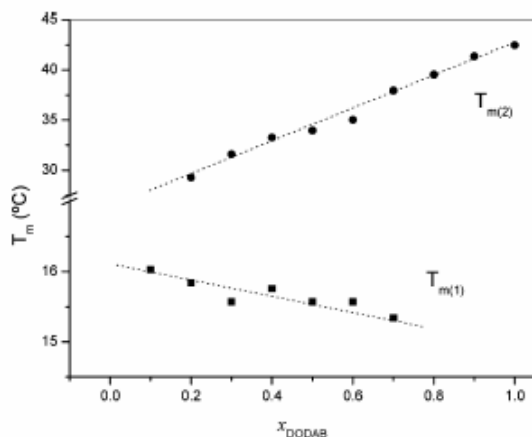


Figure 5. Effect of DODAB or DDAB molar fraction on T_m of the mixture DODAB/DDAB/water, for 1.0 mM total lipid concentration. DSC data were obtained from the second upscan.

composition, as Figures 4 and 5 indicate. In fact, the lower $T_{m(1)}$ is roughly constant with x_{DODAB} and equals T_m for the neat DDAB, but $T_{m(2)}$ decreases from T_m of neat DODAB when x_{DDAB} is augmented (see also Tables 1 and 2). For a DODAB molar fraction around 0.2–0.8 (or 0.2–0.7 in the second upscan) two main peaks are present, indicating the presence of two different populations of DDAB-rich and DODAB-rich liposomes, with well-defined melting temperatures, $T_{m(1)}$ and $T_{m(2)}$.

The neat DODAB liposomes exhibit two additional peaks that are related to the pretransition ($T_s \approx 33.2$ °C) and posttransition ($T_p \approx 53$ °C) temperatures, as reported before.²⁵ In the presence of a small amount of DDAB, the posttransition temperature vanishes, but the pretransition temperature remains; upon increasing further the amount of DDAB the upper $T_{m(2)}$ decreases and the main peak approaches and overlaps the pretransition peak, thus resulting in a broad peak (Figures 1 and 2). The effects of solutes and cosurfactants on the pre- and posttransition temperatures of DODAB liposomes have been reported, and it is shown that these peaks are sensitive to cosolutes and cosurfactants, in addition to the surfactant concentration itself (they tend to increase intensity with surfactant concentration).³¹

One should remember that it is an ordinary procedure running two or more DSC scans to check reproducibility. In some respects, the second (or higher) upscan does not fit the first one, for example, due to kinetic control; in this case, as discussed above, a longer pre-scanning time is required,³⁰ or alternatively the system may not be reversible, giving different traces. After the first cooling, the neat DDAB sample requires a longer time to attain equilibrium before being rescanned, as Figure 3 suggests. This can explain the absence of a peak in the second DSC upscan for DDAB/water shown in Figure 2. Note that these traces give slightly higher $T_m = 16.2$ °C relative to that reported in Table 1 ($T_m = 15.6$ °C). Upon sample dilution to 1.0 mM, we got the same 16.2 °C for T_m . Since this was a new sample preparation, we may infer that the actual T_m for DDAB lies in the range 15.6–16.2 °C, in good accord with literature data.²⁸ The mean T_m obtained from these two values is 15.9 °C.

First Upscan. According to Figure 4, the lower $T_{m(1)}$ for the neat DDAB is 15.6 °C as obtained by the first DSC upscan, in good agreement with data from the literature.^{28,29} Upon increasing x_{DODAB} (thus decreasing x_{DDAB}), $T_{m(1)}$ remains roughly constant and equals T_m for the neat DDAB, showing that DODAB does not affect the DDAB T_m until $x_{\text{DODAB}} \approx 0.8$, when the corresponding transition peak vanishes, probably because of the low intensity of the DSC signal owing to the low x_{DODAB} (~ 0.2), that is, partially solubilized within the bilayers of DODAB liposomes. When x_{DODAB} exceeds 0.2, a second peak appears around 30 °C, corresponding to the upper melting temperature $T_{m(2)}$. As x_{DODAB} is further increased, $T_{m(2)}$ increases linearly to attain the T_m for 1.0 mM neat DODAB ($x_{\text{DODAB}} = 1$). These results indicate that the DDAB incorporation into DODAB liposomes yields a higher bilayer fluidity of DODAB-rich liposomes, leading to a decrease in the DODAB melting temperature $T_{m(2)}$, as x_{DDAB} is increased. DODAB, on the other hand, poorly incorporates into the DDAB-rich liposomes, thus leaving the DDAB T_m roughly constant. Overall, the results suggest that DODAB and DDAB do not mix ideally to get homogeneous mixed DODAB/DDAB liposomes with, say, a T_m varying systematically between $T_{m(1)}$ and $T_{m(2)}$ for the neat lipids. It seems that DDAB has more affinity for DODAB than the reverse, as can be inferred by the monotonic decrease in $T_{m(2)}$ upon increasing x_{DODAB} and constancy of $T_{m(1)}$ upon increasing x_{DDAB} . Probably this is related to the shorter chain length of DDAB relative to DODAB, which favors the binding of DDAB to the DODAB liposomes.

Tables 1 and 2 summarize the parameters T_m , $\Delta T_{1/2}$, and ΔH associated with the lower and upper melting temperatures for the DODAB/DDAB/water system obtained from the first and second upscans (discussed below). Accordingly, as x_{DODAB} increases, the cooperativity (as measured by the peak width) of the lower transition does not change very much ($\Delta T_{1/2(1)}$ is grossly constant), but that for the upper transition tends to decrease ($\Delta T_{1/2(2)}$ increases). This indicates a higher solubility of DDAB into DODAB liposomes than the opposite, since mixed lipids exhibit a less cooperative melting transition relative to a neat lipid. The enthalpy of the upper transition $\Delta H_{(2)}$ increases with x_{DODAB} , but decreases for the lower transition, after an initial steep increase at low x_{DDAB} ; that is, $\Delta H_{(1)}$ increases with increasing x_{DDAB} . One should note that the values of the melting enthalpy for DDAB and DODAB shown in Tables 1 and 2 were calculated per mole of DDAB and DODAB in each liposome population. These values should be calculated per mole of lipids within each population of liposomes, but this is an unknown parameter. Thus, we refer to this calculated enthalpy as an apparent enthalpy, since we

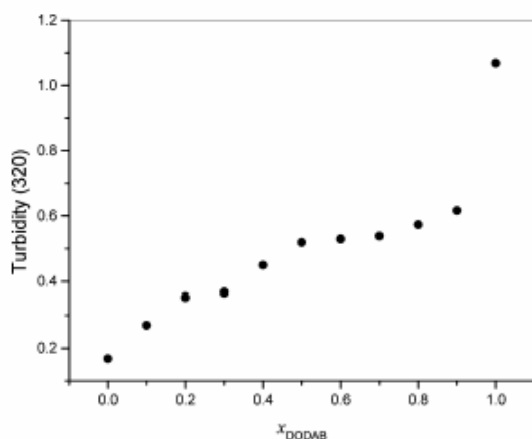


Figure 6. Turbidity (320 nm) as a function of DODAB molar fraction for the mixture DODAB/DDAB/water and 1.0 mM total lipid concentration.

cannot precisely determine from the experiments presented here the actual concentrations of these surfactants in each population.

Second Upscan. The second upscan gives roughly the same result as the first scan, except for the lower $T_{m(1)}$ that decreases slightly with x_{DODAB} (instead of being constant as observed for the first scan) (Figure 5). In this case, after the first upscan, there is a bit higher affinity of DDAB liposomes for DODAB molecules, so that the incorporation of some DODAB molecules into DDAB liposomes takes place, $T_{m(1)}$ decreasing slightly. Alternatively, the decrease in $T_{m(1)}$ may be due to kinetic effects as discussed above, but this is less probable, since T_m does not depend on the number of scans (whether first or second), as suggested by Figure 3 and Table 3. One should remember that there is a general trend of the liposome T_m to vary with the concentration of added surfactant, and the extent of this change depends on the surfactant and liposome characteristics.^{10,11} The stronger affinity of DODAB toward DDAB liposomes relative to that suggested by the first upscan is probably related to an additional amount of DODAB molecules that join the DDAB-rich liposomes during the second upscan. Also, the decrease in $T_{m(1)}$ upon addition of DODAB indicates that a few more DODAB molecules are solubilized into DDAB-rich liposomes, to form DODAB-in-DDAB liposomes. Otherwise, if DDAB-in-DODAB liposomes were formed, an increase in $T_{m(1)}$ would be observed, since the surfactant T_m increases with the surfactant chain length; that is, $T_{m(2)}$ is always larger than $T_{m(1)}$.³²

Grossly the same behavior was observed for the parameters obtained from the second upscan (Table 2) relative to those obtained from the first upscan (Table 1); an exception is for the lower $T_{m(1)}$, which decreases slightly instead of being constant, as discussed above. Furthermore, for $x_{\text{DODAB}} = 0.6, 0.7,$ and 0.8 , the peaks for the pretransition and the main transition temperatures overlap, and we used the deconvolution method to calculate the area of the overlapped peaks and thus the chain melting enthalpy for this upper transition. The apparent ΔH_{T_2} was calculated per mole of DODAB as discussed above for the data shown in Table 1.

Turbidity Results. Figure 6 shows the effect of x_{DODAB} on the turbidity, measured at 320 nm and 22 °C, for mixed DDAB/DODAB aqueous dispersions. It can be seen that as the DODAB molar fraction is increased the turbidity increases smoothly up

[32] Feitosa, E.; Jansson, J.; Lindman, B. *Chem. Phys. Lipids*, in press.

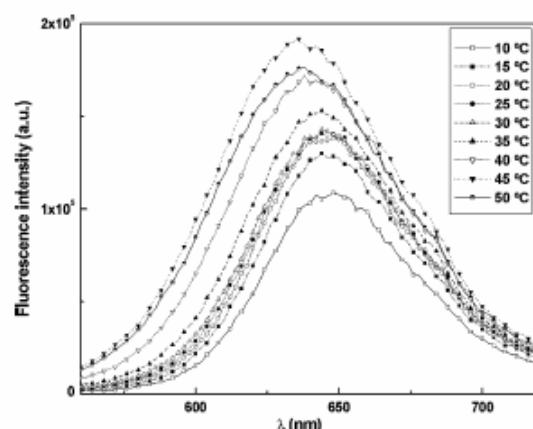


Figure 7. Nile Red emission spectra in DODAB liposomes at several temperatures ($\lambda_{\text{exc}} = 550$ nm).

to $x_{\text{DODAB}} \approx 0.9$. Then the turbidity increases steeply to attain the turbidity for the neat DODAB liposomes (Figure 6), indicating a change of size or liposome structure.

The hydrodynamic radius (R_h) of the cationic liposomes investigated here was reported before.^{33–36} For DDAB and DODAB spontaneously formed liposomes, $R_h = 350$ Å³³ and 3370 Å,³⁴ respectively. After bath sonication of the dispersion, R_h of the DODAB liposomes drops to 22 Å,³⁵ or 325 Å after tip sonication.³⁶

Fluorescence Results. Nile Red in the Neat DODAB and DDAB Liposomes. Nile Red is a well-known solvatochromic probe, which in polar media exhibits a red shift in the emission maximum, together with fluorescence quenching. Owing to its capability to establish H-bonds with protic solvents, Nile Red fluorescence in water is very weak and red shifted ($\lambda_{\text{max}} \approx 660$ nm).¹⁸ Nile Red has been used as a lipid probe, due to its hydrophobic nature.^{19–22} Figure 7 shows the emission spectra of Nile Red incorporated into pure DODAB liposomes at different temperatures. Accordingly, the fluorescence intensity increases until ca. 45 °C, corresponding grossly to the melting temperature T_m of neat DODAB, and decreases thereafter.

A significant blue shift in the emission spectrum is also observed with the temperature increase in the DODAB gel phase (until ca. 45 °C), giving an indication that Nile Red feels a more hydrophobic environment when the temperature is raised. This effect exceeds the usual fluorescence quenching with temperature (due to the increase of the competitive nonradiative processes). At low temperature (10 °C), the Nile Red emission maximum ($\lambda_{\text{max}} \approx 650$ nm) is close to the value in water,¹⁸ indicating that the probe is located in a water-rich environment. In the fluid liquid-crystalline phase (50 °C), the opposite behavior is observed (lower emission intensity and a small red shift).

For DDAB liposomes, the Nile Red fluorescence intensity decreases with increasing temperature (Figure 8), as expected from the increase of nonradiative pathways. A monotonic red shift is observed when the temperature increases. In the temperature range investigated (10–50 °C), Nile Red seems not to be sensitive to the DDAB transition temperature ($T_m \approx 16$ °C; see Table 1).

[33] Marques, E. F.; Rogev, O.; Khan, A.; Miguel, M. G.; Lindman, B. *J. Phys. Chem.* 1999, 103, 8353.

[34] Feitosa, E.; Karlsson, G.; Edwards, K. *Chem. Phys. Lipids*, in press.

[35] Feitosa, E.; Brown, W. *Langmuir* 1997, 13, 4810.

[36] Cuccovia, I. M.; Feitosa, E.; Chaimovich, H.; Sepulveda, L.; Reed, W. *J. Phys. Chem.* 1990, 94, 3722.

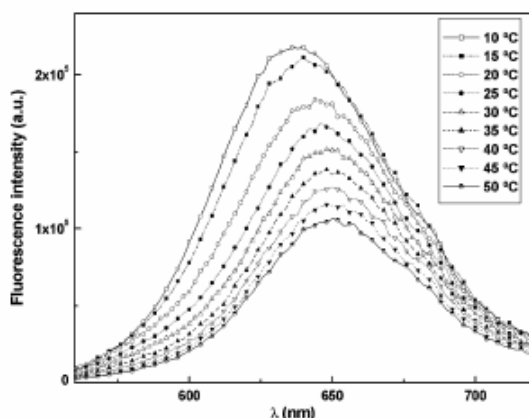


Figure 8. Nile Red emission spectra in DDAB liposomes at several temperatures ($\lambda_{exc} = 550$ nm).

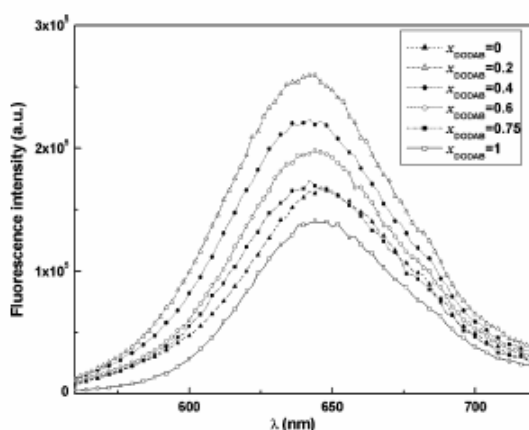


Figure 9. Nile Red emission spectra in DODAB/DDAB mixed liposomes, at several DODAB molar fractions, at 25 °C ($\lambda_{exc} = 550$ nm).

Nile Red Fluorescence in DDAB/DODAB Mixed Systems. Figure 9 shows the emission spectra for DDAB/DODAB mixed liposomes at 25 °C, at various DODAB molar fractions, x_{DODAB} . In all cases, the emission spectrum is a broad structureless band, but the relative fluorescence yield of Nile Red depends on the surfactant molar fraction. The lower fluorescence emission of Nile Red in neat DODAB liposomes ($x_{DODAB} = 1$) compared to that for the neat DDAB ($x_{DODAB} = 0$) indicates that Nile Red is more exposed to the water phase in the neat DODAB liposomes (which are in the gel phase, i.e., below T_{m2}) ≈ 43 °C) relative to the neat DDAB ones (which are in the liquid-crystalline phase, i.e., above T_{m1}) ≈ 16 °C). When the DDAB fraction increases (DODAB decreases), the emission intensity of Nile Red also increases (except for the neat DDAB). This indicates that when DDAB molecules incorporate into DODAB liposomes, Nile Red can penetrate deeper into the liposome bilayer, thus being less exposed to water. This is probably caused by the increasing fluidity of the membrane upon DDAB addition. In neat DDAB liposomes ($x_{DODAB} = 0$), Nile Red emission is significantly lower than for $x_{DODAB} = 0.2$, indicating that DDAB liposomes are smaller structures with a higher curvature, as shown by turbidity measurements, where the probe environment is more water rich.

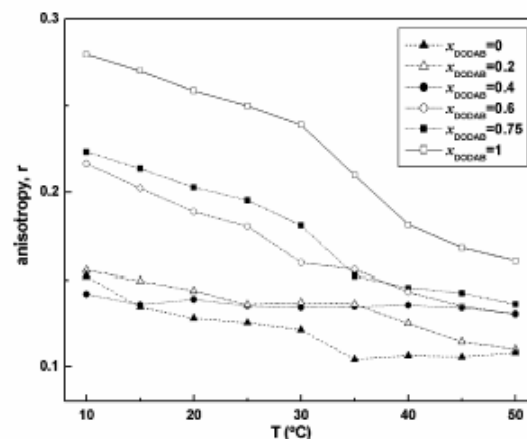


Figure 10. Nile Red steady-state anisotropy in DODAB/DDAB mixed liposomes with increasing temperature for several DODAB molar fractions.

Figure 10 shows the average steady-state anisotropy of Nile Red in DODAB/DDAB liposomes with increasing temperature for several surfactant molar fractions. The anisotropy, r , is given by eq 2, where I_{VV} and I_{VH} are the emission spectra obtained

$$r = \frac{I_{VV} - GI_{VH}}{I_{VV} + 2GI_{VH}} \quad (2)$$

with vertical and horizontal polarization, respectively (for excitation with vertically polarized light), and G is the instrumental correction factor, given by

$$G = I_{HV}/I_{HH} \quad (3)$$

where I_{HV} and I_{HH} are the emission spectra obtained with vertical and horizontal polarization (for excitation with horizontally polarized light).

The steady-state anisotropy has a pronounced decrease upon gel to liquid-crystalline transition. The results in Figure 10 indicate that the DODAB transition temperature is lower in the mixed systems, while the phase transition is attenuated, being completely removed for lower fractions of DODAB ($x_{DODAB} \leq 0.4$).

Figure 11 shows the variation of the total fluorescence intensity ($I_{total} = I_{VV} + 2GI_{VH}$) with temperature for several lipid concentrations. For neat DODAB liposomes ($x_{DODAB} = 1$) a maximum is observed around the phase transition temperature (ca. 45 °C), followed by a decrease in emission intensity. At high DODAB concentrations ($x_{DODAB} > 0.5$), a similar but weaker trend can be seen, with the emission maximum now being observed around 40 °C.

For higher DDAB concentrations ($x_{DODAB} \leq 0.6$), a slight emission maximum is observed at 10–15 °C. This can be an indication of the presence of quasi-neat DDAB liposomes, as inferred from DSC results. Above 15 °C and $x_{DODAB} \leq 0.4$, the emission decreases with temperature, indicating that the systems rich in DDAB are mainly in the liquid-crystalline phase above 15 °C (DDAB T_m).

The DODAB-rich systems ($x_{DODAB} \geq 0.6$) are predominantly in the gel phase until ca. 35 °C, with the transition temperature depending on the DODAB content (ca. 40 °C for 75% DODAB and between 35 and 40 °C for 60% DODAB). These figures are in good agreement with those obtained by DSC reported above.

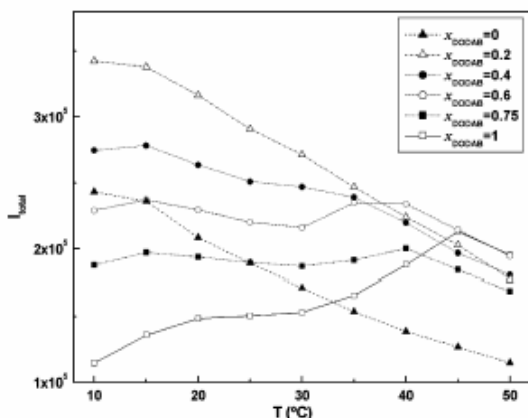


Figure 11. Variation of Nile Red total fluorescence intensity in DODAB/DDAB mixed liposomes with increasing temperature for several DODAB molar fractions.

Conclusions

The melting temperature (or gel to liquid-crystalline phase transition temperature) of mixed cationic liposomes composed of DDAB and DODAB were investigated by DSC and fluorescence of Nile Red. Depending on the surfactant composition, the system exhibits one or two melting temperatures, $T_{m(1)}$ and $T_{m(2)}$, owing to the existing two liposome populations with very distinctive characteristics. At room temperature, the population of DODAB-rich liposomes is in the gel state while

the other population of DDAB-rich liposomes is in the liquid-crystalline state. Accordingly, the upper $T_{m(2)}$ of DDAB-in-DODAB liposomes decreases with x_{DDAB} , owing to the incorporation of DDAB into the DODAB bilayer, and the mixed liposomes are in the gel state at room temperature. Therefore, DDAB increases the fluidity of DDAB-in-DODAB liposomes. When DDAB is the major component, DODAB seems to migrate to less extent into the DDAB bilayer, probably due to its longer chains, and the lower $T_{m(1)}$ is roughly constant (first DSC upscan) or decreases slightly (second DSC upscan) with increasing x_{DODAB} . These results suggest that there is more affinity of DDAB for DODAB liposomes than the reverse, resulting in a higher incorporation of DDAB into DODAB-rich liposomes than the opposite.

Nile Red fluorescence results corroborate that DDAB-rich systems are in the liquid-crystalline phase and that DODAB-rich systems are mainly in the gel phase, the transition temperature depending on the DDAB content.

We do not discard the hypothesis that a significant incorporation of DODAB into DDAB vesicles may exist, but without any variation in T_m of neat DDAB. In fact, fluorescence results indicate that the presence of a small fraction of DODAB in DDAB-rich liposomes causes a pronounced effect in Nile Red emission. Further investigation on this system and other similar systems is under way by our group.

Acknowledgment. We thank Dr. W. Loh (Unicamp) for kindly supplying the micro DSC equipment for the calorimetric experiments. F.R.A. thanks CNPq for a Ph.D. grant.

LA053238F

Artigo 4



Vesicle–micelle transition in aqueous mixtures of the cationic dioctadecyldimethylammonium and octadecyltrimethylammonium bromide surfactants

Fernanda Rosa Alves^a, Maria Elisabete D. Zaniquelli^b, Watson Loh^c, Elisabete M.S. Castanheira^d,
 M. Elisabete C.D. Real Oliveira^d, Eloi Feitosa^{a,*}

^a Physics Department, São Paulo State University, IBILCE/UNESP, Rua Cristóvão Colombo, 2265, São José do Rio Preto, SP, CEP: 15054-000, Brazil

^b Instituto de Química, Universidade de São Paulo, Ribeirão Preto, SP, Brazil

^c Instituto de Química, Universidade Estadual de Campinas, Campinas, SP, Brazil

^d Physics Department, University of Minho, Campus de Gualtar, 4710-057 Braga, Portugal

Received 27 June 2007; accepted 15 August 2007

Available online 19 August 2007

Abstract

The vesicle–micelle transition in aqueous mixtures of dioctadecyldimethylammonium and octadecyltrimethylammonium bromide (DODAB and C₁₈TAB) cationic surfactants, having respectively double and single chain, was investigated by differential scanning calorimetry (DSC), steady-state fluorescence, dynamic light scattering (DLS) and surface tension. The experiments performed at constant total surfactant concentration, up to 1.0 mM, reveal that these homologous surfactants mix together to form mixed vesicles and/or micelles, depending on the relative amount of the surfactants. The melting temperature T_m of the mixed DODAB–C₁₈TAB vesicles is larger than that for the neat DODAB in water owing to the incorporation of C₁₈TAB in the vesicle bilayer. The surface tension decreases sigmoidally with C₁₈TAB concentration and the inflection point lies around $x_{\text{DODAB}} \approx 0.4$, indicating the onset of micelle formation owing to saturation of DODAB vesicles by C₁₈TAB molecules. When $x_{\text{DODAB}} > 0.5$ C₁₈TAB molecules are mainly solubilised by the vesicles, but when $x_{\text{DODAB}} < 0.25$ micelles are dominant. Fluorescence data of the Nile Red probe incorporated in the system at different surfactant molar fractions indicate the formation of micelle and vesicle structures. These structures have apparent hydrodynamic radius R_H of about 180 and 500–800 nm, respectively, as obtained by DLS measurements. © 2007 Elsevier Inc. All rights reserved.

Keywords: DODAB; C₁₈TAB; Surfactant; DSC; Tensiometry; Light scattering; Melting temperature; Nile Red; Steady-state fluorescence

1. Introduction

In aqueous solution surfactants can form a variety of colloidal aggregates and phases depending on the surfactant concentration. When a micelle-forming surfactant is mixed with a vesicle-forming surfactant in aqueous solution, within the range of concentrations that favours the micelle or vesicle formation of the neat surfactants, vesicle–micelle transition occurs, and the intermediate aggregate structures formed in the mixed system depend on the surfactant composition, chemical structure and solvent characteristics. In case these surfactants

mix ideally together, the structures of the mixed aggregates are usually investigated in order to elucidate the mechanism of the vesicle–micelle transition.

Cationic vesicles from dioctadecyldimethylammonium bromide (DODAB) in aqueous solution can easily be formed by simply mixing the surfactant molecules in water, followed by warming the mixture to around 60 °C, that is, safely above the gel to liquid-crystalline state transition, $T_m \approx 43$ °C [1–6]. The so prepared vesicle dispersions are stable for months even when stored at a temperature below T_m , for example, at the fridge temperature (5 °C). The properties of these vesicles can be mechanically modified by sonicating or extruding the dispersion [3], or by adding co-solutes or co-surfactants to the dispersion [4–11]. The T_m of DODAB in aqueous dispersions

* Corresponding author. Fax: +55 17 3221 22 47.
 E-mail address: eloi@ibilce.unesp.br (E. Feitosa).

can be raised or lowered on addition of co-surfactants [7]; the dependence of DODAB T_m on the co-surfactant concentration is determined by the nature of the co-surfactant, like the chain length and head group polarity [4–8]. For example, non-ionic and zwitterionic surfactants reduce the T_m of DODAB until complete solubilisation of DODAB molecules by the surfactants and the vesicle–micelle transition is complete, and the decrease in T_m has been ascribed to the formation of “softer” mixed bilayer [4,5]. The surfactant counterion also plays an important role in the thermotropic phase behaviour of charged vesicles in general and cationic vesicles in particular. It has been reported that in the absence of inorganic salts like NaBr or NaCl, the T_m is larger for the chloride homologue (DODAC) than for DODAB, owing to the specific affinity of these counter ions to the vesicle interfaces [10]. Furthermore, NaCl rises whereas NaBr lowers the T_m of DODAB, as reported [9].

Anionic [11,12] and cationic [7,13] surfactants also modify the T_m of DODAB and DODAC (dioctadecyldimethylammonium chloride). Sodium dodecyl sulphate (SDS) yields fusion of DODAB vesicles, while sodium cholate (NaC) solubilises DODAC to form micelles that fuse into large aggregates [12], SDS increases [11] but NaC decreases [12] the T_m of DODAB and DODAC, respectively. Alkyltrimethylammonium salts (C_n TAB, $n = 12–18$) may reduce, increase or leave constant the T_m of DODAB, depending on the relative chain length of these surfactants [7,13].

In this communication it is reported that when mixed the single chain cationic surfactant octadecyltrimethylammonium bromide (C_{18} TAB) with DODAB, T_m of DODAB increases slightly while a second even higher melting temperature appears at higher $x_{C_{18}TAB}$. At low concentrations and above the Krafft temperature ($T_k \approx 38^\circ\text{C}$ in water) C_{18} TAB self-assembles as globular and bilayer (disk-like) micelle structures [14], as suggested in this communication. The melting temperature, hydrodynamic radius, surface tension and fluorescence emission of the hydrophobic probe Nile Red, are reported for the DODAB/ C_{18} TAB aqueous mixtures to gain information on the mechanism on the vesicle–micelle transition.

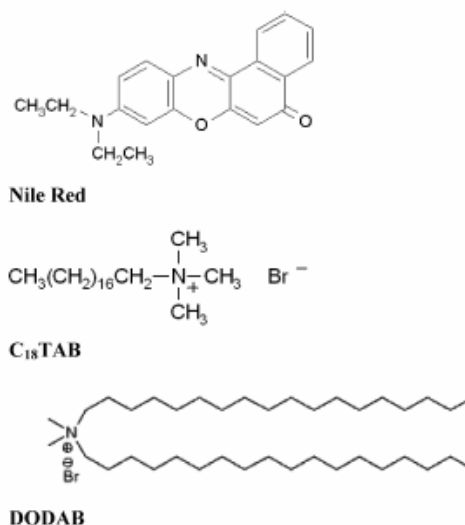
2. Experimental

2.1. Materials

Dioctadecyldimethylammonium bromide (DODAB) purity 95%, octadecyltrimethylammonium bromide (C_{18} TAB) purity 98% and 9-(diethyl-amino)-5H-benzo[α]phenoxazin-5-one (Nile Red or NR) were used as supplied by Aldrich. Ultra pure Milli-Q-Plus water was used in sample preparation. Scheme 1 shows the molecular structures of DODAB, C_{18} TAB and Nile Red.

2.2. Sample preparation

DODAB and C_{18} TAB (1.0 mM) aqueous solutions were prepared by weighing the surfactants and warming the dispersion



Scheme 1. Molecular structures of Nile Red, C_{18} TAB and DODAB.

to 60 and 50 $^\circ\text{C}$, respectively, that is, safely above the melting ($T_m \approx 43^\circ\text{C}$) [3] and Kraft ($T_k \approx 38^\circ\text{C}$) [14] temperatures of these systems.

Mixed DODAB/ C_{18} TAB aqueous dispersions were prepared at total surfactant concentration of 0.5 mM for light scattering measurements and 1.0 mM for fluorescence, surface tension and DSC measurements and varying the individual surfactant concentrations. All the experiments were performed at a constant total surfactant concentration and varying the surfactant molar fractions. The data are presented as a function of the DODAB molar fraction, x_{DODAB} given by Eq. (1), such that $x_{DODAB} + x_{C_{18}TAB}$ equal unity

$$x_{DODAB} = \frac{[DODAB]}{[C_{18}TAB] + [DODAB]} \quad (1)$$

For fluorescence measurements, Nile Red was introduced in the 1.0 mM surfactant systems by injecting 10 μL of a 10^{-3} M stock solution of the probe in ethanol. The final concentration of Nile Red in the solutions is ca. 3 μM . The solutions were then cooled to room temperature and left standing for several hours (ca. 24 h) to stabilize.

2.3. Fluorescence

Fluorescence measurements were performed using a Spex Fluorolog 2 spectrofluorimeter, equipped with a temperature controlled cuvette holder. Polarized emission spectra were recorded using Glan–Thompson polarizers. All spectra were corrected for the instrumental response of the system.

2.4. Surface tension (γ)

The surface tension of DODAB/ C_{18} TAB/water solutions was measured by the drop-volume technique. Drops of the solution were gradually extruded through a capillary and the volume

determined to obtain γ , as previously described [2,14,15]. The measurements were made at 40 °C to prevent crystal formation.

2.5. Dynamic light scattering

Dynamic light scattering (DLS) measurements were made using a Zeta Sizer 3000 HS equipped with 10 mW He–Ne ion laser operating at $\lambda = 633$ nm was used as light source. From the measured normalized intensity time correlation function, we obtained, through the inverse Laplace transform analysis, the relaxation time distribution, and from the moments of this distribution the diffusion coefficients of the particles were determined [16]. The apparent hydrodynamic radius was then obtained using the Stokes–Einstein equation

$$R_H = \frac{kT}{6\pi\eta_0 D}, \quad (2)$$

where D is the mean diffusion coefficient, k is the Boltzmann constant, T is the absolute temperature and η_0 is the solvent viscosity.

2.6. Differential scanning calorimetry (DSC)

A VP-DSC (MicroCal, Northampton, MA) calorimeter equipped with 0.542 ml twin cells for the reference and sample solutions was used. The measurements were performed with the scan rate of 1 °C/min and temperature range of 5–80 °C. The two cells filled with water were run as baseline reference. From the thermograms we obtained T_m , which is the temperature at the peak maximum, the enthalpy change of this transition, which is proportional to the area under the transition peak, and the transition cooperativity, which is inversely proportional to the peak width. Details on the DSC methods and setup can be found elsewhere [4–6].

3. Results and discussion

When C₁₈TAB (critical micelle concentration, CMC \approx 0.34 mM at 40 [14] and 30 °C [17] and DODAB (critical vesicular concentration, CVC \approx 0) [2] are mixed together in water, either vesicles or micelles or both can be formed, depending on the surfactant concentration, temperature and ionic strength, since the structure of these surfactant aggregates depends individually on these parameters [9,14]. In this communication, it is reported the effect of the surfactant concentration and temperature on some physical properties of the DODAB/C₁₈TAB/water system.

Above CMC and at room temperature (ca. 25 °C), neat C₁₈TAB in water precipitates as hydrated crystals (HC) within ca. 24 h of preparation, since the system is below the Krafft temperature ($T_k \approx 38$ °C) [14]. DODAB, on the other hand, has quite low CVC [2] and is poorly soluble in water below $T_m \approx 43$ °C. Above this critical temperature DODAB forms large unilamellar vesicles (LUV) at concentrations up to ca. 1 mM [1–11,13].

In presence of up to ca. $x_{\text{DODAB}} = 0.25$ ($x_{\text{C}_{18}\text{TAB}} > 0.75$) the dispersion is rich in C₁₈TAB micelles and there are some HC precipitates at 25 °C in equilibrium with mixed vesicles; above $x_{\text{DODAB}} \approx 0.25$ the dispersion is bluish and rich in vesicle structures, and most of the C₁₈TAB molecules are either incorporated in the vesicle bilayers or free in solution as monomers. The phase diagram for the DODAB/C₁₈TAB/water system for 1.0 mM total surfactant concentration and 25 °C is shown in the supporting materials (Fig. SM1). It indicates the region of vesicle dispersion (L₁), $x_{\text{DODAB}} > 0.25$ and that of crystal precipitates in vesicle dispersion (L₁ + HC), $x_{\text{DODAB}} < 0.25$. Most probably the unbound C₁₈TAB surfactants precipitate as hydrated crystals. The phase diagram was constructed by preparing a number of samples having different compositions that were kept standing for months at 25 °C before the phase border being defined. The samples were observed by naked eyes and the properties of surfactant mixtures at varying surfactant concentration were monitored by a number of techniques, as discussed below. For all experimental data the error does not exceed 5%.

3.1. Surface tension results

The surface tension (γ) data for the DODAB/C₁₈TAB/water system were collected at 40 °C (slightly above T_k of neat C₁₈TAB in water and below T_m of neat DODAB in water) and constant 1.0 mM total surfactant concentration (Fig. 1). For $x_{\text{DODAB}} = 1$ (neat DODAB in water) γ approaches that of pure water (ca. 72.0 mN/m), owing to the very low CVC of DODAB in water [2]. In presence of up to $x_{\text{C}_{18}\text{TAB}} \approx 0.5$ ($x_{\text{DODAB}} > 0.5$), there is no significant change in γ , indicating that C₁₈TAB is solubilised into the vesicle bilayer to form mixed DODAB–C₁₈TAB vesicles instead of adsorbing at the air/water interface. At higher C₁₈TAB content, however, γ decreases sigmoidally, with the inflection point around $x_{\text{DODAB}} \approx 0.4$, to attain the minimum value of ca. 36 mN/m, similar to the value of neat C₁₈TAB in water [14]. The decrease in γ is most

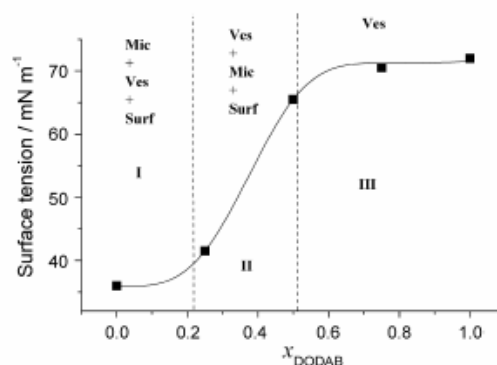


Fig. 1. The effect of DODAB (or C₁₈TAB) molar fraction on the surface tension of water–air interface for the DODAB/C₁₈TAB/water system. The total surfactant concentration is 1.0 mM and data obtained at 40 °C. It indicates regions dominated by micelles (I), micelles and vesicles (II), and vesicles (III). Ves = vesicle, Mic = micelle, Surf = surfactant.

probably due to saturation of the vesicle bilayer by C₁₈TAB and the excess surfactant monomers that remain free in solution act at the air–water interface of the system. For $x_{\text{DODAB}} < 0.25$ the solution is dominated by C₁₈TAB–DODAB mixed micelles. Finally, neat C₁₈TAB (1.0 mM) in water assembles as micelles, as reported [14].

3.2. Dynamic light scattering (DLS) results

DLS data were collected at 25 °C and constant 0.5 mM total surfactant concentration, and the mean apparent hydrodynamic radius (R_H) of the aggregates monitored as a function of x_{DODAB} (Fig. 2). At higher concentrations DODAB vesicles scatter too much light, thus being not suitable for the data analyses [1]. Accordingly, for the neat DODAB vesicles $R_H \approx 544$ nm and in presence of increasing amount of C₁₈TAB

(decreasing x_{DODAB}) R_H tends to increase to a maximum value of $R_H \approx 820$ nm when $x_{\text{DODAB}} \approx 0.3$, and then it decreases to the value of R_H for the neat C₁₈TAB micelles, $R_H \approx 180$ nm. The large micelle size has to do with the trend of C₁₈TAB to assemble as disk-like micelles, although globular structures can be found as reported [14].

The vesicle growth may be attributed to the incorporation of C₁₈TAB into the DODAB bilayer to favour larger vesicle formation. The R_H maximum at $x_{\text{DODAB}} \approx 0.3$ corresponds to the onset of micelle formation. Beyond this point ($x_{\text{DODAB}} < 0.3$), R_H decreases to attain the value of the neat C₁₈TAB micelles. The decrease in R_H is most probably related to the formation of increasing amount of mixed micelles in equilibrium with a decreasing amount of mixed DODAB vesicles. Since the micelles are smaller than the vesicles, the mean size reported might be the average size of the vesicle and micelle populations.

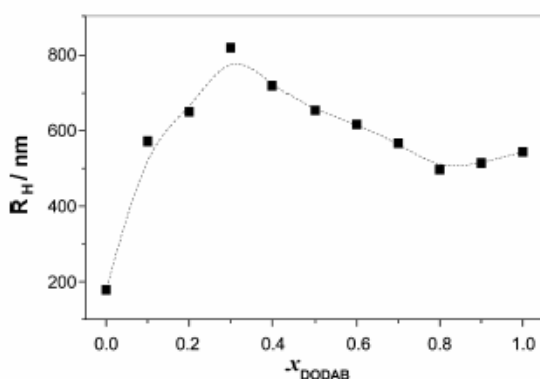


Fig. 2. The effect of DODAB (or C₁₈TAB) molar fraction on the apparent hydrodynamic radius (R_H) of the surfactant aggregates in the DODAB/C₁₈TAB/water system, at the total surfactant concentration of 0.5 mM (25 °C). The dashed line is just a guide for the eyes.

3.3. Differential scanning calorimetry (DSC) results

The DSC traces for 1.0 mM total surfactant concentration in mixed DODAB/C₁₈TAB aqueous dispersions are shown in Fig. 3 for varying surfactant concentrations. T_m , melting enthalpy (ΔH) and peak width ($\Delta T_{1/2}$) related to the main transition are also shown in Figs. 4 and 5 and Table SM1, as function of x_{DODAB} . Accordingly, the neat DODAB/water dispersion ($x_{\text{DODAB}} = 1$) exhibits a small pre-transition peak around $T_s = 33.3$ °C, in addition to the main transition at $T_m = 42.5$ °C, as reported [3]. The pre- and main transitions are related to the transitions from the gel phase to the rippled gel phase and from this to the liquid-crystalline (LC) phase, respectively, upon raising the temperature [18,19]. Since the pre-transition vanishes in presence of a small amount of C₁₈TAB (Fig. 3), mixed C₁₈TAB–DODAB vesicles exhibit a direct gel–LC phase transition.

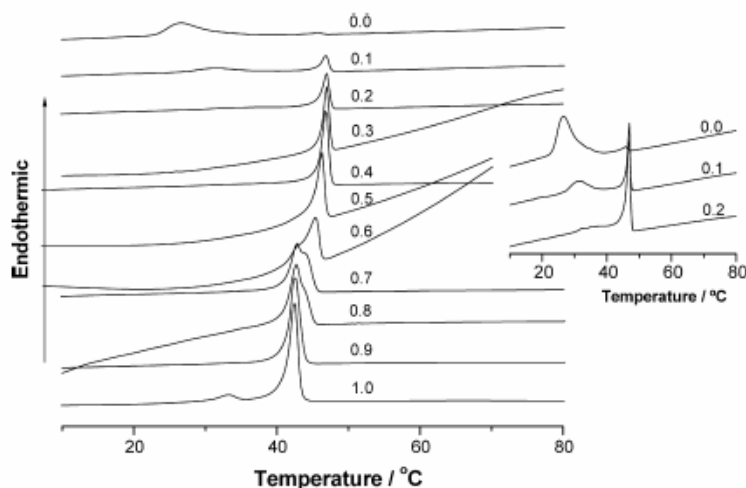


Fig. 3. DSC upscan thermograms for the mixture DODAB/C₁₈TAB/water, for 1.0 mM total surfactant concentration and varying DODAB molar fraction (numbers beside the curves). Inset shows the expanded thermograms for $x_{\text{DODAB}} = 0, 0.1$ and 0.2 .

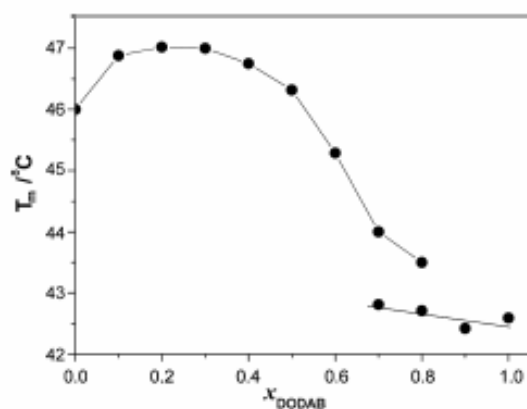


Fig. 4. The effect of DODAB (or C_{18}TAB) molar fraction on the melting temperature (T_m) of the cationic mixed DODAB/ C_{18}TAB aqueous dispersions.

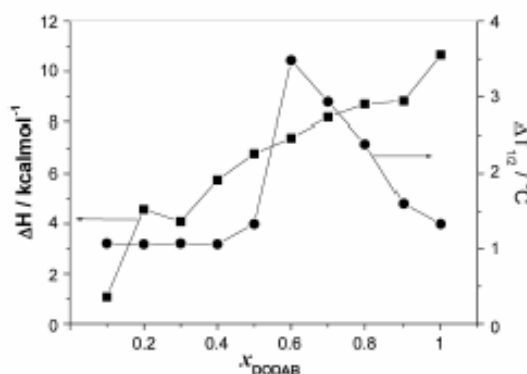


Fig. 5. The effect of DODAB (or C_{18}TAB) molar fraction on the enthalpy change (ΔH) and width of the melting peak ($\Delta T_{1/2}$) for the mixed DODAB/ C_{18}TAB aqueous dispersions.

Even though the vesicle dispersions are quite polydisperse [1,2], the width of the main transition peak is rather narrow [3], thus indicating a little dependence of T_m on the vesicle curvature and structure (like multilamellar or multistructural), and does not change with surfactant concentration except for the intermediate range of $x_{\text{DODAB}} = 0.5\text{--}0.9$ where there is some peak overlapping, indicating that C_{18}TAB is solubilised in different vesicle populations, according to the two-population model for the vesicle dispersions of DODAB [1]. In this range of concentration the large values of $\Delta T_{1/2}$ (Fig. 5) are meaningless since they are related to peak overlapping instead of single transition peaks.

The peak related to the main transition for neat DODAB in water is slightly shifted upward, that is, T_m increases slightly on increasing $x_{\text{C}_{18}\text{TAB}}$ up to ca. 0.3 wt%, when a new peak appears at a slightly higher temperature overlapping the main transition peak. By further increasing the amount of C_{18}TAB , the intensity of the main peak decreases while the intensity of the additional peak becomes more pronounced. Finally, the main peak disappears around ca. $x_{\text{DODAB}} \approx 0.5$ (Fig. 3), indicating

the presence of mixed vesicles dominated by C_{18}TAB that exhibit higher T_m .

The presence of two main transitions associated to the main peak can be explained by the presence of two populations of vesicles in the neat DODAB aqueous dispersion, that differ mainly in size and structure (multilamellar vs. multistructural) [1], and also to the different surfactant packing of DODAB and C_{18}TAB which determines the vesicle curvature. Since T_m tends to increase with vesicle size [3], the lower and higher temperature main peaks may be related to the higher- and lower-curvature vesicles, respectively. Since C_{18}TAB yields vesicle growth (Fig. 2), the population of smaller vesicles may be reduced in comparison with the larger ones. Thus, as the relative concentration of C_{18}TAB increases, the peak intensity for the C_{18}TAB -rich vesicles increases, while the one for DODAB-rich vesicles decreases to disappear around the equimolar concentration of the surfactants.

Up to $x_{\text{C}_{18}\text{TAB}} \approx 0.3$ ($x_{\text{DODAB}} \geq 0.7$), T_m is slightly higher (Fig. 4), thus indicating that the C_{18}TAB monomers are incorporated into the DODAB vesicles to form mixed DODAB- C_{18}TAB vesicles with the C_{18}TAB monomers distributed homogeneously within the DODAB bilayer, such that the mixed vesicles exhibit similar characteristics to the neat DODAB vesicles. For x_{DODAB} lower than 0.7, there is a pronounced increase in T_m until x_{DODAB} approaches 0.3, when $T_m \approx 47^\circ\text{C}$ and mixed DODAB- C_{18}TAB micelles are formed. In fact the higher T_m comes from a second peak in the thermogram that initially overlaps with the original peak, and these two peaks may be due to solubilisation of C_{18}TAB in different vesicle populations. When the amount of C_{18}TAB is further increased, T_m remains roughly constant, indicating that the C_{18}TAB monomers are not solubilised anymore by the (saturated) vesicle bilayers.

Fig. 3 insert indicates a rather broad peak at $T_k^* \approx 26.7^\circ\text{C}$ for neat C_{18}TAB in water. This critical temperature is lower than that expected for the Krafft point of this system (ca. 38°C) [14] and may be related to a transition in the micelle structure, since at this concentration and temperature the rate of crystal formation is much slower than the DSC scan rate. In presence of small amount of DODAB T_k^* increases but the peak intensity decreases to vanish around $x_{\text{DODAB}} \approx 0.2$. The sharper peak above 40°C comes from the main transition.

Interestingly C_{18}TAB exhibits in addition to the peak at $T_k^* = 26.7^\circ\text{C}$, an additional peak centered at $T_m = 46^\circ\text{C}$. Neither these peaks have to do with the Krafft phenomenon. Even though the origin for these peaks is not clear, the smaller one at $T_m = 46^\circ\text{C}$ is most probably related to the trend of C_{18}TAB to form bilayer-like structures, as reported [14]. Upon addition of DODAB, the peak at T_m increases intensity whereas the one at T_k^* is inhibited. According to Fig. 4 T_m initially increases to a maximum plateau around 47°C and then it decreases to values comparable to that of neat DODAB, meaning that the vesicle bilayers dominated by C_{18}TAB are more compact than those dominated by DODAB.

The melting enthalpy decreases monotonically with the amount of C_{18}TAB concentration (Fig. 5), also indicating that the C_{18}TAB -rich bilayer is more densely packed relative to that of DODAB. Fig. 5 also shows the effect of x_{DODAB} on the

width $\Delta T_{1/2}$ of the main transition peak. The larger $\Delta T_{1/2}$ for $x_{\text{DODAB}} \approx 0.5$ – 0.9 is due to the overlap of the two main peaks that might be related to the two populations of DODAB vesicles present in solution that mainly differ by the relative fraction of C_{18}TAB solubilised into the vesicle bilayers. Except for the region of peak overlap, the width of all single peaks is rather narrow, indicating high cooperativity of the main transition. In fact the peaks are narrower for the C_{18}TAB -rich than for the DODAB-rich vesicles.

3.4. Fluorescence results

The fluorescence probe Nile Red (NR) has been extensively used as a probe for lipid aggregates, such as vesicles, due to its hydrophobic nature that allow it to be incorporated in the bilayer moiety [20–23]. In addition, this probe exhibits solvatochromic behaviour and in polar media it is observed a red shift in the emission maximum, together with fluorescence quenching, due to the capability of NR to establish hydrogen bonds with protic solvents [24]. As a consequence, the NR emission in water is very weak with $\lambda_{\text{max}} \approx 660$ nm [25].

Fig. 6 shows the emission spectra of NR incorporated in the DODAB/ C_{18}TAB /water system at 25 °C, for selected surfactant molar fractions. The fluorescence intensity increases when x_{DODAB} decreases ($x_{\text{C}_{18}\text{TAB}}$ increases). The lower fluorescence emission for the neat DODAB/water system ($x_{\text{DODAB}} = 1$) indicates that NR feels a water-rich environment in DODAB vesicles. In fact, the maximum emission wavelength for $x_{\text{DODAB}} = 1$, $\lambda_{\text{max}} \approx 650$ nm, is close to the value for pure water ($\lambda_{\text{max}} \approx 660$ nm) [25], probably due to the fact that at room temperature (below $T_m = 42.5$ °C) DODAB vesicle bilayers are in the gel phase, thus hindering the probe to penetrate deeper in the lipid bilayer.

When x_{DODAB} decreases, the emission intensity increases monotonically (Fig. 6), indicating that NR becomes less exposed to water in the mixed aggregates. This can be explained by the formation of larger structures with a lower curvature, due to the incorporation of C_{18}TAB into the DODAB bilayer, as shown by the light scattering data (Fig. 2). At higher C_{18}TAB content ($x_{\text{DODAB}} < 0.3$), the further increase in NR fluorescence intensity may be justified by the formation of an increasing amount of mixed micelles, where NR feels a more fluid (less viscous) environment and may achieve a deeper penetration.

The variation of the maximum emission wavelength (λ_{max}) of NR with increasing x_{DODAB} (Fig. 6 insert) indicates the same trend. At 25 °C (below T_m), in the gel phase, λ_{max} decreases with decreasing x_{DODAB} , indicating an increasing hydrophobicity of the local environment of NR when the relative amount of C_{18}TAB is increased. An opposite behavior of λ_{max} is observed at 55 °C (above T_m), in the liquid-crystalline phase, where NR feels a more hydrophobic environment at higher x_{DODAB} . These results indicate that the bilayer fluidity depends on temperature and surfactant composition, and plays an important role in the probe location in the mixed systems.

Fig. 7 shows the average steady-state fluorescence anisotropy, r , of NR in DODAB/ C_{18}TAB /water mixtures, obtained at increasing temperature, for x_{DODAB} varying from 0 to 1. The anisotropy is given by

$$r = \frac{I_{\text{VV}} - GI_{\text{VH}}}{I_{\text{VV}} + 2GI_{\text{VH}}}, \quad (3)$$

where I_{VV} and I_{VH} are the intensity of the emission spectra obtained with vertical and horizontal polarization, respectively (for vertically polarized excitation light), and $G = I_{\text{HV}}/I_{\text{HH}}$ is the instrument correction factor, where I_{HV} and I_{HH} are the

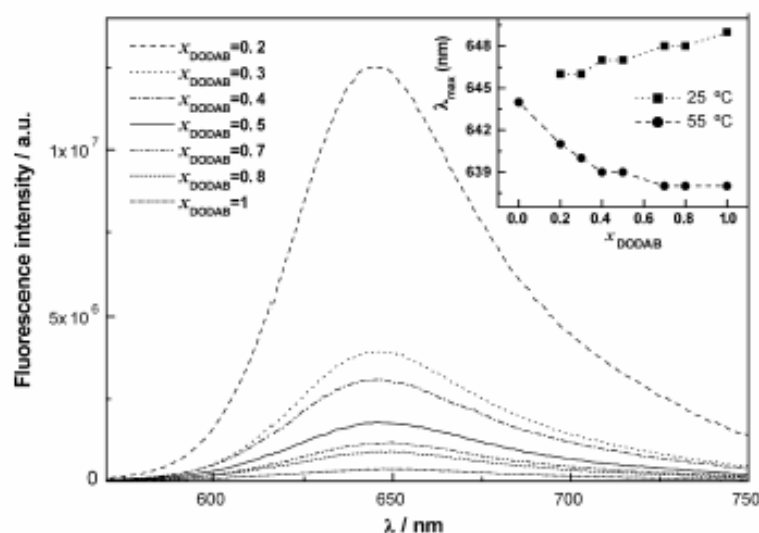


Fig. 6. Fluorescence spectra of Nile Red in DODAB/ C_{18}TAB /water mixed systems for several x_{DODAB} at 25 °C ($\lambda_{\text{exc}} = 550$ nm). Inset: Maximum emission wavelength of Nile Red in DODAB/ C_{18}TAB /water mixed systems in water, below 25 °C and above 55 °C the melting temperature, as a function of x_{DODAB} .

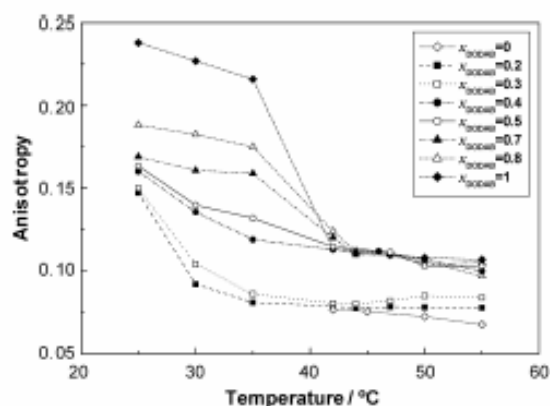


Fig. 7. Steady-state anisotropy of Nile Red in DODAB/C₁₈TAB/water mixed systems for selected DODAB molar fractions.

emission intensities obtained with vertical and horizontal polarization (for horizontally polarized excitation light).

A high fluorescence anisotropy value is related to a low degree of rotation of the fluorescence probe. Therefore, anisotropy variations are indicative of changes in fluidity of the probe environment. When temperature increases above T_m , a decrease in anisotropy is observed resulting from the decrease in the medium viscosity in the liquid-crystalline phase.

For neat DODAB vesicles ($x_{\text{DODAB}} = 1$) the anisotropy is high below T_m , in the gel phase, and exhibits a pronounced decrease upon the gel to liquid-crystalline transition, as previously observed [6]. For the mixed surfactant systems and temperature below 35 °C, the anisotropy decreases monotonically with the decrease in the DODAB content, indicating an average increase in fluidity of the mixed aggregates.

In the liquid-crystalline phase the anisotropy of the mixed systems for $x_{\text{DODAB}} > 0.3$ is similar to the value obtained for neat DODAB vesicles. However, a different behaviour was observed for $x_{\text{DODAB}} \leq 0.3$, where the anisotropy approaches the value for neat C₁₈TAB in water. This indicates that for ca. $x_{\text{DODAB}} > 0.3$, the aggregates are dominated by mixed vesicles, while for lower x_{DODAB} , the aggregates are dominated by mixed micelles. This is supported by the surface tension data that approach the value for the neat DODAB/water system when $x_{\text{DODAB}} > 0.5$ (Fig. 1). Since the CMC of C₁₈TAB in water at 40 °C is ca. 0.34 mM [14], it is possible that some mixed micelles and vesicles co-exist when $x_{\text{DODAB}} < 0.5$. This could explain the strong attenuation of the phase transition in the anisotropy plots for $x_{\text{DODAB}} = 0.4$ and 0.5 (Fig. 7).

Fig. 8 shows the variation of the total fluorescence intensity, $I_{\text{total}} = I_{\text{VV}} + 2GI_{\text{VH}}$, with temperature for three different DODAB molar fractions (for other values of x_{DODAB} similar data were obtained—results not shown). In the mixed surfactant systems, a maximum is observed around 47 °C, close to T_m . Below this temperature, in the gel phase, it can be observed a slight increase in fluorescence intensity followed by a steep rise around T_m . This may be due to an increase in bilayer fluidity (chain melting), causing a deeper penetration of NR in the mixed aggregates. This behavior exceeds the usual fluo-

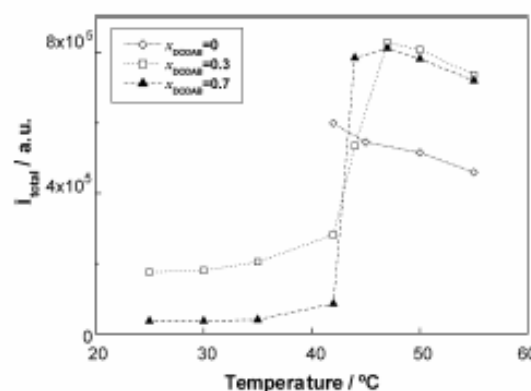


Fig. 8. Total intensity of fluorescence ($I_{\text{total}} = I_{\text{VV}} + 2GI_{\text{VH}}$) of Nile Red in DODAB/C₁₈TAB/water mixed systems for selected DODAB molar fractions.

rescence quenching with temperature, due to the increase in the competitive non-radiative processes, as observed for the neat C₁₈TAB system ($x_{\text{DODAB}} = 0$). Above DODAB T_m , in the liquid-crystalline phase, the emission intensity decreases with increasing temperature, which is the usual behavior.

The less abrupt increase in I_{total} for $x_{\text{DODAB}} = 0.3$ relative to $x_{\text{DODAB}} = 0.7$ may reflect the lower transition temperature for the latter molar fraction (Fig. 4 and Table SM1). However, the fluorescence measurements are not sensitive enough to small variations in T_m as observed by DSC.

4. Conclusions

Based in the present results of differential scanning calorimetry, dynamic light scattering, NR fluorescence and tensiometry the following conclusions can be outlined: At 1 mM DODAB and C₁₈TAB form vesicles and micelles, respectively. By mixing these surfactants mixed vesicles and/or micelles are formed. The melting temperature (T_m) for the mixed vesicles is higher than that for neat DODAB, so as the hydrodynamic radii for the mixed micelles and mixed vesicles. In the gel phase the average fluidity of the aggregates increases with the increasing amount of C₁₈TAB, while in the liquid-crystalline phase two regions are distinguished, one with the presence of vesicle structures ($x_{\text{DODAB}} > 0.3$) and the other dominated by higher fluid mixed micelles.

Association colloids with well defined and controlled properties, such as melting temperature, size and polydispersity, can thus be formed by mixing surfactants aiding the possible development of structures that contain domains of solubilisation for specific solute molecules for different applications.

Acknowledgments

E.R.A. and E.F. thank CNPq for PhD and research grant (Grant 304543/2006-3), respectively. E.F. also thanks FAPESP for supporting his visit to Universidade do Minho (Grant 07/51039-3). E.M.S.C. and M.E.C.D.R.O. thank FCT-Portugal for funding through Centro de Física of Universidade do Minho.

Supporting material

The online version of this article contains additional supplementary material.

Please visit DOI: 10.1016/j.jcis.2007.08.027.

References

- [1] E. Feitosa, G. Karlsson, K. Edwards, *Chem. Phys. Lipids* 140 (2006) 66.
- [2] E. Feitosa, W. Brown, *Langmuir* 13 (1997) 4810.
- [3] E. Feitosa, P.C.A. Barreiros, G. Olofsson, *Chem. Phys. Lipids* 105 (2000) 201.
- [4] P.C.A. Barreiros, G. Olofsson, N.M. Bonassi, E. Feitosa, *Langmuir* 18 (2002) 1024.
- [5] E. Feitosa, N.M. Bonassi, W. Loh, *Langmuir* 22 (2006) 4512.
- [6] E. Feitosa, F.R. Alves, A. Niemiec, M.E.C.D. Real Oliveira, E.M.S. Castanheira, A.L.F. Baptista, *Langmuir* 22 (2006) 3579.
- [7] A. Kacperska, *J. Thermochim. Anal.* 45 (1995) 703.
- [8] M.J. Blandamer, B. Briggs, M.D. Butt, P.M. Cullis, M. Waters, J.B.F.N. Engberts, D. Hoekstra, *J. Chem. Soc. Faraday Trans.* 90 (1994) 727.
- [9] E. Feitosa, P.C.A. Barreiros, *Prog. Colloid Polym. Sci.* 128 (2004) 163.
- [10] C.R. Berutti, E. Feitosa, R.M. Fernandez, M.T. Lamy-Freund, *Chem. Phys. Lipids* 111 (2001) 93.
- [11] J. Cocquyt, U. Olsson, G. Olofsson, P. Van der Meer, *Langmuir* 20 (2004) 3906.
- [12] F.R. Alves, E. Feitosa, *Thermochim. Acta* 450 (2006) 76.
- [13] M.J. Blandamer, B. Briggs, P.M. Cullis, A. Kacperska, J.B.F.N. Engberts, D. Hoekstra, *J. Indian Chem. Soc.* 70 (1993) 347.
- [14] M. Swanson-Vethamuthu, E. Feitosa, W. Brown, *Langmuir* 14 (1998) 1590.
- [15] E. Tornberg, *J. Colloid Interface Sci.* 60 (1977) 50.
- [16] W. Brown, *Dynamic Light Scattering. The Method and Some Applications*, Clarendon Press, Oxford, 1993.
- [17] J. Mata, D. Varade, P. Bahadur, *Thermochim. Acta* 428 (2005) 147.
- [18] P.L. Luisi, B.E. Straub, in: *Reverse Micelles—Biological and Technological Relevance of Amphiphilic Structures in Aqueous Media*, Plenum Press, New York, 1984.
- [19] D.F. Evans, H. Wennerström, *The Colloidal Domain*, Wiley-VCH, New York, 1994.
- [20] P. Greenspan, S.D.J. Fowler, *Lipid Res.* 26 (1985) 781.
- [21] I. Krishnamoorthy, G. Krishnamoorthy, *J. Phys. Chem. B* 15 (2001) 1484.
- [22] P.J.G. Coutinho, E.M.S. Castanheira, M.C. Rei, M.E.C.D. Real Oliveira, *J. Phys. Chem. B* 106 (2002) 12841.
- [23] G. Hungerford, E.M.S. Castanheira, A.L.F. Baptista, P.J.G. Coutinho, M.E.C.D. Real Oliveira, *J. Fluoresc.* 15 (2005) 835.
- [24] A. Csér, K. Nagy, L. Biczók, *Chem. Phys. Lett.* 360 (2002) 473.
- [25] G. Hungerford, E.M.S. Castanheira, M.E.C.D. Real Oliveira, M.G. Miguel, H.D. Burrows, *J. Phys. Chem. B* 106 (2002) 4061.

Artigo 5



Thermotropic phase behavior in aqueous mixtures of dioctadecyldimethylammonium bromide and alkyltrimethylammonium bromide surfactant series studied by differential scanning calorimetry

Fernanda Rosa Alves, Eloi Feitosa*

Physics Department, IBRICE/UNESP, Rua Cristovão Colombo 2365, São Paulo State University, São José do Rio Preto, CEP: 13054-000 SP, Brazil

ARTICLE INFO

Article history:

Received 24 November 2007
Received in revised form 5 March 2008
Accepted 10 March 2008
Available online 30 March 2008

Keywords:

DODAB
 C_n TAB
DSC
Melting temperature
Vesicles
Micelles

ABSTRACT

The effect of the micelle-forming surfactant series alkyltrimethylammonium bromide (C_n TAB, $n=12, 14, 16$ and 18) on the thermotropic phase behavior of dioctadecyldimethylammonium bromide (DODAB) vesicles in water was investigated by differential scanning calorimetry at constant 5.0 mM total surfactant concentration and varying individual surfactant concentrations. The pre-, post- and main transition temperatures (T_i , T_p and T_m), melting enthalpy (ΔH) and peak width of the main transition ($\Delta T_{1/2}$) are reported as a function of the surfactant molar fraction. No clear dependence of these parameters on the C_n TAB chain length was found. At 5 mM, neat DODAB in water exhibits two transition temperatures, $T_i=32.1$ and $T_m=42.7$ °C, as obtained from the DSC upscans, but not a clear T_p . For every n , except $n=12$, T_i vanishes as C_n TAB concentration increases and approaches CMC. T_m behaves differently for different n , the longer C_{14} TAB and C_{16} TAB decrease, while C_{18} TAB increases T_m with increasing concentration. The data indicate that changes in T_m , T_i , T_p and ΔH of the transition are related not only to the extent of C_n TAB affinity to DODAB but also to the surfactant chain length. Accordingly, C_{18} TAB yields a more compact bilayer, thus increasing T_m , while C_{14} TAB and C_{16} TAB yield a less organized bilayer and reduce T_m . C_{12} TAB does not much affect T_i and T_m , although it yields $T_p \approx 51.6$ °C.

© 2008 Elsevier B.V. All rights reserved.

1. Introduction

Unilamellar vesicles consist of a lipid bilayer separating an aqueous solution from the bulk phase, forming roughly spherical structures with an inner aqueous core [1,2]. In general, the vesicle characteristics, such as size and stability, depend on the method of preparation. Vesicles can be prepared by sonication, extrusion, surfactant removal or spontaneously, that is, without sonication or extrusion [1,2]. Owing to their structural similarity to cell membranes, vesicles have attracted considerable interest as membrane models [1–4] and as drug delivery vehicles. Cationic vesicles are appropriate for DNA compaction [2]. On heating, the vesicle bilayer exhibits a transition temperature (T_m) characteristic of the system, ascribed to a gel to liquid crystalline state transition [3,4]. Vesicles may also present pre- and post-transition temperatures, T_i and T_p , respectively. These temperatures can be monitored to gain insight on the vesicle structure in different media and conditions.

In excess water, dioctadecyldimethylammonium bromide (DODAB) molecules assemble spontaneously above $T_m \approx 43$ °C and at low concentrations (typically 1.0 mM) as large unilamellar vesicles, that is, without sonication or extrusion [5,6]. At higher concentrations, in addition to unilamellar vesicles, they assemble as more complex structures such as multilamellar and multistructural vesicles yielding additional transitions [7,8]. The structural organization and properties of DODAB vesicles thus depend on the surfactant concentration, solvent and vesicle preparation method [5–10]. Up to 5 mM DODAB, however, the concentration has a minor effect on the transition temperatures [5].

Co-surfactants may have pronounced effects on the vesicle properties owing to their solubilization into the vesicle bilayer that changes the bilayer fluidity, thus affecting the transition temperatures. Anionic, nonionic and zwitterionic surfactants reduce the T_m of DODAB [11–13]. Cationic surfactants, however, may increase, decrease or leave constant DODAB T_m [14,15].

Except for C_{12} TAB, the CMC (critical micellar concentration) of C_n TAB ($n=14, 16$ and 18) is below 5 mM, and these surfactants interact with DODAB vesicles either as monomers or micelles. The CMC of C_n TAB in water is $15.2, 3.98, 1.00$ and 0.35 mM, for $n=12, 14, 16$ and 18 , respectively [16]. The Krafft temperature, on the other

* Corresponding author. Tel.: +55 17 3221 2240; fax: +55 17 3221 2247.
E-mail address: efoi@ibrice.unesp.br (E. Feitosa).

hand, increases almost linearly with the chain length [17]. DODAB exhibits a critical vesicle concentration (CVC) close to zero [6]. Thus, in the experiments the C_n TAB concentration is either below or above CMC, whereas DODAB concentration is always above CVC. In that way, the system is appropriate to investigate the effect of C_n TAB monomers and micelles on DODAB vesicles.

The aim of this study was to investigate the effect of the chain length of C_n TAB ($n = 12, 14, 16$ and 18) on the thermotropic phase behavior of DODAB vesicles at constant 5.0 mM total surfactant concentration and varying surfactant ratio.

2. Experimental

2.1. Materials

DODAB was purchased from Aldrich. Hexadecyltrimethylammonium bromide (C_{16} TAB) was supplied by Sigma, whereas dodecyl- (C_{12} TAB), tetradecyl- (C_{14} TAB) and octadecyltrimethylammonium (C_{18} TAB) bromides were obtained from Fluka. All surfactants were used as received. Ultrapure water of Milli-Q-Plus quality was used in sample preparations.

2.2. Sample preparation

DODAB and C_n TAB dispersions were prepared by simple dilution of 5.0 mM surfactant in water at room temperature (25 °C). For complete dissolution DODAB and C_{18} TAB aqueous mixtures were warmed to 60 and 45 °C, respectively, that is, above $T_m \approx 43$ °C [6] and the Krafft temperatures ($T_K \approx 38$ °C) [18] of DODAB and C_{18} TAB. All the other dispersions of the C_n TAB surfactants were prepared by simply mixing the appropriate amount of the surfactant at room temperature (25 °C), since at this temperature they are above T_K [17].

Mixed DODAB/ C_n TAB aqueous dispersions were prepared by mixing appropriate volumes of the 5.0 mM dispersions of these surfactants to have 5.0 mM total surfactant concentration and varying ratios of the individual surfactant concentrations. The data are presented as a function of the molar fraction of surfactant. For example, for the mixture of DODAB and C_n TAB, the molar fraction of DODAB is $x_{\text{DODAB}} = [\text{DODAB}]/[\text{TOTAL}]$, where brackets account for molar concentration and $[\text{TOTAL}] = 5.0$ mM.

2.3. Differential scanning calorimetry (DSC)

A VP-DSC (MicroCal, Northampton, MA) calorimeter with 0.542 ml twin cells for the reference and sample solutions was used to obtain the thermograms. Measurements were performed at a scan rate of 1 °C/min from 5 to 80 °C allowing the system to be either below or above the Krafft temperature of the C_n TAB/DODAB/water system, especially for $n = 16$ and 18 . Prior the DSC experiments the samples were left standing at 25 °C for at least 48 h to check for precipitate formation. Precipitate formation was observed only for the C_{18} TAB-containing system, as indicated by the phase diagram shown in Fig. 8 of the supplementary material. Those samples that formed precipitates were warmed to become clear before being transferred to the DSC cell. After the experiments the samples were left standing for months at 25 °C to check for precipitate formation. Once again, only the C_{18} TAB-containing system exhibited precipitates. The baseline reference was obtained with both cells filled with water. The melting temperature (T_m , i.e., the temperature of the peak maximum), and melting enthalpy (ΔH) were determined from the peak area, and the cooperativity of the transition by the peak width ($\Delta T_{1/2}$) at the peak half height. For the pre- and post-transition peaks, only the transition temperatures T_S and T_D were obtained because they were not well defined. MicroCal Origin, v.5.0, was used for data acquisition and analyses. Further details on the DSC can be found in previous publications [5,8,13,19].

3. Results and discussion

At 5.0 mM $T_m \approx 43$ °C of neat DODAB is the same as that of 1.0 mM often investigated [5]. At 5.0 mM DODAB, more pronounced pre- and post-transitions were expected, which could be used to investigate the effects of C_n TAB. However, the DSC traces in Figs. 1 and 2 reveal that DODAB concentration has little effect on the size of these peaks.

The melting temperature T_m , enthalpy ΔH and peak width $\Delta T_{1/2}$ are shown in Figs. 3–5, as functions of the C_n TAB molar fraction ($x_{C_n\text{TAB}}$). The neat DODAB dispersion ($x_{\text{DODAB}} = 1.0$) exhibits two endothermic transition temperatures, $T_S = 32.1$ °C and $T_m = 42.7$ °C. The post-transition temperature (T_D) reported in previous publications [5,8,19] does not appear even in the enlarged curves, although it is induced by the presence of C_{12} TAB, as Fig. 9 in the supplementary material indicates. C_{12} TAB reduces slightly and linearly

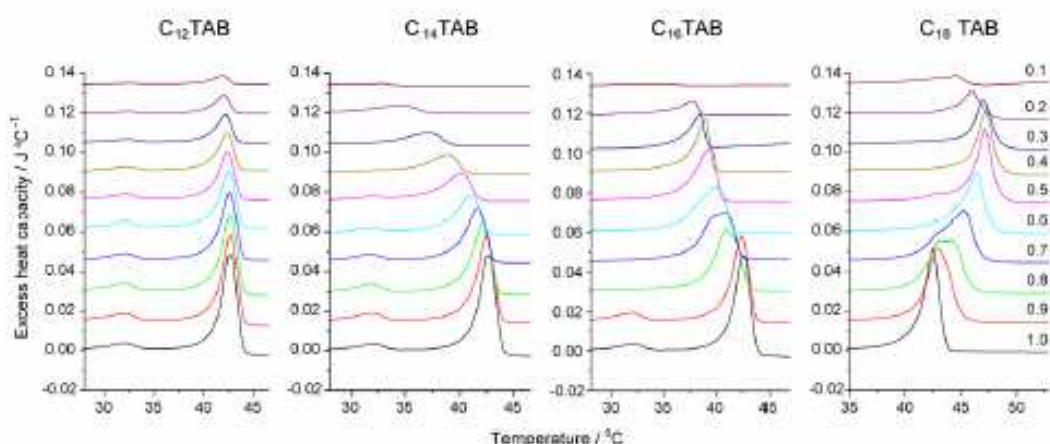


Fig. 1. DSC upscan thermograms from mixtures of DODAB/ C_n TAB/water, $n = 12, 14, 16$ and 18 , 5.0 mM total surfactant concentration, and $x_{\text{DODAB}} = 0.1, 0.2, 0.3, \dots, 1.0$, as indicated. To avoid overlap, the curves were offset by 0.015 J °C⁻¹ from each other.

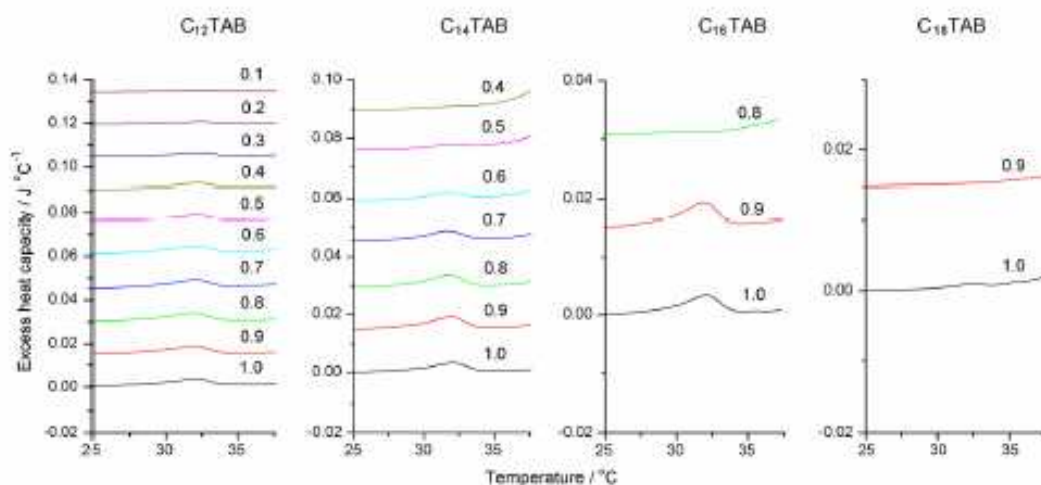


Fig. 2. Same as Fig. 1, except for the enlarged traces around the pre-transition temperature T_5 .

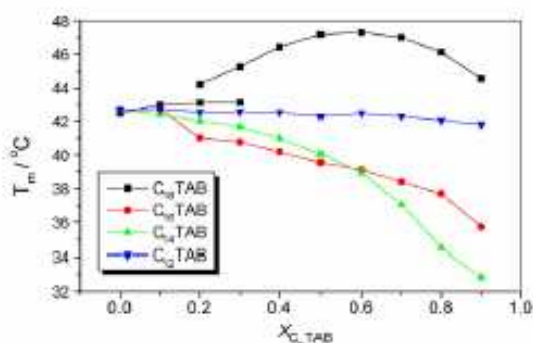


Fig. 3. The effect of C_n TAB molar fraction (x_{C_nTAB}) on the melting temperature T_m of the mixed cationic C_n TAB-DODAB vesicles in water.

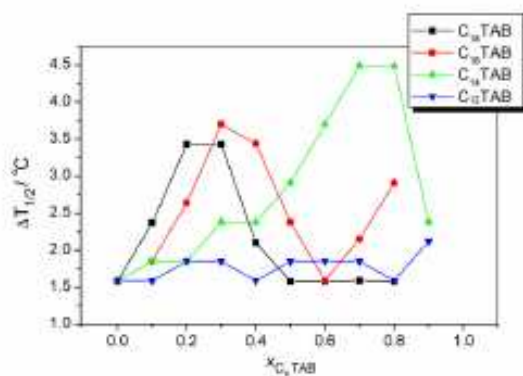


Fig. 4. The effect of C_n TAB molar fraction (x_{C_nTAB}) on the width peak at half-height $\Delta T_{1/2}$ of the mixed cationic C_n TAB-DODAB vesicles in water.

T_p , yielding $T_p = 51.6^\circ\text{C}$ upon extrapolation of the fitting curve to zero C_{12} TAB concentration (Fig. 10 in the supplementary material), in good agreement with previously reported $T_p \approx 53^\circ\text{C}$ [5,8,19].

The enlarged thermograms around the pre-transition temperature (Fig. 2) indicate that the longer the C_n TAB chain length, the stronger the inhibition of the pre-transition peak. C_{12} TAB thus exhibits minor effect on T_5 (Fig. 6), probably because it is already in a more disordered state. The post-transition temperature (T_p) can only be poorly discerned for the thermograms of the C_{12} TAB-containing systems (Fig. 9 in supplementary material), but cannot be seen for $n = 14$ –18. Furthermore, T_p decreases only slightly and linearly with C_{12} TAB concentration (Fig. 10 in the supplementary materials).

The DSC curves (Figs. 1 and 2) indicate that T_5 is rather sensitive to C_n TAB concentration and chain length. T_5 vanishes when $x_{C_{18}TAB} < 0.1$, $x_{C_{16}TAB} \approx 0.2$ and $x_{C_{14}TAB} \approx 0.6$, whereas C_{12} TAB does not inhibit the pre-transition at all. Even though the T_5 values are not well defined, because the peaks are very weak, they clearly indicate that the pre-transition is inhibited around the surfactant CMC.

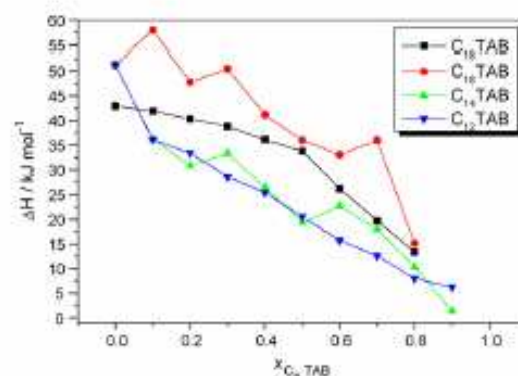


Fig. 5. The effect of C_n TAB molar fraction (x_{C_nTAB}) on the melting enthalpy ΔH of the mixed cationic C_n TAB-DODAB vesicles in water.

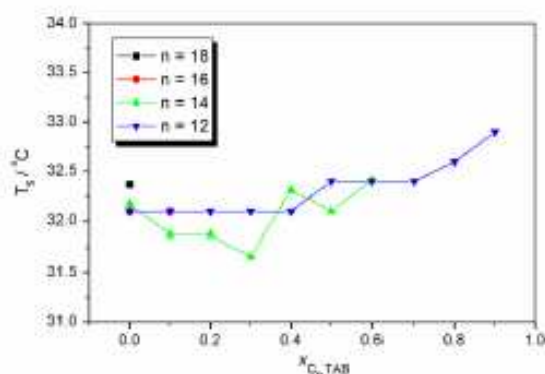


Fig. 6. The effect of C_n TAB molar fraction (x_{C_nTAB}) on the pre-transition temperature T_p of the mixed cationic C_n TAB-DODAB vesicles in water.

Since T_s exists only when C_n TAB concentration is below CMC, a fraction of monomers might be solubilized in the vesicle bilayer to form mixed C_n TAB-DODAB vesicles; above CMC the C_n TAB monomers have more affinity to the micelle, rather than the vesicle structure.

The main peak position in the thermograms gives the melting temperature (T_m), shown in Fig. 3 as a function of x_{C_nTAB} . Up to $x_{C_{18}TAB} \approx 0.6$, T_m increases to a maximum value about 47.2 °C, meaning that C_{18} TAB stabilizes the gel state of the DODAB-based vesicles, due to the solubilization of monomers into the DODAB bilayer, as reported for 1.0 mM total surfactant concentration [15]. Above this concentration, T_m decreases to values even higher than that for neat DODAB in water. Note that around 0.2–0.3 C_{18} TAB there are two melting temperatures due to solubilization of C_{18} TAB into two different vesicle populations, as reported [7,15]. The opposite effect was observed for C_{14} TAB and C_{16} TAB that shift T_m downward in temperature. C_{12} TAB does not much affect T_m of DODAB, indicating weaker interaction.

The main transition, which is related to the melting of the surfactant hydrocarbon chains, is influenced by perturbation caused by C_n TAB molecules solubilized into the vesicle bilayer. The bell-shaped variation of T_m with increasing x_{C_nTAB} (Fig. 3) indicates that the mixed C_{18} TAB-DODAB bilayer is more densely packed than that of neat DODAB. In presence of C_{14} TAB and C_{16} TAB the chains become more mobile, increasing the disorder of the surfactant chains, thus reducing T_m . The shorter C_{12} TAB molecules do not much affect T_m , T_s or T_p since they stay as monomers in solution below CMC = 15.2 mM [19] or, alternatively, the solubilized monomers are short enough to disturb the vesicle bilayers.

According to Fig. 3, the effect of C_n TAB chain length on T_m depends on the relative amount of the surfactants. First, C_{12} TAB does not affect T_m because its concentration is lower than CMC. Up to $x_{C_nTAB} \approx 0.1$ there is no effect of C_n TAB on T_m . Above this point and up to $x_{C_nTAB} \approx 0.6$ both C_{14} TAB and C_{16} TAB decrease T_m with a slightly stronger effect of C_{16} TAB, whereas C_{18} TAB increases T_m to a maximum value around 47 °C. Beyond $x_{C_nTAB} \approx 0.6$ C_{14} TAB exhibits a stronger decreasing effect on T_m relative to C_{16} TAB. C_{18} TAB also decreases T_m , however, to a value (45 °C) higher than that of neat DODAB (43 °C). These data indicate that there is no clear relationship between T_m and the C_n TAB chain length, with C_{18} TAB exhibiting the unusual behavior of increasing T_m . Overall, surfactants reduce T_m [11,13,14].

Fig. 4 shows the effect of the surfactant molar fraction on the width of the main transition peaks, $\Delta T_{1/2}$. $\Delta T_{1/2}$ does not vary much with x_{C_nTAB} , indicating that the transition is rather cooperative, that is, it takes place in a rather narrow range of temperature, between

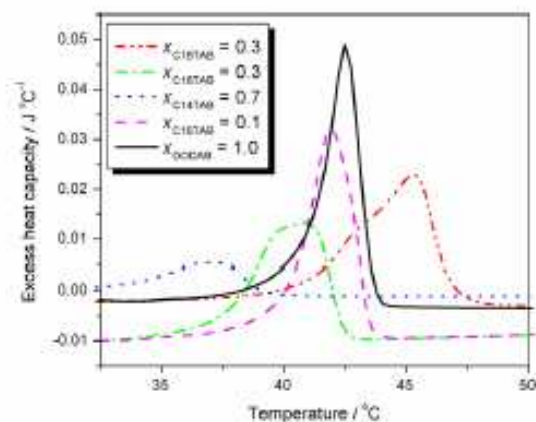


Fig. 7. DSC upscan thermograms from selected mixtures of C_n TAB-DODAB in water, indicating peak overlaps.

1.5 and 2.0 °C. The broadening of $\Delta T_{1/2}$ on addition of C_n TAB, for $n = 14$ –18, is due to peak overlaps. C_{18} TAB and C_{14} TAB broaden the peaks at low and high concentrations, respectively, while C_{16} TAB broaden the peaks both at low and high concentrations.

The peak overlap is due to sharp transitions that occur in a narrow range of temperature due to the vesicle polydispersity, since the vesicle curvature affects T_m [5]. The appearance of the extra peak at $x_{C_{18}TAB} = 0.5$ has been attributed to a vesicle population rich in C_{18} TAB in addition to the ordinary DODAB-rich vesicles [15]. A detailed analysis of the broader peaks clearly indicates peak overlaps (Fig. 7). Surprisingly this figure also indicates that even the narrower peaks for neat DODAB and the C_{12} TAB-DODAB vesicles are composed of peak overlaps. Such overlaps were attributed to different populations of DODAB vesicles differing mainly in size (rather than in structure) to explain the effect of C_{18} TAB on increasing T_m [15].

In the presence of a small amount of DODAB, broad (overlapped) peaks appear (Fig. 11, supplementary material) owing to multiple transitions in the C_{16} TAB- and C_{18} TAB-containing systems. This is the usual behavior of higher amount of cosurfactants, such as C_n TAB, since they exhibit specific transitions themselves [15]. Transitions for C_{18} TAB in water were previously reported indicating that this surfactant assembles as a bilayer in addition to micelle structures [15,18].

The enthalpy change (ΔH) associated to the main transition for neat DODAB in water lies between 43 and 51.5 kJ mol⁻¹ (Fig. 5) in good agreement with data previously reported for similar systems [8,11,19]. Accordingly, ΔH decreases with increasing x_{C_nTAB} , indicating that the addition of C_n TAB favors the main transition. The data, however, indicate no clear relationship between ΔH and the chain length.

4. Conclusions

The thermotropic phase behavior of the aqueous mixtures of DODAB and C_n TAB (for $n = 12$ –18) was investigated by DSC at 5.0 mM total surfactant concentration and varying surfactant ratios. The systems allow the investigation of the C_n TAB-DODAB vesicle interaction below and above CMC. The results indicate that not only the chain length, but also the relative concentration of C_n TAB influences the main-, pre- and post-transition temperatures (T_m , T_s and T_p). Accordingly, vesicles are formed even in the presence of very small amounts of DODAB (high amount of C_n TAB). C_{12} TAB does not

affect T_m and T_3 since its concentration is much lower than CMC. It yields, however, a $T_p \approx 51.6^\circ\text{C}$ that cannot be viewed in the DSC traces (Fig. 1) for neat DODAB. For $n = 14$ –18, upon increasing C_n TAB concentration the pre-transition is completely inhibited when concentration approaches CMC. C_{14} TAB and C_{16} TAB decrease, whereas C_{18} TAB increases T_m . According to the peak width, for all C_n TAB-DODAB mixtures the main transition is cooperative even though it is composed of overlapped narrow peaks, for larger n the peaks are broader owing as well to peak overlaps. The melting enthalpy is lowered on increasing C_n TAB concentration, indicating that the surfactant favors the melting transition. The C_n TAB-DODAB systems thus offer excellent opportunity to deal with mixed cationic vesicles with well-defined characteristics and high potential application as membrane mimetic systems as well as vehicle for drug delivery.

Acknowledgements

FRA and EF acknowledge CNPq for PhD and research (Grant 304543/2006-3) grants, respectively. Dr. W. Loh (UNICAMP) is acknowledged for kindly supplying the DSC equipment.

Appendix A. Supplementary data

Supplementary data associated with this article can be found, in the online version, at doi:10.1016/j.tca.2008.03.017.

References

- [1] J.H. Fendler, *Membrane Mimetic Chemistry*, Wiley-Interscience, New York, 1982.
- [2] D.D. Lasic, *Liposomes. From Physics to Applications*, Elsevier, Amsterdam, 1993.
- [3] G. Cevec, D. Marsh, *Phospholipid Bilayers-Physical Principles and Models*, v. 5, New York, 1987.
- [4] J.H.E.N. Engberts, D. Hoeskestra, *Biochim. Biophys. Acta* 1241 (1995) 323–340.
- [5] E. Feltosa, P.C.A. Barreleim, G. Olafsson, *Chem. Phys. Lipids* 105(2000)201–213.
- [6] E. Feltosa, W. Brown, *Langmuir* 13 (1997) 4810–4816.
- [7] E. Feltosa, G. Karlsson, K. Edwards, *Chem. Phys. Lipids* 140 (2006)65–74.
- [8] E. Feltosa, P.C.A. Barreleim, *Progr. Colloid Polym. Sci.* 128 (2004) 163–168.
- [9] C.R. Benatti, E. Feltosa, R.M. Fernandez, M.T. Lamy-Freund, *Chem. Phys. Lipids* 111 (2001)93–104.
- [10] R.O. Brito, E.F. Marques, *Chem. Phys. Lipids* 137 (2005) 18–28.
- [11] E. Feltosa, N.M. Bonassi, W. Loh, *Langmuir* 22 (2006) 4512–4517.
- [12] J. Cocquyt, U. Olsson, G. Olafsson, P. Van der Meeren, *Langmuir* 20 (2004) 3906–3912.
- [13] P.C.A. Barreleim, G. Olafsson, W. Brown, K. Edwards, N.M. Bonassi, E. Feltosa, *Langmuir* 18 (2002) 1024–1029.
- [14] A. Kacperska, *J. Thermochem. Anal.* 45(1995) 703–714.
- [15] F.R. Alves, M.E.D. Zaniquelli, W. Loh, E.M.S. Castanheira, M.E.C.D. Real Oliveira, E. Feltosa, *J. Colloid Interf. Sci.* 316 (2007) 132–139.
- [16] J. Mata, D. Varade, P. Bahadur, *Thermochim. Acta* 428 (2005) 147–155.
- [17] T.W. Dawey, W.A. Ducker, A.R. Hayman, J. Simpson, *Langmuir* 14 (1998) 3210–3213.
- [18] M. Swanson-Vethamuthu, E. Feltosa, W. Brown, *Langmuir* 14 (1998) 1500–1505.
- [19] E. Feltosa, F.R. Alves, A. Niemić, M.E.C.D. Real Oliveira, E.M.S. Castanheira, A.L.F. Baptista, *Langmuir* 22 (2006) 3579–3585.

Artigo 6

Vesicle-micelle transitions in DODAB- C_n TAB aqueous mixtures studied by differential scanning calorimetry and turbidity

Eloi Feitosa,^{1,*} Fernanda R. Alves¹ and Watson Loh²

¹Department of Physics, Sao Paulo State University, Sao Jose do Rio Preto, SP, Brazil

²Institute of Chemistry, University of Campinas (UNICAMP), Campinas, SP, Brazil

*Correspondence address:

Eloi Feitosa

Physics Dept., IBILCE/UNESP

Rua Cristovao Colombo, 2265

Sao Jose do Rio Preto, SP - Brazil

CEP: 15054-000

Voice: +55 17 3221 22 40

Telefax: +55 17 3221 22 47

e-mail: eloi@ibilce.unesp.br

Abstract

The effect of C_n TAB, $n = 12-18$, on 1.0 mM DODAB vesicles was studied by differential scanning calorimetry and turbidity to monitor changes in the melting temperature, T_m , and vesicle-micelle transition. The longer is the chain length, the lower the C_n TAB concentration necessary for the complete vesicle-micelle transition. For all these systems investigated the vesicle-micelle transition follows a three-stage transition. Below CMC, C_n TAB solubilizes into DODAB vesicles that swell; above CMC, C_n TAB partitions between DODAB vesicles and C_n TAB micelles until complete solubilization of DODAB to form mixed micelles. Within the intermediate stage mixed vesicles and micelles co-exist. As a result, all surfactants, but C_{18} TAB, decrease T_m .

Keywords: Cationic vesicles, DODAB, C_n TAB, DSC, turbidity.

Introduction

In excess water, quaternary ammonium-based surfactants, like DODAB or CTAB, self-assemble either as micelle or bilayer structures depending mainly on whether they are single or double tailed and on their chain length. The individual properties of these surfactants, either as monomer or aggregates in aqueous solutions, including CMC (critical micelle concentration), CVC (critical vesicle concentration), Krafft point, melting temperature, aggregate size, degree of counterion dissociation among others, are already described in the literature [1-21].

Under appropriate conditions C_n TAB self-assemble as micelle [7] while DODAB as vesicle [8,11] structures. Such individual surfactant characteristics raise the following question: what kind of structures can be formed in aqueous mixtures of these surfactants? Previous investigations indicate that, in excess of C_n TAB or DODAB, micelles or vesicles are formed, respectively [12-13]. More detailed information on the vesicle-micelle transition in C_n TAB-DODAB mixtures, however, is still missing.

Because aqueous solutions of these individual surfactants have potential applications in many formulations, mixed DODAB- C_n TAB aqueous solutions are widely appropriate for industrial or scientific applications, considering that pure compounds are scarce and expensive for industrial purposes. Detailed investigation is required on the physico-chemical properties of the aqueous mixtures of surfactants in general and DODAB- C_n TAB in particular. The purpose of the present investigation to elucidate how C_n TAB affects the properties of DODAB vesicles when increasing amount of C_n TAB is added to a vesicle dispersion leaving constant the DODAB concentration. The data are compared to similar studies previously reported [14-19].

Special attention concerns on whether the C_n TAB concentration is below or above CMC and on it affects the DODAB- C_n TAB interaction. DSC and turbidity measurements

provide clear information on the presence of vesicle or micelle structures, and DSC is capable of following how DODAB T_m varies on increasing the C_n TAB concentration.

Materials and methods

C_n TAB (alkyltrimethylammonium bromide) and DODAB (dioctadecyldimethylammonium bromide) (both from Sigma) were used as purchased, without further purification. Milli-Q quality water was used in sample preparations. According to the literature, the CMC of DODAB in water is close to zero [8], while those for C_n TAB are 15.2, 3.98, 1.0 and 0.34 mM, for $n = 12, 14, 16$ and 18 , respectively [3,7].

Sample preparation: Stock solutions of C_n TAB micelles and DODAB vesicles were prepared by weighing the appropriate amount of these surfactants and water to obtain the desired concentration. The DODAB/water mixtures were warmed to $55\text{ }^\circ\text{C}$ to complete dissolution of the surfactant and then stored at room temperature, while the C_n TAB/water mixtures were warmed to a safe temperature above the Krafft point of these surfactants [2,3]. Only C_{18} TAB has Krafft point above $25\text{ }^\circ\text{C}$ (room temperature), so that the C_{18} TAB/water samples were mixed at $40\text{ }^\circ\text{C}$, while all the other surfactant solutions were mixed at $25\text{ }^\circ\text{C}$. All samples were stored at room temperature. Before being diluted or mixed with DODAB the C_{18} TAB stock solution was warmed to ca $45\text{ }^\circ\text{C}$ to dissolve the crystals.

The DODAB- C_n TAB mixtures were prepared by weighing in glass flasks appropriate amount of the micelle and vesicle solutions, taking care for the micelle solution to be above the Krafft temperature (T_K) to ensure the homogeneous condition. T_K was obtained for C_{18} TAB micelles and mixed DODAB/ C_{18} TAB mixtures either by DSC (the DSC thermogram exhibits a sharp peak around T_K) or by stepwise warming the sample until complete dissolution of the crystals, according to visual observation of the sample.

Turbidity data were obtained by an UV-vis spectrophotometer (Cary 100) at $\lambda = 400$ nm, and the DSC data were collected by a microcalorimeter, model VP-DSC (MicroCal), at the scan rate of 1 °C/min, within the temperature range of 5-85 °C. Details on the DSC experimental setup can be found elsewhere [12].

Results and discussion

The effect of C_n TAB concentration on the turbidity of 1.0 mM DODAB vesicles is shown in Fig. 1. The curves resemble those previously reported for the effect of nonionic and zwitterionic surfactants on DODAB or DODAC vesicles [17,19], and on phospholipid liposomes [20,21]. By adding oxyethylene-based surfactants ($C_{12}E_n$) to DODAB vesicles there is an initial increase followed by a decrease in turbidity to values close to zero compatible with formation of micelle systems, indicating that the vesicle-micelle transition takes place in three stages as described before [17,19]. First mixed vesicles are formed and then, in the intermediary region, mixed vesicles and micelles co-exist in equilibrium. Finally there are only mixed micelles in solution. Similar mechanism of vesicle-micelle transition seems to occur for the systems DODAB- C_n TAB here investigated.

Accordingly, the initial mixed vesicles are slightly larger than the neat DODAB vesicles, as revealed by the greater turbidity, and the complete vesicle-micelle transition obeys the sequence $n = 18 < 16 < 14 < 12$, indicating that the longer the chain length, the stronger the interaction and the smaller the amount of C_n TAB required to complete the vesicle-micelle transition. Fig. 1 also indicates that the vesicle-micelle transition is smoother for C_{12} TAB and steeper for C_{18} TAB. Surprisingly, C_{14} TAB exhibits a stronger effect on the vesicle-micelle transition than C_{16} TAB. The reason for such an unusual behavior is not clear for us, although the data also indicate that C_{14} TAB has a stronger effect within the intermediary region.

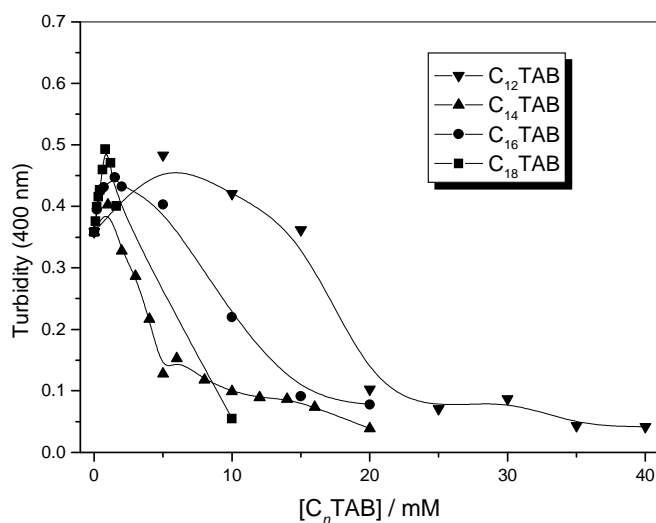


Figure 1 – Turbidity of DODAB- C_n TAB-water system, at constant 1.0 mM DODAB and varying C_n TAB ($n = 12-18$). Measurements at 25 °C.

Fig. 2 shows the DSC thermograms obtained from the second upscans for the DODAB- C_n TAB systems, for $n = 12-18$. The first and second scans gave rather similar results except for neat C_{18} TAB, as discussed below (see Fig. 3a). Accordingly, the addition of C_n TAB to a DODAB vesicle dispersion affects the thermotropic behavior of the vesicles in a way that depends on the surfactant chain length (n), and on the relative amount of these surfactants. One should notice that in presence of C_{18} TAB the DSC main peak may be broaden due to the superposition of narrower peaks, as Fig.3b illustrates the presence of three peaks enveloped by the broad peak for 1.0 mM DODAB and 0.4 mM C_{18} TAB. The formation of multiple (overlapping) peaks is due to the interaction of C_{18} TAB with different vesicle structures [11] resulting in mixed polydisperse structures with characteristic phase behavior.

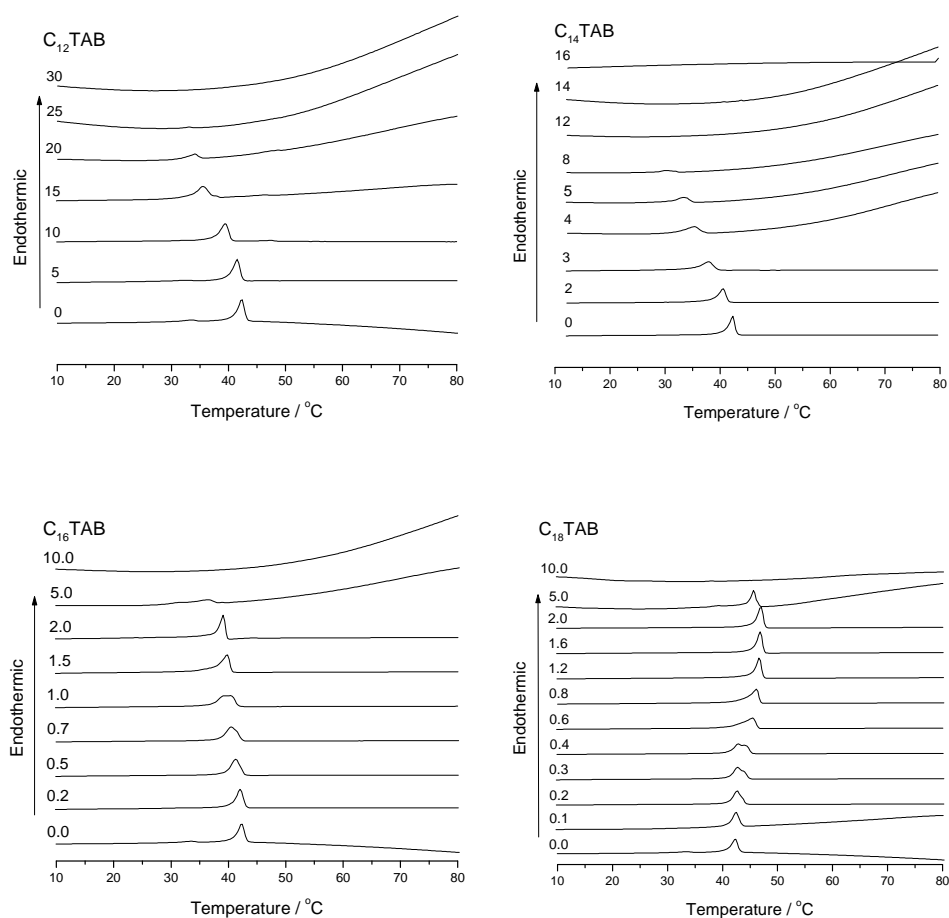


Figure 2 – Second DSC upscans for the DODAB/ C_n TAB system, at constant 1.0 mM DODAB and varying C_n TAB ($n = 12-18$).

The first and second DSC upscan thermograms for neat C_{18} TAB in water (Fig. 3a) gives information on the “melting” temperature of the C_{18} TAB bilayer as well as on the Krafft temperature of this surfactant in water in good agreement with previously reported data [3]. In that study it was reported that C_{18} TAB molecules assemble in aqueous solution as spherical and disk-like micelles, with the “melting” temperature $T_m = 34$ °C. The population of C_{18} TAB disk-like aggregates increases with surfactant concentration and ionic strength [3] and, as a result, the intensity of the DSC peak associated with the melting temperature increases [12]. Based on the present DSC data, we report $T_m = 33$ °C and a Krafft temperature $T_K = 37.0$ °C (Fig. 3a) for 15 mM C_{18} TAB. In this figure, the sharp peak characteristic for T_K does not

appear in the second upscan because after cooling the sample the crystals were not formed prior the beginning of the second scan.

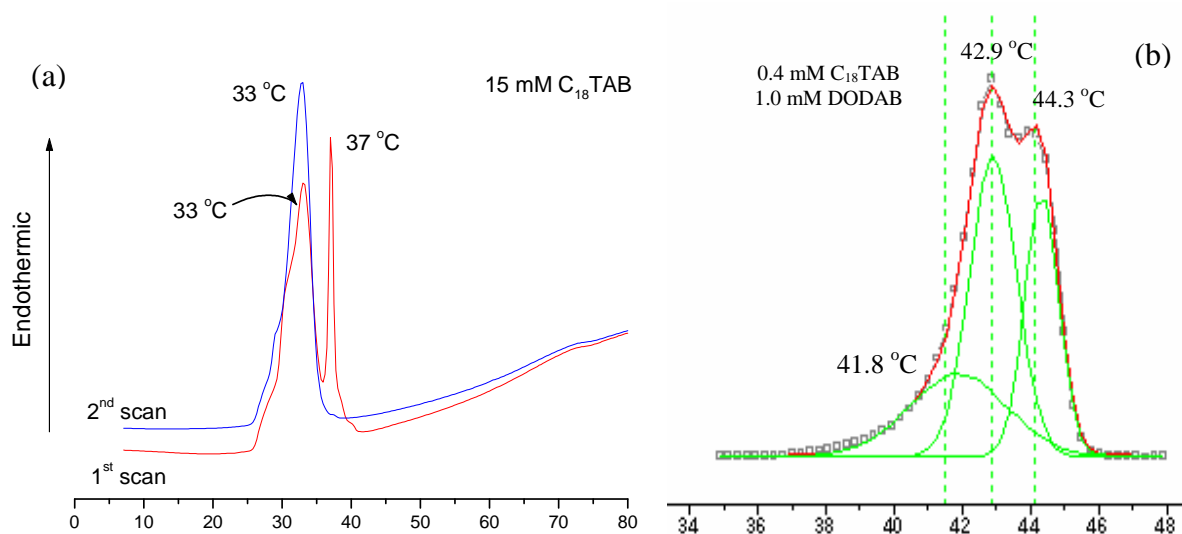


Figure 3: (a) First (red line) and second (blue line) DSC upscans for neat C₁₈TAB 15.0 mM in water. (b) Deconvolution of a typical broad DSC peak associated to the main transition for 1.0 mM DODAB and 0.4 mM C₁₈TAB.

In presence of DODAB vesicles no Krafft transition was detected in excess DODAB, when all C₁₈TAB molecules are solubilized into the vesicles to form mixed DODAB-C₁₈TAB mixed vesicles. After saturation, however, C₁₈TAB free micelles are formed and the mixtures exhibit a similar T_K to that of neat C₁₈TAB in water (T_K = 37.0 °C), indicating that neat C₁₈TAB micelles are in equilibrium with mixed DODAB-C₁₈TAB vesicles. The effect of C₁₈TAB concentration on T_K, in presence of constant 1.0 mM DODAB, was obtained by visual observation of the sample submitted to a stepwise increase in temperature from 5 °C up to T_K, the temperature at which the precipitates disappear.

The effect of the C_nTAB concentration on the melting temperature (T_m) is shown in Fig. 4. Accordingly, C_nTAB reduces T_m when *n* equals 12-16, but increases T_m when *n* = 18 from 42.4 °C to a maximum value of ca. 47 °C when C₁₈TAB concentration equals about 2.5 fold the DODAB concentration (Fig. 4), at a concentration much higher than the CMC of

C_{18} TAB (equals 0.34 mM) [3]. Beyond this concentration T_m decreases to attain the value of neat C_{18} TAB in water (33 °C), indicating that in excess C_{18} TAB, DODAB molecules are solubilized in the C_{18} TAB bilayers or disk-like micelles. The precise structure of the C_{18} TAB-rich aggregates requires further investigation. However, as the turbidity of these samples is rather low, the aggregates should be small and may possibly be disk-like micelles, or pre-vesicle structures.

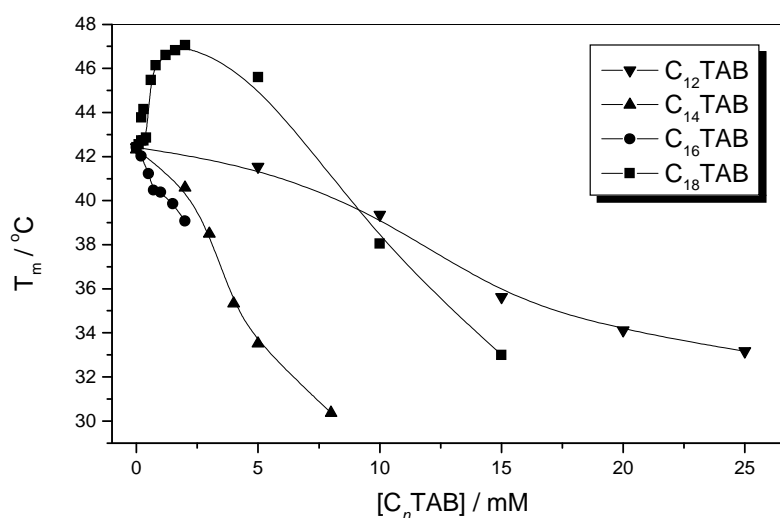


Figure 4: The effect of C_n TAB concentration on the melting temperature (T_m) of the DODAB/ C_n TAB system, at constant 1.0 mM DODAB. The point for 15 mM C_{18} TAB corresponds to neat surfactant (without DODAB).

For $n = 14-16$ T_m is lowered, smoothly for $n = 12$ (higher CMC) and more pronounced for $n = 14$ and 16, indicating stronger affinity of DODAB vesicles for C_n TAB, when $n = 14$ and 16. These surfactants are solubilized in the vesicle bilayer leaving it more fluid, thus reducing the melting temperature. The unusual effect of C_{18} TAB on T_m of DODAB vesicles has been discussed before and the increase in T_m was attributed to the formation of more densely packed bilayer structures [12,13], followed by a decrease of the population of the “ordinary” vesicles. A possible explanation for such a behavior is that the terminal CH_3 group

of the shorter C_n TAB ($n = 12-16$) forces the DODAB chains to bend, leaving the bilayer less densely packed.

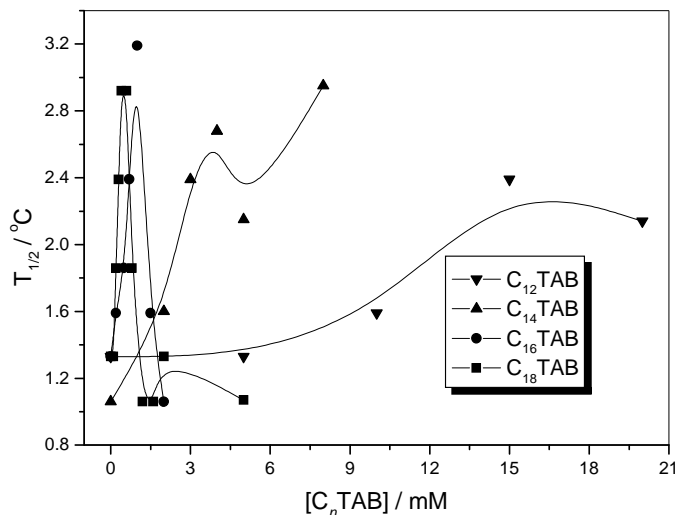


Figure 5: The effect of C_n TAB concentration on the peak width ($\Delta T_{1/2}$) of the DODAB/ C_n TAB system, at constant 1.0 mM DODAB.

The melting enthalpy (ΔH) of neat DODAB vesicles and C_{18} TAB bilayers are about 40 and 29 kJmol^{-1} , respectively, as calculated from the peak area, while the DODAB peak width ($\Delta T_{1/2}$) is about 1.2 $^{\circ}\text{C}$, indicating a rather narrow peak. On addition of C_{18} TAB both ΔH and $\Delta T_{1/2}$ vary in different ways. Unfortunately the calculation of the melting enthalpy involves the unknown surfactant concentration within the vesicles. For this reason, ΔH has not been calculated. The peak width is shown in Fig. 5 as a function of C_n TAB concentration. Accordingly, the broad peaks exhibit high $\Delta T_{1/2}$ due to overlapping peaks (Fig.3b) indicating the coexistence of bilayer structures with different curvatures. In this sense Fig. 5 indicates how the peak width varies with surfactant concentration. The lack of a systematic behavior in these systems reflects the polydispersity of the bilayer structures yielded by the addition of C_n TAB.

Furthermore, different population of vesicles may respond differently to the presence of C₁₈TAB, yielding formation of different bilayer-like structures giving rise to overlapping DSC peaks, as Fig. 3b indicates. The deconvolution of the main DSC peak for the sample containing 1.0 mM DODAB and 0.4 mM C₁₈TAB, indicates the presence of three peaks, characteristic of populations of different bilayer structures.

Conclusions

When C_nTAB is added to DODAB vesicles a vesicle-micelle transition is observed. The present data show that the vesicle-micelle transition depends on the surfactant chain length and the relative DODAB/C_nTAB concentration. The longer is the chain length, the greater the affinity of DODAB vesicles for C_nTAB. For $n < 18$, C_nTAB decreases the melting temperature, T_m, leaving the bilayer more fluid, as expected for most surfactants. For $n = 18$ (same size as DODAB) T_m increases, indicating that the longer C₁₈TAB compacts the bilayer, increasing T_m.

Mixtures of surfactants are often used to modify and control the structure and properties of association colloid systems aiming specific applications in a variety of scientific and industrial systems. This investigation provides information on how the properties of cationic surfactant aggregates, including vesicles and micelles, may be varied by varying the surfactant composition to achieve different purposes.

Acknowledgements

FRA and EF thank CNPq for PhD and research grant (Grant 304543/2006-3), respectively.

WL thanks FAPESP for supporting the calorimetric studies.

References

- [1] I.M. Cuccovia, E. Feitosa, H. Chaimovich, L. Sepulveda, W. Reed, *J. Phys Chem.* 94 (1990) 3722.
- [2] T.W. Davey, W.A. Ducker, A.R. Hayman, J. Simpson, *Langmuir* 14 (1998) 3210.
- [3] M. Swanson-Vethamuthu, E. Feitosa, W. Brown, *Langmuir* 14 (1998) 1590.
- [4] D.B. Nascimento, R. Rapuano, M.M. Lessa, A.M. Carmona-Ribeiro, *Langmuir* 14 (1998) 7387.
- [5] C.R. Benatti, E. Feitosa, R.M. Fernandez, Lamy-Freund, M.T. *Chem. Phys. Lipids* 111 (2001) 93.
- [6] R.O. Brito, E.F. Marques, *Chem. Phys. Lipids* 137 (2005) 18.
- [7] J. Mata, D. Varade, P. Bahadur, *Thermochimica Acta* 428 (2005) 147.
- [8] E. Feitosa, W. Brown, *Langmuir* 13 (1997) 4810.
- [9] E. Feitosa, P.C.A. Barreleiro, *Progr. Colloid Polym. Sci.* 128 (2004) 163.
- [10] E. Feitosa, P.C.A. Barreleiro, G. Olofsson, *Chem. Phys. Lipids* 105, (2000) 201.
- [11] E. Feitosa, G. Karlsson, K. Edwards, *Chem. Phys. Lipids* 140 (2006) 66.
- [12] F.R. Alves, M.E.D. Zaniquelli, W. Loh, E.M.S. Castanheira, M.E.C.D. Real Oliveira, E. Feitosa, *J. Colloid Interface Sci.* 316 (2007) 132.
- [13] F.R. Alves, E. Feitosa, *Thermochimica Acta*, 472 (2008) 41.
- [14] A. Kacperska, *J. Thermoch. Analysis* 45 (1995) 703.
- [15] M.J. Blandamer, B. Briggs, P.M. Cullis, P. Last, J.B.F.N. Engberts, A. Kacperska, *J. Therm. Anal. Cal.* 55 (1999) 29.
- [16] P.C.A. Barreleiro, G. Olofsson, E. Feitosa, *Progr. Colloid Polym. Sci.* 116 (2000) 33.
- [17] P.C.A. Barreleiro, G. Olofsson, W. Brown, K. Edwards, N.M. Bonassi, E. Feitosa, *Langmuir* 18 (2002) 1024.
- [18] J. Cocquyt, U. Olsson, G. Olofsson, P. Van der Meeren, *Langmuir* 20 (2004) 3906-3912.

[19] E. Feitosa, N.M. Bonassi, W. Loh, *Langmuir* 22 (2006) 4512.

[20] M. Johnsson, K. Edwards, *Langmuir* 16 (2000) 8632.

[21] M. Johnsson, N. Bergstrand, *Colloids Surf. B* 34 (2004) 69.